The Complete Research Report

Project Name…

Heat Transfer and Pressure Drop Characteristics of Nanofluids Flowing Through Microchannel Heat Sinks

Investigator…

Asst. Prof. Dr. Weerapun Duangthongsuk

July 2014

Project code: MRG5580118

The Complete Research Report

Project Name…

Heat Transfer and Pressure Drop Characteristics of
Nanofluids Flowing Through Microchannel Heat Sinks

Researcher…

Asst. Prof. Dr. Weerapun Duangthongsuk
Mechanical Engineering Department
Faculty of Engineering
Southeast Asia University

Supported by the Thailand Research Fund (TRF)

บทคัดย่อ

รหัสโครงการ: MRG5580118

ชื่อโครงการ: ลักษณะเฉพาะการถ่ายเทความร้อนและความดันลดของของไหลนาโนที่ไหลผ่านอุปกรณ์ระบายความร้อนที่มีช่องทางการไหลขนาดเล็ก

ชื่อนักวิจัย:
ผศ. ดร. วีระพันธ์ ด้วงทองสุข
สาขาวิชาวิศวกรรมเครื่องกล คณะวิศวกรรมศาสตร์ มหาวิทยาลัยเอเชียอาคเนย์

E-mail Address: wdaungthongsuk@yahoo.com, weerapund@sau.ac.th

ระยะเวลาโครงการ : 2 ปี นับตั้งแต่ 2 กรกฎาคม 2012 – 30 มิถุนายน 2014

งานวิจัยนี้เป็นการศึกษาเชิงทดลองในการหาค่าสมรรถนะทางความร้อนและลักษณะของความดันลด ที่เกิดขึ้นภายในอุปกรณ์ระบายความร้อนที่ใช้ของไหลนาโนเป็นของไหลทำงาน โดยอุปกรณ์ระบายความร้อนที่ใช้ในการทดลองมี 2 ลักษณะ คือ แบบที่มีลักษณะเป็นครีบแท่งกลมที่มีขนาดเล็กมาก (Miniature circular pin fin ,MCFHS) และครีบแท่งเหลี่ยมที่มีขนาดเล็กมาก (Miniature square pin fin, MSFHS) นอกจากนั้นของไหลนาโนที่ใช้ในการทดลองก็มี 2 ชนิด คือ ชนิดที่ใส่อนุภาคของ ZnO และ SiO_2 ลงในน้ำ โดยมีความเข้มข้นโดยปริมาตรเท่ากับ 0.2, 0.4 และ 0.6 vol.% และไหลผ่านอุปกรณ์ระบายความร้อนภายใต้สภาวะฟลักซ์ความร้อนคงที่ โดยการศึกษานี้ได้รายงานผลของลักษณะของครีบระบายความร้อน, ความเข้มข้นของของไหลนาโน และเลขเรย์โนลด์ ที่มีต่อสมรรถนะการถ่ายเทความร้อนและความดันลดที่เกิดขึ้น สำหรับสภาวะที่ใช้ในการทดลอง คือ เลขเรย์โนลด์อยู่ระหว่าง 700 และ 3,700 อุณหภูมิของของไหลเท่ากับ 15 องศาเซลเซียส ฟลักซ์ความร้อนอยู่ระหว่าง 2 ถึง 5 วัตต์ต่อตารางเซนติเมตร สำหรับเส้นผ่านศูนย์กลางไฮดรอลิกซ์ของช่องทางการไหลของอุปกรณ์ระบายความร้อนทั้ง 2 แบบ ถูกออกแบบให้เท่ากันที่ 1.2 มิลลิเมตร และพื้นที่ผิวการถ่ายเทความร้อนของอุปกรณ์ระบายความร้อนแบบครีบแท่งกลมและครีบแท่งเหลี่ยม เท่ากับ 1,430 และ 1,565 ตารางมิลลิเมตร ตามลำดับ และทำมาจากอลูมิเนียมขนาดประมาณ 28 x 30 มิลลิเมตร โดยข้อมูลจากการทดลองของของไหลนาโนจะถูกนำไปเปรียบเทียบกับข้อมูลการทดลองของน้ำ จากผลการทดลองพบว่าสมรรถนะในการถ่ายเทความร้อนของของไหลนาโนจะมีค่าสูงกว่าน้ำ และแปรผันตามเลขเรย์โรลด์และความเข้มข้นของของไหลนาโน โดยของไหลนาโนชนิดใส่อนุภาคของ SiO_2 ลงในน้ำให้ค่าสมรรถนะการถ่ายเทความร้อนที่สูงกว่าน้ำระหว่าง 4 ถึง 13

เปอร์เซ็นต์ ส่วนของไหลนาโนชนิดใส่อนุภาคของ ZnO ลงในน้ำ ให้ค่าสมรรถนะการถ่ายเทความร้อนที่สูงกว่าน้ำระหว่าง 7 ถึง 20 เปอร์เซ็นต์ นอกจากนั้นจากผลการทดลองยังพบว่าอุปกรณ์ระบายความร้อนแบบครีบแท่งกลมให้ค่าสมรรถนะการถ่ายเทความร้อนที่ดีกว่าครีบแบบแท่งเหลี่ยม ในส่วนของความดันลดนั้น จากผลการทดลองพบว่าผลของอนุภาคนาโน, ความเข้มข้นและลักษณะของครีบระบายความร้อนมีผลต่อค่ากำลังงานในการปั๊มของไหลน้อยมากสุดท้าย ในการศึกษานี้ได้นำข้อมูลจากการทดลองทั้งหมด มาสร้างสหสัมพันธ์สำหรับทำนายค่าเลขนัสเซลและความดันลด จากการไหลของของไหลนาโนที่ไหลผ่านอุปกรณ์ระบายความร้อนแบบที่มีครีบแท่งกลมและครีบแท่งเหลี่ยมขนาดเล็ก ซึ่งรูปแบบของสมการจะมีรูปแบบที่ง่ายต่อการใช้งาน

คำหลัก : ระบายความร้อนด้วยของไหลนาโน, อุปกรณ์ระบายความร้อน, เลขนัสเซล, กำลังงานในการปั๊ม

Abstract

Project Code: MRG5580118

Project Title: Heat Transfer and Pressure Drop Characteristics of Nanofluids flowing Through Microchannel Heat Sinks

Investigator:

Asst. Prof. Dr. Weerapun Duangthongsuk

Mechanical Engineering Department, Faculty of Engineering,

Southeast Asia University

E-mail Address: wdaungthongsuk@yahoo.com, weerapund@sau.ac.th

Project Period: 2 July 2012 – 30 June 2014

The research reports an experimental investigation on the thermal performance and pressure drop features of the nanofluid-cooled heat sinks with miniature circular pin fin (MCFHS) and square pin fin (MSFHS) structure. ZnO and SiO_2 nanoparticles dispersed in DI water with particle concentrations of 0.2, 0.4 and 0.6 vol.% are used as working fluids and flow through both heat sinks under constant heat flux condition. The effect of pin fin configuration, particle concentration and Reynolds number on the heat transfer performance and pressure drop are presented. Reynolds number ranging between 700 and 3,700, fluid temperature of 15 ^{o}C and heat flux ranged between 2 and 5.W/cm^2 are tested. Hydraulic diameter of MCFHS and MSFHS are equally designed at 1.2 mm, and the heat transfer area of MCFHS and MSFHS is around 1,430 and 1,565 mm^2, respectively. MCFHS and MSFHS are made from aluminum material with dimension about 28x30 mm. The data for nanofluid-cooled heat sink are used to compare with the data for water-cooled heat sinks. The experimental results indicated that the heat transfer coefficient increased with increasing Reynolds number and particle concentrations. The data also showed that the heat transfer performance of nanofluid-cooled heat sink was larger than the water-cooled heat sink around 4-13% for SiO_2-water nanofluid and 7-20% for ZnO-water nanofluid. MCFHS gave larger heat transfer performance than the MSFHS at a given condition. For pressure drop data, the measured data showed that particle types, particle concentration and channel

configurations had a small effect on the pumping power. Finally, the heat transfer and pressure drop correlation were proposed in the simple form to predict the Nusselt number and pressure drop of nanofluid-cooled heat sink with pin fin structures.

Keywords : nanofluid-cooled, heat sink, Nusselt number, pumping power

Output จากโครงการวิจัยที่ได้รับทุนจาก สกว.

1. ผลงานตีพิมพ์ในวารสารวิชาการนานาชาติ

   - Duangthongsuk, W. and Wongwises, S., “A Critical Overview on the Heat Transfer Performance and Flow Characteristics of Nanofluids-Cooled Heat sink”, in preparation
   - Duangthongsuk, W. and Wongwises, S., “Effect of Nanofluids Types on the Thermal Performance and Pressure Drop of Miniature Circular Pin Fin Heat Sink”, in preparation
   - Duangthongsuk, W. and Wongwises, S., “A Comparison of the Heat Transfer Performance of nanofluid-Cooled Heat Sinks with Different Miniature pin fin Configurations”, in preparation

2. การนำผลงานวิจัยไปใช้ประโยชน์
   - เชิงพาณิชย์ (มีการนำไปผลิต/ขาย/ก่อให้เกิดรายได้ หรือมีการนำไปประยุกต์ใช้โดยภาคธุรกิจ/บุคคลทั่วไป)
   - เชิงนโยบาย (มีการกำหนดนโยบายอิงงานวิจัย/เกิดมาตรการใหม่/เปลี่ยนแปลงระเบียบข้อบังคับหรือวิธีทำงาน)
   - เชิงสาธารณะ (มีเครือข่ายความร่วมมือ/สร้างกระแสความสนใจในวงกว้าง)
   - เชิงวิชาการ (มีการพัฒนาการเรียนการสอน/สร้างนักวิจัยใหม่)

3. อื่นๆ
   - An Experimental Study on the Heat Transfer Performance and Flow Characteristics of Nanofluids Flowing Through Microchannel Heat Sink with Different Configurations, การประชุมวิชาการประจำปี “**นักวิจัยรุ่นใหม่.. พบ..เมธีวิจัยอาวุโส สกว**.” ครั้งที่ 14, 23 - 25 ตุลาคม พ.ศ. 2557 , จอมเทียน, ชลบุรี

ACKNOWLEDGEMENT

This research work would not have been possible without the help and active collaboration of many people to whom I acknowledge my indebtedness and sincere gratitude and appreciation.

Firstly, I would like to express sincere thanks to the Thailand Research Fund (TRF), the Office of the Higher Education Commission, and the Southeast Asia University to provide financial support (Grant No. MRG5 5 8 0 1 1 8) for this study. I am very grateful to thanks my mentor, Prof. Dr. Somchai Wongwises, for his valuable suggestion, attentive interest, guidance and kind recommendations in the present research. Thank you the student in the Mechanical Engineering Department, Southeast Asia University for their help.

CONTENTS

LIST OF TABLES

LIST OF FIGURES

LIST OF SYMBOLS

A	=	area, m^2
B	=	base thickness, mm
C_p	=	specific heat, J/kgK
d	=	nanoparticle diameter, m
D_H	=	hydraulic diameter, m
h	=	heat transfer coefficient, W/m^2K
I	=	electric current, A
k	=	thermal conductivity, W/mK
$\ell 1$	=	heat sink width, mm
$\dot{m}$	=	mass flow rate, kg/s
Nu	=	Nusselt number
n	=	number of pin fin
Pow	=	pumping power, W
ΔP	=	Pressure drop, Pa
Pr	=	Prandtl number
q	=	heat flux, W/m^2
Q	=	heat transfer rate, W
Re	=	Reynolds number
T	=	temperature, ^oC
t	=	fin height, mm
u	=	mean velocity, m/s
V	=	voltage, Volt

$\dot{V}$ = volume flow rate, m^3/s

W = heat sink length / width, mm

Greek symbols

ϕ = volume fraction

$\varnothing$ = fin diameter, mm

ρ = density, kg/m^3

μ = viscosity, kg/ms

Subscript

ch = channel

h = heating fluid

hs = heat sink

in = inlet

m = mean

out = outlet

p = particles

nf = nanofluid

s = surface

TS = test section

wall = wall

CHAPTER 1 INTRODUCITON

1.1 Rationale

Now a day, the next generation of the modern electronic device (such as electronic chip) turn into smaller and high heat flux will be generated. Because of limitation of the heat transfer area, unprecedented high load was created. Thus, removing of high heat generated from these equipment is a major target for designing the future electronic system. In general, there are three approaches for increasing the cooling performance of advanced electronic devices with high level of heat generation. The first is to find an optimum geometry of cooling devices in which the cooling performance is maximized. The second is to reduce the channel diameter for enhancing the heat transfer coefficient which is reported by Tuckerman and Pease [1]. The last is to improve the heat transfer performance of coolants. So, using of nanofluid as coolant is a new idea to increase the cooling performance of the advanced electronic devices. In order to solve this problem, concept of nanofluids combined with heat sinks with optimum configuration and small size of flow channel can be established and are expected for effective heat removing from modern electronic system. Using of some ultra-fine solid particles for dispersing in the common heat transfer fluid was firstly introduced in 1993 by Masuda et al., [2]. Later, in 1995, Choi [3] was first introduced the name of “Nanofluids” which means that the conventional fluids with nanoparticle suspension. Many researchers stated that replacing of common heat transfer fluids with nanofluids provided greater heat transfer performance than that of the common base fluids for several times. At the same time, no or tiny penalty drop in pressure were obtained (Daungthongsuk and Wongwises [4, 5, 6 and 7]). Similarly, concept of microchannel heat sink (MCHS) was first explored by Tuckerman and Pease [1] in the 1981. Their results showed that MCHS gave high heat

transfer removal potential. . They were also suggested that in order to increase the heat transfer performance, decreasing in the channel diameter should be done. Finally, heat sinks with optimal structure called “miniature pin fin configuration (MPF)” was an alternative way to improve the heat transfer performance of the heat sink. Thus, the present work was aimed to study the advantage of different ways for enhancing the heat transfer performance of nanofluid-cooled microchannel heat sink with miniature circular fin (MCFHS) and square fin (MSFHS) configuration. Two different types of nanoparticle were tested. Moreover, pressure drop across the heat sink block was also investigated.

1.2 Objectives

1. To investigate the heat transfer performance and pressure drop characteristics of nanofluids flowing through miniature heat sinks with circular fin (MCFHS) and square fin (MSFHS) structure and having small size of flow channel.

2. To study the effects of the Reynolds number, particle concentration and channel configuration (MCFHS and MSFHS) of heat sinks on the heat transfer performance and pressure drop characteristics of nanofluids-cooled heat sink compared with water cooled- heat sink.

3. To propose the new correlations to predict the Nusselt number and pressure drop of nanofluid-cooled heat sinks for practical use.

1.3 Scope

1. Heat sinks made from aluminum material with dimension of around 28x30 mm are tested.

2. Two miniature pin fin configurations with circular (MCFHS) and square fin (MSFHS) are compared.

3. The SiO_2 and ZnO nanoparticles suspended in DI water with particle concentrations of 0.2, 0.4 and 0.6 vol.% are used as coolant.

4. A 100 W electric heater is used to supply heat load to the each test sections. .

5. Inlet fluid temperature is about 15 ^oC.

1.4 Significance and Usefulness

1. The results obtained from this study are expected to be suitable for applying the nanofluid-cooled heat sinks to practical use.

2. The experimental system can be used to study the other types of the nanofluids and test sections.

3. The new heat transfer and pressure drop correlations can be used to predict the thermal and flow behaviors of nanofluid-cooled heat sink which give more accuracy.

CHAPTER 2 FUNDAMENTAL AND LITERATURE REVIEW

The purpose of this chapter is to describe the fundamental and basic theory of nanofluids and heat sink, respectively. Moreover, review the literature mentioning the heat transfer performance and flow characteristics of nanofluids flowing through heat sink with microchannel configuration and pin fin arrangement including the experimental and numerical investigations. The detail of above mentioned is expressed in the following subsection.

2.1 Fundamental of Nanofluids

2.1.1 Making of Nanofluids

Materials for base fluids and nanoparticles are diverse. Stable and highly conductive nanofluids are produced by one- and two-step production methods. Both approaches to creating nanoparticle suspensions suffer from agglomeration of nanoparticles, which is a key issue in all technology involving nanopowders. Thus, synthesis and suspension of nearly nonagglomerated or monodispersed nanoparticles in liquids is the key to significant enhancement in the thermal properties of nanofluids (Das et al. [8]).

2.1.2 Nanoparticles Materials and Conventional Base Fluids

Modern fabrication technology provides great opportunities to process materials actively at nanometer scales. Nanostructured or nanophase materials are made of nanometer-sized substances engineered on the atomic or molecular scale to produce either new or enhanced physical properties not exhibited by conventional bulk solids. All physical mechanisms have a critical length scale below which the physical properties of materials are changed. Therefore, particles smaller than 100 nm exhibit

properties different from those of conventional solids. The noble properties of nanophase materials come from the relatively high surface area/volume ratio, which is due to the high proportion of constituent atoms residing at the grain boundaries. The thermal, mechanical, optical, magnetic, and electrical properties of nanophase materials are superior to those of conventional materials with coarse grain structures. Consequently, research and development investigation of nanophase materials has drawn considerable attention from both material scientists and engineers (Duncan and Rouvray, [9]).

1. Nanoparticle material types. Nanoparticles used in nanofluids have been made of various materials, such as oxide ceramics (Al_2O_3, CuO), nitride ceramics (AlN, SiN), carbide ceramics (SiC, TiC), metals (Cu, Ag, Au), semiconductors (TiO_2, SiC), carbon nanotubes, and composite materials such as alloyed nanoparticles Al70Cu30 or nanoparticle core–polymer shell composites. In addition to nonmetallic, metallic, and other materials for nanoparticles, completely new materials and structures, such as materials "doped" with molecules in their solid–liquid interface structure, may also have desirable characteristics (Das et al. [8]).

2. Host liquid types. Many types of liquids, such as water, ethylene glycol, and oil, have been used as host liquids in nanofluids (Das et al. [8]).

2.1.3 Methods of Nanoparticle Manufacture

Fabrication of nanoparticles can be classified into two broad categories: physical processes and chemical processes (Kimoto et al. [10], Granqvist and Buhrman [11]). Currently, a number of methods exist for the manufacture of nanoparticles. Typical physical methods include inert-gas condensation (IGC), developed by Granqvist and Buhrman [11], and mechanical grinding. Chemical methods include chemical vapor

deposition (CVD), chemical precipitation, microemulsions, thermal spray, and spray pyrolysis. A sonochemical method has been developed to make suspensions of iron nanoparticles stabilized by oleic acid (Suslick et al., [12]). The current processes for making metal nanoparticles include IGC, mechanical milling, chemical precipitation, thermal spray, and spray pyrolysis. Most recently, Chopkar et al. [13] produced alloyed nanoparticles Al70Cu30 using ball milling. In ball milling, balls impart a lot of energy to slurry of powder, and in most cases some chemicals are used to cause physical and chemical changes. These nanosized materials are most commonly produced in the form of powders. In powder form, nanoparticles are dispersed in aqueous or organic host liquids for specific applications (Das et al. [8]).

2.1.4 Dispersion of Nanoparticles in Liquids

Stable suspensions of nanoparticles in conventional heat transfer fluids are produced by two methods: the two-step technique and the single-step technique. The two-step method first makes nanoparticles using one of the above-described nanoparticle processing techniques and then disperses them into base fluids. The single-step method simultaneously makes and disperses nanoparticles directly into base fluids. In either case, a well-mixed and uniformly dispersed nanofluid is needed for successful production or reproduction of enhanced properties and interpretation of experimental data. For nanofluids prepared by the two-step method, dispersion techniques such as high shear and ultrasound can be used to create various particle–fluid combinations. Most nanofluids containing oxide nanoparticles and carbon nanotubes reported in the open literature are produced by the two-step process. If nanoparticles are produced in dry powder form, some agglomeration of individual nanoparticles may occur due to strong attractive van der Waals forces between nanoparticles. This undesirable

agglomeration is a key issue in all technology involving nanopowders. Making nanofluids using the two-step processes has remained a challenge because individual particles quickly agglomerate before dispersion, and nanoparticle agglomerates settle out in the liquids. Well-dispersed stable nanoparticle suspensions are produced by fully separating nanoparticle agglomerates into individual nanoparticles in a host liquid. In most nanofluids prepared by the two-step process, the agglomerates are not fully separated, so nanoparticles are dispersed only partially. Although nanoparticles are dispersed ultrasonically in liquid using a bath or tip sonicator with intermittent sonication time to control overheating of nanofluids, this two-step preparation process produces significantly poor dispersion quality. Because the dispersion quality is poor, the conductivity of the nanofluids is low. Therefore, the key to success in achieving significant enhancement in the thermal properties of nanofluids is to produce and suspend nearly monodispersed or nonagglomerated nanoparticles in liquids.

A promising technique for producing nonagglomerating nanoparticles involves condensing nanophase powders from the vapor phase directly into a flowing low-vapor pressure fluid. This approach, developed in Japan 20 years ago by Akoh et al. [14] which is called the VEROS (vacuum evaporation onto a running oil substrate) technique. VEROS has been essentially ignored by the nanocrystalline-materials community because of subsequent difficulties in separating the particles from the fluids to make dry powders or bulk materials. Based on a modification of the VEROS process developed in Germany (Wagener et al. [15]) Moreover, Eastman et al. [16] developed a direct evaporation system that overcomes the difficulties of making stable and well-dispersed nanofluids. The direct evaporation–condensation process yielded a uniform distribution of nanoparticles in a host liquid. In this much-longed-for way to making

nonagglomerating nanoparticles, they obtained copper nanofluids with excellent dispersion characteristics and intriguing properties. The thermal conductivity of ethylene glycol, the base liquid, increases by 40% at a Cu nanoparticle concentration of only 0.3 vol%. This is the highest enhancement observed for nanofluids except for those containing carbon nanotubes. However, the technology used by Eastman et al. has two main disadvantages. First, it has not been scaled up for large-scale industrial applications. Second, it is applicable only to low-vapor-pressure base liquids. Clearly, the next step is to see whether they can compete with the chemical one-step method described below. Zhu et al. [17] developed a one-step chemical method for producing stable Cu-in-ethylene glycol nanofluids by reducing copper sulfate pentahydrate ($CuSO_4 \cdot 5H_2O$) with sodium hypophosphite ($NaH_2PO_2 \cdot H_2O$) in ethylene glycol under microwave irradiation. They claim that this one-step chemical method is faster and cheaper than the one-step physical method. The thermal conductivity enhancement approaches that of Cu nanofluids prepared by a one-step physical method developed by Eastman et al. [18]. Although the two-step method works well for oxide nanoparticles, it is not as effective for metal nanoparticles such as copper. For nanofluids containing high-conductivity metals, it is clear that the single-step technique is preferable to the two-step method (Das et al. [8]).

The first-ever nanofluids with carbon nanotubes, nanotubes-in-synthetic oil (PAOs), were produced by a two-step method (Choi et al. [19]). Multiwalled carbon nanotubes (MWNTs) were produced in a CVD reactor, with xylene as the primary carbon source and ferrocene to provide the iron catalyst. MWNTs having a mean diameter of~25 nm and a length of~50μm contained an average of 30 annular layers. Chopkar et al. [13] used ball milling to produce $Al_{70}Cu_{30}$ nanoparticles and dispersed

their alloyed nanoparticles in ethylene glycol (Das et al. [8]).

2.2 Heat Sink

2.2.1 Heat Transfer Principle [20]

A heat sink transfers thermal energy from a higher temperature device to a lower temperature fluid medium. The fluid medium is frequently air, but can also be water, refrigerants or oil. If the fluid medium is water, the heat sink is frequently called a cold plate. In thermodynamics a heat sink is a heat reservoir that can absorb an arbitrary amount of heat without significantly changing temperature. Practical heat sinks for electronic devices must have a temperature higher than the surroundings to transfer heat by convection, radiation, and conduction.

To understand the principle of a heat sink, consider Fourier's law of heat conduction. Joseph Fourier was a French mathematician who made important contributions to the analytical treatment of heat conduction. Fourier's law of heat conduction, simplified to a one-dimensional form in the *x*-direction, shows that when there is a temperature gradient in a body, heat will be transferred from the higher temperature region to the lower temperature region. The rate at which heat is transferred by conduction, Q, is proportional to the product of the temperature gradient and the cross-sectional area through which heat is transferred.

$$Q = -kA\frac{dT}{dx} \tag{2.1}$$

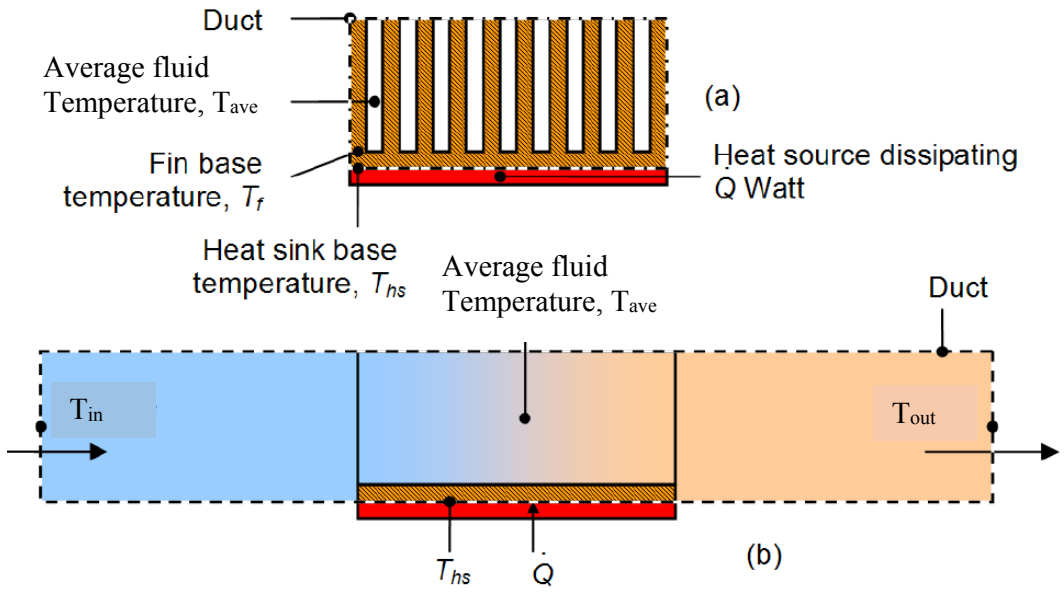

Figure 2.1 Heat transfer behavior across the heat sink [20]

Consider a heat sink in a duct, where fluid flows through the duct, as shown in Figure 2.1. It is assumed that the heat sink base is higher in temperature than the fluid. Applying the conservation of energy, for steady-state conditions, and Newton's law of cooling to the temperature nodes shown in Figure 2.1 gives the following set of equations.

$$Q = \dot{m} C_P (T_{out} - T_{in}) \tag{2.2}$$

$$Q = \frac{T_{hs} - T_{ave}}{R_{hs}} \tag{2.3}$$

where

$$T_{ave} = \frac{T_{in} + T_{out}}{2} \tag{2.4}$$

Using the mean fluid temperature is an assumption that is valid for relatively short heat sinks. When compact heat exchangers are calculated, the logarithmic mean air temperature is used. $\dot{m}$ is the mass flow rate in kg/s.

The above equations show that

- When the fluid flow through the heat sink decreases, this results in an increase in the average fluid temperature. This in turn increases the heat sink base temperature. And additionally, the thermal resistance of the heat sink will also increase. The net result is a higher heat sink base temperature.
- The inlet fluid temperature relates strongly with the heat sink base temperature. For example, if there is recirculation of fluid in a product, the inlet fluid temperature is not the surrounding temperature. The inlet fluid temperature of the heat sink is therefore higher, which also results in a higher heat sink base temperature.
- If there is no fluid flow around the heat sink, energy cannot be transferred.
- A heat sink is not a device with the "magical ability to absorb heat like a sponge and send it off to a parallel universe".

2.2.2 Thermal Resistance

For semiconductor devices used in a variety of consumer and industrial electronics, the idea of *thermal resistance* simplifies the selection of heat sinks. The heat flow between the semiconductor die and ambient air is modeled as a series of resistances to heat flow; there is a resistance from the die to the device case, from the case to the heat sink, and from the heat sink to the ambient air. The sum of these resistances is the total thermal resistance from the die to the ambient air. Thermal resistance is defined as temperature

rise per unit of power, analogous to electrical resistance, and is expressed in units of degrees Celsius per watt (°C/W). If the device dissipation in watts is known, and the total thermal resistance is calculated, the temperature rise of the die over the ambient air can be calculated.

The idea of thermal resistance of a semiconductor heat sink is an approximation. It does not take into account non-uniform distribution of heat over a device or heat sink. It only models a system in thermal equilibrium, and does not take into account the change in temperatures with time. Nor does it reflect the non-linearity of radiation and convection with respect to temperature rise. However, manufacturers tabulate typical values of thermal resistance for heat sinks and semiconductor devices, which allows selection of commercially manufactured heat sinks to be simplified.

Commercial extruded aluminium heat sinks have a thermal resistance (heat sink to ambient air) ranging from 0.4 °C/W for a large sink meant for TO3 devices, up to as high as 85 °C/W for a clip-on heat sink for a TO92 small plastic case. The popular 2N3055 power transistor in a TO3 case has an internal thermal resistance from junction to case of 1.52 °C/W. The contact between the device case and heat sink may have a thermal resistance of between 0.5 up to 1.7 °C/W, depending on the case size, and use of grease or insulating mica washer.

2.2.3 Fin Arrangements

A pin fin heat sink is a heat sink that has pins that extend from its base. The pins can be cylindrical, elliptical or square. A pin is by far one of the more common heat sink types available on the market. A second type of heat sink fin arrangement is the straight fin.

These run the entire length of the heat sink. A variation on the straight fin heat sink is a cross cut heat sink. A straight fin heat sink is cut at regular intervals.

In general, the more surface area a heat sink has, the better it works. However, this is not always true. The concept of a pin fin heat sink is to try to pack as much surface area into a given volume as possible. As well, it works well in any orientation. Kordyban has compared the performance of a pin fin and a straight fin heat sink of similar dimensions. Although the pin fin has 194 cm^2 surface area while the straight fin has 58 cm^2, the temperature difference between the heat sink base and the ambient air for the pin fin is 50 °C. For the straight fin it was 44 °C or 6 °C better than the pin fin. Pin fin heat sink performance is significantly better than straight fins when used in their intended application where the fluid flows axially along the pins rather than only tangentially across the pins.

Figure 2.2 Sample of heat sink types (pin, straight and flared fin heat sink) [20]

2.2.4 Engineering Applications

Heat dissipation is an unavoidable by-product of electronic devices and circuits. In general, the temperature of the device or component will depend on the thermal resistance from the component to the environment, and the heat dissipated by the component. To ensure that the component temperature does not overheat, a thermal engineer seeks to find an efficient heat transfer path from the device to the environment.

The heat transfer path may be from the component to a printed circuit board (PCB), to a heat sink, to air flow provided by a fan, but in all instances, eventually to the environment.

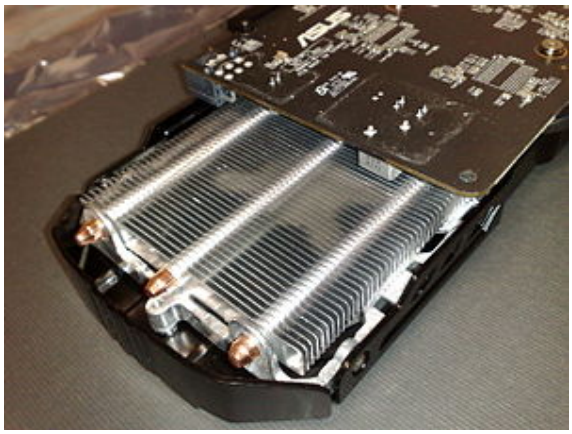

Figure 2.3 Cooling system of an Asus GTX-650 graphics card [20]

Two additional design factors also influence the thermal/mechanical performance of the thermal design:

- The method by which the heat sink is mounted on a component or processor. This will be discussed under the section attachment methods.
- For each interface between two objects in contact with each other, there will be a temperature drop across the interface. For such composite systems, the temperature drop across the interface may be appreciable. This temperature change may be attributed to what is known as the thermal contact resistance. Thermal interface materials (TIM) decrease the thermal contact resistance.

2.3 Literature Review

The concept of nanofluid-cooled heat sink is a new way to increase the cooling performance of the electronic cooling system. The published articles on deriving the heat transfer performance and flow characteristics of nanofluid flowing through heat sink with small size of flow channel (MCHS) and miniature pin fin (MPFHS) configuration are discussed as follows:

2.3.1 Experimental Approach

Some existing published articles which involve the heat transfer performance and flow feature of nanofluids flowing through MCHS and MPFHS are discussed as follows:

Jung and colleague [21] investigated the heat transfer coefficient and friction factor of nanofluid-cooled MCHS, experimentally. Al_2O_3-water nanofluids flowing through MCHS with rectangular channel under laminar flow condition were tested. The measured data indicated that the heat transfer coefficient of nanofluid was greater than that of water approximately 30% and increased with increasing particle concentration. Moreover, the pressure drop of nanofluid agrees well with that of water data.

Ho et al. [22] reported on an experiment which studied the heat transfer performance of MCHS using Al_2O_3-water nanofluid as coolant and flowing under laminar flow condition. MCHS made from copper consists of 25 parallel rectangular microchannels was used as the test section. Their data demonstrated that the heat transfer coefficient of nanofluid was significantly larger than that of base liquid. Moreover, use of nanofluid creates a small penalty in pressure drop.

Roberts and Walker [23] experimental investigation on the heat transfer performance and pressure drop characteristics of nanofluids flowing in commercial electronics cooling systems. Al_2O_3-water nanofluids were tested. The results indicated that addition of nanoparticles in the commercial cooling system can increase the heat transfer performance of MCHS.

Jasperson et al. [24] experimental investigated on the thermal performance, hydraulic performance and cost of manufacturing of micro channel and micro pin fin heat sink. Micro channels and micro pin-fin were made from copper and having same height and width (670 x 200 □m). At flow rates above 60 GPM, the results showed that pin fin heat sinks gave larger heat transfer performance than those of the micro channel heat sinks. However, at low flow rate, vice versa trend were observed.

Escher and colleges [25] presented the experimental investigation on the heat transfer characteristic and flow behavior of SiO_2-water nanofluids flow in three different channel widths MCHS in laminar flow regime. Particle volume fraction of 5, 16 and 31 vol.% and channel width of 50, 100 and 200 mm were used. The measured data were used to compare with the data for one-dimensional model. Their results illustrated that the thermal conductivity had small effect on the MCHS performance. Furthermore, they also suggested that the heat capacity and density of fluid had significant effect on the heat transfer enhancement of MCHS.

Fazeli et al. [26] experimentally and numerically investigated the heat transfer performance of a miniature heat sink using SiO_2-water nanofluids at particle fraction of 3.5, 4.0, 4.5 and 5.0 vol.% as a coolant. Experimental data described that using of

nanofluid instead of water significantly augmented the heat transfer coefficient and decrease in the thermal resistance around 10%.

Kalteh and co-workers [27] reported the heat transfer performance of Al_2O_3-water nanofluid flowing through a wide MCHS with dimensions of 94.3x28.1x0.58 mm (LxWxH) under laminar flow condition, both experimentally and numerically. Particle mass fractions used in their study were 0.1 and 0.2 wt.%. The measured data illustrated that the heat transfer coefficient of nanofluids was 22% higher than the common base fluid for particle fraction of 0.2 wt.% and decreased with increasing particle size. Moreover, they recommended that to simulate the heat transfer performance of nanofluid-cooled MCHS, the two-phase model was more suitable than the homogeneous model.

Selvakumar and Suresh [28] presented an experimental investigation on the heat transfer performance and pumping power of the CuO-water nanofluid flowing through MCHS with cross-sectional of 0.3x2 mm (WxH) under turbulent flow regime. The results indicated that the Nusselt number and pumping power of nanofluids were about 30% and 15.11% larger than the common base fluid for the fraction of 0.2 vol.%, respectively.

Nitiapiruk et al. [29] investigated on the cooling performance and pressure drop characteristic of nanofluid-cooled MCHS, experimentally. Particle fraction used in their study were 0.5, 1.0 and 2.0 vol.% and flow through 0.5x0.8 mm (WxH) MCHS under laminar flow regime. Effect of thermophysical models on the thermal performance was also presented. Similar to the other researchers, the results showed that the use of

nanofluids as coolant gave higher heat transfer potential than the pure water about 1.24 times for particle fration of 2.0 vol.%. Their also claimed that the archaic model proposed by Maxwell in (1892) for thermal conductivity can be used to predict the Nusselt number of nanofluid-cooled MCHS and gave very good agreement compared with the other models.

Deshmukh and Warkhedkar (30) studied the air side thermal performance of fully shrouded elliptical pin fin heat sink under combined natural and forced convection, experimentally. A theoretical model was used to predict the effect of various configuration (inline and staggered layout), heat transfer and flow parameters on the thermal resistance of the heat sink. The results indicated that as the fin bundle void fraction increased with increasing the fin spacing in longitudinal and transverse directions which resulted increases in the heat transfer coefficient. Moreover, generalized heat transfer correlations were proposed for elliptical pin fin heat sink.

2.3.1 Numerical Approach

Similar to the experimental investigation, many researchers devoted to study the heat transfer behaviour and pressure drop (or pumping power) of nanofluids flow through MCHS and MPFHS. There are few articles taking the nanofluid into account as the multiphase feature. Some detailed reviews mentioned above are shown as follows:

Lee and Choi [31] presented the thermal performance of MCHS using NF_2 and NF_3 nanofluid as coolant compared with pure water and liquid nitrogen, theoretically. Their data illustrated that thermal resistances of nanofluid were lower than those of pure water

and liquid nitrogen, respectively. In contrast, cooling rate and power density of nanofluid were much larger than those for common base liquids.

Chein and Huang [32] introduced a mathematical model to predict the heat transfer coefficient and pumping power of nanofluid-cooled MCHSs. In this study, Cu nanoparticles dispersed in water with different concentrations were used as coolant. Similarly, two specific geometries of MCHSs were tested. The simulation data indicated that nanofluids gave significantly higher heat transfer performance than the base liquid and the pressure drop concided well with that of the base liquid.

Koo and Kleinstreuer [33] studied the heat transfer and flow characteristics of nanofluid-cooled MCHS, numerically. In this study, CuO nanoparticles dispersed in water and ethylene glycol were used as coolant. Their results demonstrated that heat transfer performance of ethylene glycol was larger than that of pure water. They also recommended that high thermal conductivity nanoparticle and MCHS with high aspect ratio of channel should be used.

Jang and Choi [34] presented a numerical study on the cooling performance of a MCHS using Cu-water and diamond-water nanofluids as coolant. The results showed that the diamond–water nanofluid with particle concentration of 1.0 vol.% gave higher heat transfer performance than of the base fluid approximately 10%. Moreover, the results indicated that use of nanofluids can reduce both the thermal resistance and temperature difference between the heated surface of MCHS and the working fluid. They also demonstrated that improving the thermal performance of MCHS using nanofluids as

coolant is to be the next generation cooling system for cooling the ultra-high heat flux devices.

Abbassi and Aghanajafi [35] studied the thermal behavior of MCHS using nanofluid as coolant, numerically. In this study, Cu-water was used as working fluid. The thermal dispersion model and thermal dispersion coefficient was considered for heat transfer analysis. The simulation data illustrated that the use of nanofluid resulted in a pronounced in the heat transfer performance compared with base fluid.

Chein and Chuang [36] presented the thermal performance of nanofluid-cooled MCHS and using CuO-water nanofluids as coolants. Particle concentrations of 0.2 and 0.4 vol.% were tested. At a low flow rate, the results showed that the energy absorption of nanofluids were greater than those of pure water. On the contrary, there is no contribution from heat absorption when the flow rate is high.

Tsai and Chein [37] studied the thermal performance of nanofluid-cooled MCHS, analytically. In their study, Cu-water and CNT-water nanofluids were used as the working fluid and the porous medium model was considered. Their simulation data showed that the temperature difference between MCHS surface and fluid temperature of nanofluids were smaller than those of pure water which lead to larger thermal performance.

Ghazvini and Shokouhmand [38] studied the thermal performance of a MCHS using CuO-water nanofluid as coolant, both analytically and numerically. The fin model and the porous media approach were considered in their work. It was found that the use of

nanofluids gave greater overall heat transfer coefficient than that of pure water and increased with increasing Reynolds number. Moreover, the porous media approach gave higher heat transfer coefficient ratio than the fin model.

Ebrahimi et al. [39] studied numerically the cooling performance of a nanofluid-cooled MCHS using CNTs-water nanofluid as coolant. Their data illustrated the thermal conductivity of nanofluid increase with increasing nano-layer thickness which leads to decrease in temperature gradient in MCHS.

Mohammed et al. [40] presented the heat transfer and flow characteristics of different nanofluids flow in a square shaped MCHS, numerically. The effects of particles type and Reynolds number were reported. Al_2O_3, SiO_2, Ag and TiO_2 dispersed in water were used as working fluids. The simulation results showed that nanofluids gave higher heat transfer performance than that of water and there was a small increase in pressure drop.

Shokouhmand at al. [41] simulated the heat transfer performance of the MCHS working with nanofluids in laminar and turbulent flow regime using an artificial neural network (ANN) technique. Silicon MCHS with rectangular flow channel (Cros. Sec. 100x30 μm) and Cu-water nanofluids were tested. The results showed that nanofluids can be augment the performance of MCHS without increased in the pressure drop and optimized geometry was obtained for every particle volume fraction.

Mohammed and co-worker [42] studied the heat transfer and flow characteristics of Al_2O_3-water nanofluids flowing through a rectangular shaped MCHS with cross-sectional area of 180x430 mm in laminar flow condition. Particle concentration ranged

between 1 and 5 vol.% were investigated. The simulation results illustrated that the heat transfer performance and wall shear stress increased with increasing particle fraction and no penalty drop in pressure. Moreover, the data also indicated that at particle concentration of 5 vol.%, the heat transfer coefficient of nanofluids was quite same for the data of pure water. This means that no enhancement in the high particle fraction.

Ijam and Saidur [43, 44] presented a numerical study on the heat transfer and flow characteristics of minichannel heat sink working with TiO_2-water, Al_2O_3-water and SiC-water nanofluids at particle fraction of 0.8, 1.6, 2.4, 3.2 and 4.0 vol.%. The simulation data showed that using of nanofluids as coolant provided higher heat transfer enhancement that those of the pure water up to 17%. Similarly, the pumping power of nanofluids was quite the same at a given condition.

Hung et al. [45] presented the thermal performance and pumping power of a 3-D MCHS working with Al_2O_3-water and diamond-water nanofluid, numerically. Their results demonstrated that when the particle fraction was increased, the thermal resistance of the system was first decreased and will be increased later. MCHS with smaller size of nanoparticle yield lower thermal resistance as well as pumping power. Finally, the heat transfer performance of Al_2O_3-water and diamond-water nanofluid was larger than the pure water approximately 21.6%.

Manay et al. [46] reported the heat transfer performance and pressure drop of Al_2O_3-water and CuO-water nanofluids flow in MCHS with a square channel (0.4x0.4 mm) under laminar flow condition using the finite volume method combined with the mixture model. Particle concentration of 0.5, 1.0 and 2.0 vol.% were investigated. Their

data illustrated that highest heat transfer performance was took place at particle fraction of 2.0 vol.% and Reynolds number of 100 for CuO-water nanfofluids which was about 3.21 times larger than the water.

Tokil and co-worker [47] presented the thermal performance of a interrupted microchannel heat sink (IMCHS) by using Al_2O_3-water, CuO-water and SiO_2-water nanofluids for particle fraction ranging between 1 to 4% as coolants, numerically. The results illustrated that the Nusselt number of IMCHS was higher than the common MCHS with a small rise in drop of pressure. Also, the SiO_2-water gave greater heat transfer performance than the Al_2O_3-water, CuO-water nanofluids, respectivey.

Hashemi et al. [48] determined the thermal performance of nanofluid-cooled miniature heat sink, numerically. Plate fin type heat sink and SiO_2-water nanofluids with particle concentration of 3.5, 4.0, 4.5 and 5.0 vol.% were tested under laminar flow regime. Similar to the other researchers, they identified that the use of nanofluid-cooled heat sink creates higher heat transfer performance than that of the case of water-cooled heat sink and increases with increasing particle concentration.

Tabrizi and Seyf [49] presented the entropy generation and convective heat transfer behavior of Al_2O_3-water nanofluids flowing through tangential MCHS in laminar flow regime, numerically. The results indicated that use of nanofluids can enhance the heat transfer performance of MCHS and increased with increasing particle fraction. On the contrary, the heat transfer coefficient decreased with increasing particle size. For the case of entropy generation, the results showed that the total entropy generation decreased with increasing particle fraction and decreasing particle size.

Effect of Brownian motion and particle size effect on the thermal performance of nanofluid-cooled MCHS was numerically explored by Seyl and Nikaaein [50]. Al_2O_3, ZnO and CuO nanoparticles dispersed in 60:40 (by mass) EG-water were used as coolant. The results indicated that Brownian motion had significant effect on the thermal conductivity enhancement of nanofluids and use of nanofluid can increase the heat transfer performance of MCHS. Moreover, Al_2O_3 dispersed in common base liquid have lower thermal resistance than the ZnO and CuO, respectively.

Seyl and Feizbakhshi [51] reported the heat transfer performance and pressure drop of CuO-water and Al_2O_3-water nanofluids working with micro-pin-fin MCHS, numerically. Their measured showed that the Nusselt number of CuO-water nanofluids was tiny larger than the Al_2O_3-water nanofluids and increased with increasing Reynolds number as well as particle fractions. Finally, they concluded that the Nusselt number of CuO-water nanofluids decreased with decreasing particle size while increased for Al_2O_3-water nanofluids.

Shafeie et al. [52] investigated on the convective heat transfer of heat sinks with micro pin-fin structure under laminar flow regime. A water cooled heat sink on a 1x1 cm substrate was studied. In their study, MCHSs and PFHSs with different patterns (oblique and staggered) were used. At the same pumping power, their data illustrated that the heat removal of the PFHSs was lower than the MCHSs at medium and high pumping power. However, at small pumping power, the reverse behaviors were obtained.

John and co-workers [53] presented numerical investigation on the thermal and hydraulic performance of water flows through micro pin fin heat sink with square and circle shaped. The results indicated that at Re less than 300, the heat transfer performance of circular pin fin was higher than that of the square pin fin. However, vice versa was observed at Re above 300.

As mentioned above, there are a lot of published papers revealed the use of naofluids as coolant for dissipating heat load from the various types of microchannel (MCHS) and pin-fin heat sinks (MPFHS). These attempts are done to discover the best suitable way for enhancing the heat transfer performance of high power density electronic devices, both experimentally and simulation. Heat transfer potential of MCHS and MPFHS working with nanofluids have been addressed by a number of researchers. However, experimentally research articles on the heat transfer performance and pressure drop characteristic of MCHS and MPFHS are quite small compared with the numerically investigation. Thus, the authors would like to present the alternate way to study the heat transfer and pressure drop characteristics of nanofluid-cooled heat sink which having small flow channel and small pin fin simultaneously. Heat sinks used in the present study are miniature circular pin fin (MCFHS) and square pin fin heat sink (MSFHS). They are made from aluminum material with dimension about 28 x 33 mm. Similarly, SiO_2-water and ZnO-water nanofluids with particle concentrations of 0.2, 0.4 and 0.6 vol.% are used as coolant. This study is a series works of the authors which try to find the heat transfer performance and flow characteristic of different nanofluids flowing through heat sink with different configurations.

CHAPTER 3 SAMPLE PREPARATION, EXPERIMENTAL APPARATUS AND PROCEDURE

This chapter presents the method to prepare the nanofluid solution, experimental system and experimental procedure, respectively. For the experimental system, the apparatus are conducted for measuring the convective heat transfer and pressure drop of nanofluids flow through MCFHS and MSFHS. The details are described in the following sections.

3.1 Sample Preparation

Nanofluid preparation is of crucial importance when using the nanofluid as a working fluid. The term "nanofluid" does not mean a simple mixture between solid particles and base fluid. In order to prepare nanofluids by dispersing the nanoparticles in a base fluid, proper mixing, and stabilization of the particles is required. Normally, there are three effective methods used to attain stability of suspension against sedimentation of the nanoparticles which are outlined as follows: 1) control the ph value of the suspensions, 2) add surface activators or surfactants, 3) use ultrasonic vibration. All of these techniques aim to change the surface properties of suspended nanoparticles and suppress the formation of clustering particles in order to obtain stable suspensions. In this study, two different nanoparticles are used as working fluid. Firstly, SiO_2 nanoparticles with mean diameters of 15 nm. Secondly, ZnO nanoparticles with mean diameters of 20 nm. Particle volume fractions used in this study are 0.2, 0.4 and 0.6 vol.%. Foe preparation of nanofluids, small amount of CTAB (0.01%) was first mixed with water to ensure better stability and proper dispersion of nanofluid. Nanofluid with

various concentrations were then prepared by dispersing a specific amount of the nanoparticles in the deionized water (DI water) base fluid. Moreover, an ultrasonic vibrator was used to sonicate the solution continuously for about two hours in order to break down agglomeration of the nanoparticles. The thermophysical properties of nanoparticle were expressed in the following table.

Table 3.1 Thermophysical properties of nanoparticle used in the present study

Properties	SiO_2 nanoparticle	ZnO nanoparticle
Density (kg/m^3)	2,648	5,600
Specific heat (kJ/kg ^oC)	0.742	0.514
Thermal conductivity ($W/m^{2o}C$)	1.37	13
Mean diameter, d (nm)	15	20

3.2 Convective Heat Transfer and Pressure Drop Measurement

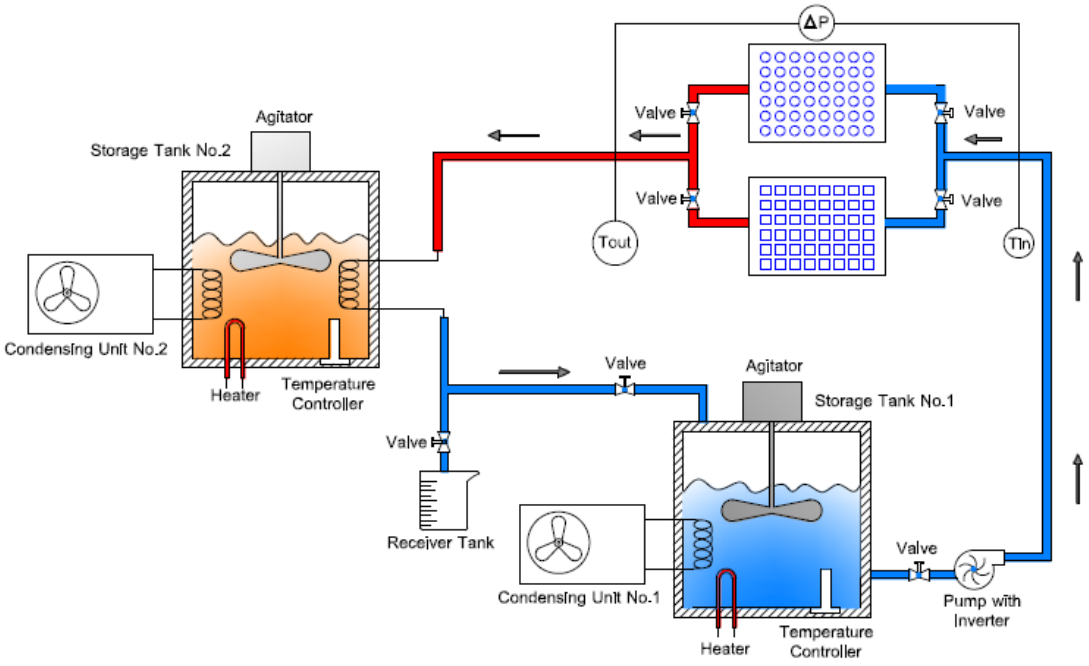

Figure 3.1 Schematic diagram of the experimental apparatus

In the present study, experimental approach is used to investigate the heat transfer performance and flow characteristics of nanofluids flow in heat sink with miniature circular pin fin (MCFHS) and square pin fin (MSFHS) structure. The experimental system is shown schematically in Figure 3.1. It mainly consists of two test sections, two storage tanks with temperature controller, a pump with inverter and a receiver tank. MCFHS and MSFHS configurations are shown in Figure 3.2. They are made from aluminum material with sized of 28x30 mm. In order to study the effect of pin fin configuration on the thermal performance and flow characteristic of nanofluid-cooled heat sinks, same hydraulic diameter of both heat sink are performed. A 80 W electric heater is attached at the bottom of the MCFHS and MSFHS to supply heat load. Two storage tanks with 15 L capacity are made from stainless steel. The storage tank No.1 with a 3.5 kW cooling coil, 2 kW electric heaters and a thermostat is used to adjust the nanofluid temperature. Similarly, the storage tank No. 2 with a 3.5 kW cooling coil and a thermostat is used to reduce the nanofluid temperature leaving from the test section to the same value of tank No.1 in order to meet steady state condition. A pump with inverter is used to adjust the nanofluids flow rate. T-type thermocouples and a differential pressure transmitter are installed at both ends of the test section to measure the bulk temperature and pressure drop of the nanofluid, respectively. Similarly, 2 thermocouples are inserted at two different positions on the surface of test section for measuring the temperature gradient in order to calculate the surface temperature of the test section. The receiver tank is used to measure the nanofluid flow rate by the time taken for a given volume of nanofluid to be discharged. Calibrations of all instruments used in this study are performed for estimating the accuracy of the measured data.

All of the T-type thermocouples were calibrated with a standard thermometer which has a maximum precision of 0.05 ^{o}C. The differential pressure transmitter was calibrated using an air operated dead weight tester. The uncertainty of the pressure measurement is ± 0.050 kPa. Moreover, the nanofluid flow rates were determined by electronic balance. The uncertainty of the electronic balance is ± 0.0006 kg. Therefore, the uncertainty of the heat transfer coefficient is around 5%. After steady state reached, wall temperatures, inlet and exit temperatures of the nanofluids, mass flow rates of the nanofluids, and pressure drop across the test section are recorded.

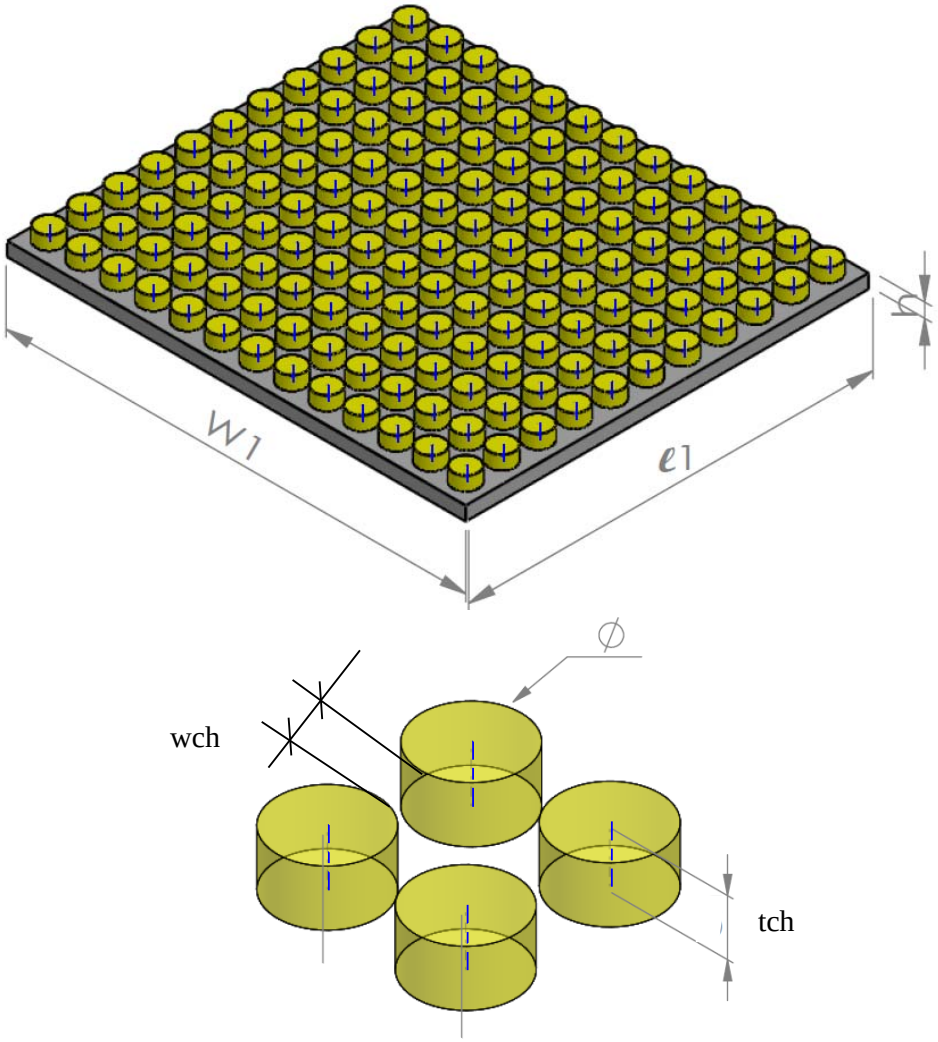

a) MCFHS

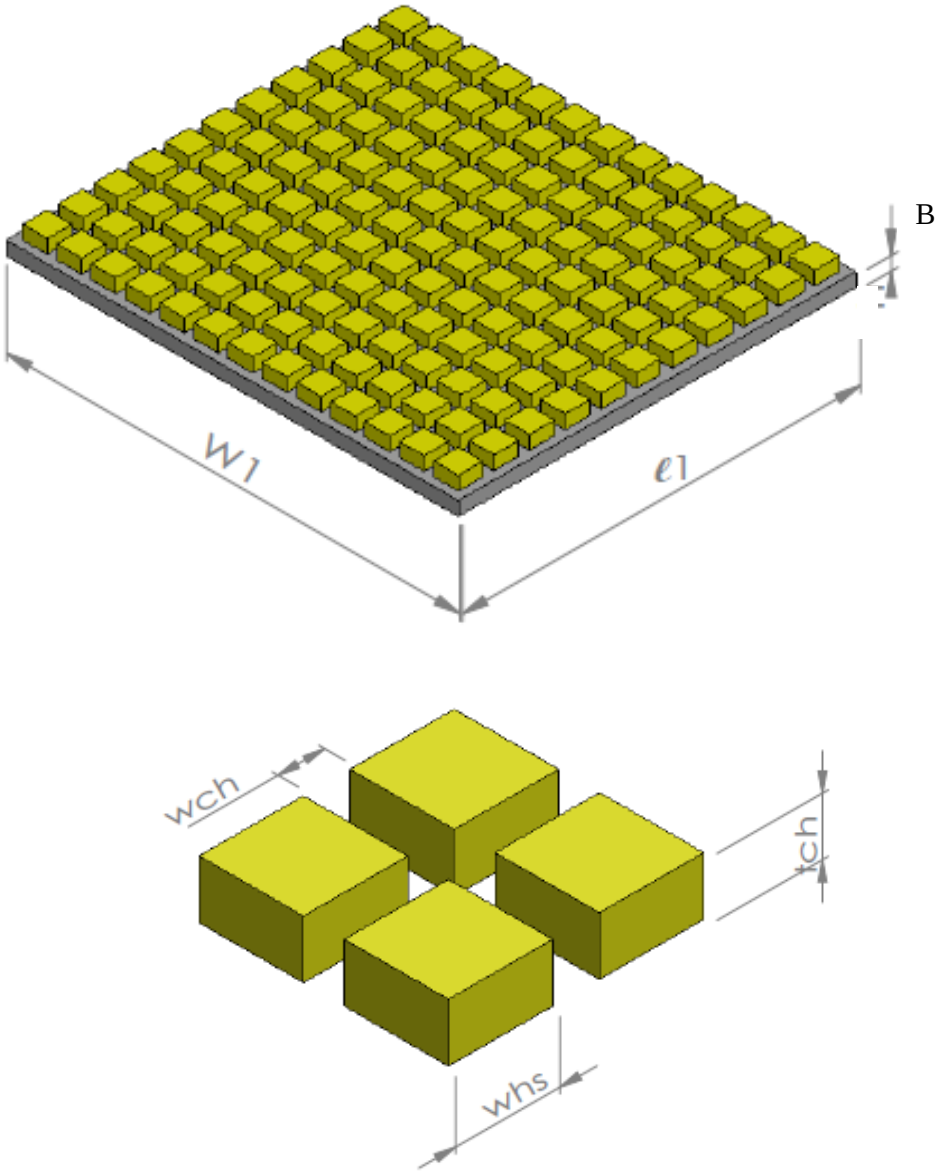

b) MSFHS

Figure 3.2 Configuration of the pin fin heat sinks used in the present study

Table 3.2 Dimension of heat sink used in the present work

Dimension	MCFHS	MSFHS
Heat sink width, $\ell 1$ (mm)	28.15	28.15
Heat sink length, W1 (mm)	33.05	33.05
Base thickness, B (mm)	1	1
Channel width, Wch (mm)	1.2	1.2
Fin width, Whs (mm)	-	1.2 x 1.2
Fin or channel height, tch (mm)	1.2	1.2
Fin diameter, ∅ (mm)	1.25	-
Hydraulic diameter of flow channel, D_H (mm)	1.2	1.2
Heat transfer surface area, As (mm2)	1,430	1,565
Number of pin fin, n	143	143

3.3 Experimental Procedure

Experiments were conducted with various mass flow rates of coolant and heat loads whereas the temperature of nanofluid was kept constant at desired values. The coolant flow rate (water and nanofluids) was adjusted using an inverter for controlling the speed of pump. The nanofluid temperature at the inlet of the test section was kept constant at a required value using the cooling coil controlled via temperature controller. Similarly, the heat load supplied to the test sections can be varied by adjusting the power of heater. During the test run, the system was allowed to approach the steady state before any data was recorded. After stabilization, inlet and exit temperatures of the nanofluids, wall temperatures, flow rates of nanofluid and pressure drop across the test section block were recorded. The test runs were done at inlet temperatures of nanofluid at 15^{o}C. The mass flow rate ranged between 0.66 and 3.3 kg/min. The heat loads of the test section were ranging between 30 and 70 W.

CHAPTER 4 DATA REDUCTION

The objective of this chapter is to explore the data reduction of the measured data. The data reduction to provide the heat transfer coefficient, Nusselt number, Reynolds number and pumping power of nanofluids flow in MCFHS and MSFHS which is concluded as follows:

4.1 Heat Transfer Performance and Pumping Power Calculation

The heat transfer performance and pumping power of nanofluids flowing through MCFHS and MSFHS can be calculated from the following equation.

The heat transfer rate into the nanofluid is calculated from:

$$Q_{nf} = \dot{m}_{nf} Cp_{nf} (T_{out} - T_{in})_{nf} \tag{4.1}$$

where Q_{nf} is the heat transfer rate of the nanofluid, Cp_{nf} is the specific heat of the nanofluid, T_{out} and T_{in} are the nanofluid temperature at outlet and inlet of the test section, respectively and $\dot{m}_{nf}$ is the mass flow rate of the nanofluid.

The heat load of the test section is defined as follows:

$$Q_{TS} = VI \tag{4.2}$$

where Q_{TS} is the heat load of the test section, V is the electric voltage and I is the electric current supplied to the heater.

In this study, the energy differences between nanofluid and heat load of the test section are approximately 10%.

The experimental heat transfer coefficient and Nusselt number of the nanofluid are computed from the following equation.

$$h_{nf} = \frac{Q_{nf}}{(T_{wall} - T_{nf})} \tag{4.3}$$

$$Nu_{nf} = \frac{h_{nf} D_H}{k_{nf}} \tag{4.4}$$

where h_{nf} is the heat transfer coefficient of the nanofluid, T_{wall} is the average temperature of the wall, T_{nf} is the bulk temperature of the nanofluid, Nu_{nf} is the Nusselt number of the nanofluid, D_H is the hydraulic diameter of the test section based on each of the flow channel width and k_{nf} is the thermal conductivity of the nanofluid.

The Reynolds number based on each of the flow channel width of the test sections is expressed as:

$$\mathrm{Re}_{nf} = \frac{\rho_{nf} u_{ch} D_H}{\mu_{nf}} \tag{4.5}$$

$$D_H = \frac{4A_{ch}}{p_{ch}} \tag{4.6}$$

where u_{ch} is the flow velocity based on each of the flow channel width, A_{ch} is the cross-sectional area of each of the flow channel width and p_{ch} is the periemter of each of the flow channel width.

Similarly to the heat transfer performance, the pumping power across the test sections is calculated from:

$$Pow = \dot{V}\Delta P \tag{4.7}$$

where Pow is the pumping power across the test sections block, ΔP is the measured pressure drop across the test section block, and $\dot{V}$ is the volume flow rate of the working fluid.

4.2 Thermophysical Properties of Nanofluid

The density and specific heat of the nanofluids presented in the above equation are calculated by use of the Pak and Cho [54] correlations, which are defined as follows:

$$\rho_{nf} = \phi\rho_p + (1-\phi)\rho_w \tag{4.8}$$

and

$$Cp_{nf} = \phi Cp_p + (1-\phi)Cp_w \tag{4.9}$$

where Cp_{nf} is the specific heat of the nanofluid, Cp_p is the specific heat of the nanoparticles and Cp_w is the specific heat of the base fluid.

For the measured thermal conductivity of nanofluids, the following equations can be used to calculate the thermal conductivity of nanofluids, which are defined as follows.

One well-known formula for calculating the thermal conductivity of nanofluid is the Hamilton and Crosser [55] model (H-C model), which is expressed in the following form:

$$k_{nf} = \left[\frac{k_p + (n-1)k_w - (n-1)\phi(k_w - k_p)}{k_p + (n-1)k_w + \phi(k_w - k_p)} \right] k_w \tag{4.10}$$

$$n = 3/\psi \tag{4.11}$$

in which n is the empirical shape factor and ψ is the sphericity, defined as the ratio of the surface area of a sphere (with the same volume as the given particle) to the surface area of the particle. The sphericity is 1 and 0.5 for the spherical and cylindrical shapes, respectively. Moreover, k_{nf} is the thermal conductivity of the nanofluid, k_p is the thermal conductivity of the nanoparticles and k_w is the thermal conductivity of the base fluid.

Murshed et al. [56] introduced the Bruggeman model to predict the thermal conductivity of nanofluids, which is defined as follows:

$$k_{nf} = \frac{1}{4}\left[(3\phi - 1)k_p + (2 - 3\phi)k_w\right] + \frac{k_w}{4}\sqrt{\Delta} \tag{4.12}$$

$$\Delta = \left[(3\phi - 1)^2 (k_p / k_w)^2 + (2 - 3\phi)^2 + 2\left(2 + 9\phi - 9\phi^2\right)(k_p / k_w)\right] \tag{4.13}$$

Wasp [57] proposed a model for calculating the thermal conductivity of nanofluids, which is expressed as follows:

$$k_{nf} = \left[\frac{k_p + 2k_w - 2\phi(k_w - k_p)}{k_p + 2k_w + \phi(k_w - k_p)} \right] k_w \tag{4.14}$$

For spherical particles, the results given by the Wasp model concur with those of the H-C model.

An alternative formula for calculating thermal conductivity was introduced by Yu and Choi [58], which is expressed in the following form:

$$k_{nf} = \left[\frac{k_p + 2k_w + 2(k_p - k_w)(1+\beta)^3 \phi}{k_p + 2k_w - (k_p - k_w)(1+\beta)^3 \phi} \right] k_w \tag{4.15}$$

where β is the ratio of the nano-layer thickness to the original particle radius. Normally β=0.1 is used to calculate the thermal conductivity of nanofluid.

Timofeeva et al. [59] suggested the effective medium theory to calculate thermal conductivity of nanofluids, which is expressed as follows:

$$k_{nf} = [1 + 3\phi] k_w \tag{4.16}$$

Similar to the thermal conductivity, the viscosities of nanofluids can be calculated from the existing well-known models, as follows:

Batchelor [60] introduced a correlation to predict the viscosity of nanofluids with spherical shape nanoparticles which is defined as:

$$\mu_{nf} = \left(1 + 2.5\phi + 6.2\phi^2\right)\mu_w \tag{4.17}$$

Drew and Passman [61] suggested the well-known Einstein equation for calculating viscosity, which is applicable to spherical particles in volume fractions less than 5.0 vol.% and is defined as follows:

$$\mu_{nf} = (1 + 2.5\phi)\mu_w \tag{4.18}$$

Brinkman [62] has modified the Einstein equation to a more generalised form which is expressed as follows:

$$\mu_{nf} = \frac{1}{(1-\phi)^{2.5}}\mu_w \tag{4.19}$$

Furthermore, Wang et al. [63] proposed a model for calculating the viscosity of nanofluids which is defined as:

$$\mu_{nf} = \left(1 + 7.3\phi + 123\phi^2\right)\mu_w \tag{4.20}$$

where ϕ is the volume concentration, μ_{nf} is the viscosity of the nanofluid and μ_w is the viscosity of the base fluid.

Furthermore, Duangthongsuk and wongwises [64] presented the thermal conductivity and viscosity correlation to predict the thermal conductivity and viscosity of nanofluid with temperature dependent. The correlations were expressed as follows:

For thermal conductivity

$$\frac{k_{nf}}{k_w} = a + b\phi \tag{4.21}$$

where a and b are constant values which are described as follows:

Temperature (ºC)	**a**	**b**
15	1.0225	0.0272
25	1.0204	0.0249
35	1.0139	0.0250

For viscosity

$$\frac{\mu_{nf}}{\mu_w} = \left(a + b\phi + c\phi^2\right) \tag{4.22}$$

where a, b and c are constant values as follows:

Temperature (ºC)	**a**	**b**	**c**
15	1.0226	0.0477	-0.0112
25	1.013	0.092	-0.015
35	1.018	0.112	-0.0177

The properties of the nanofluid shown in the above equations are evaluated from water and nanoparticles at average bulk temperature.

CHAPTER 5 RESULTS AND DISCUSSION

The objective of this chapter is to present the results and discussion of the heat transfer performance and pumping power of the SiO_2-water and ZnO-water nanofluids flowing through MCFHS and MSFHS. The results of the present study were expressed as follows:

5.1 Data for SiO_2-Water Nanofluids

5.1.1 For Miniature Circular Fin Heat Sink (MCFHS)

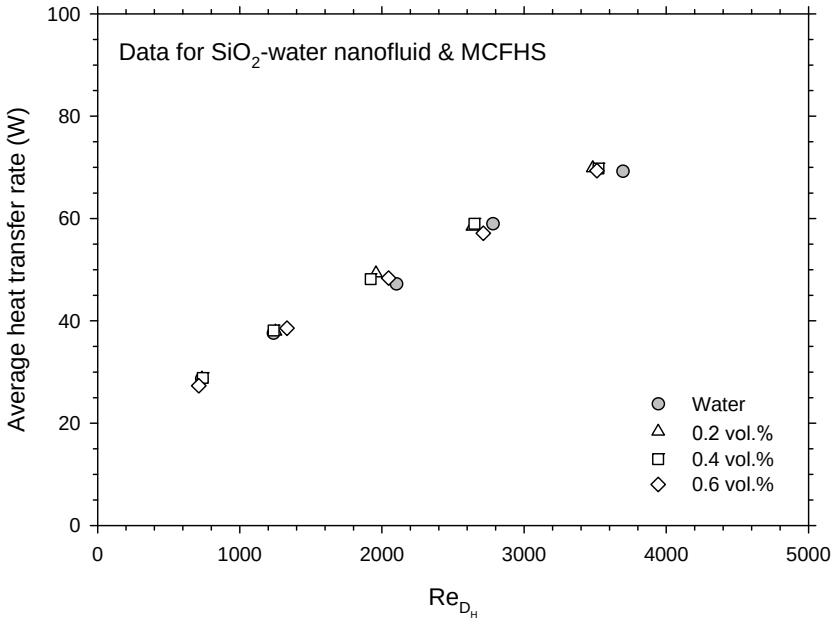

Figure 5.1 Variation of the average heat transfer rate as a function of Reynolds number and particle volume concentration (data for MCFHS)

The average heat transfer rates used in the present study are shown in Figure 5.1. It can be clearly seen that the heat transfer rate of nanofluids are rather higher than that of the

pure water under the same mass flow rate. This is an advantage of using of nanofluid to replace the conventional heat transfer fluids.

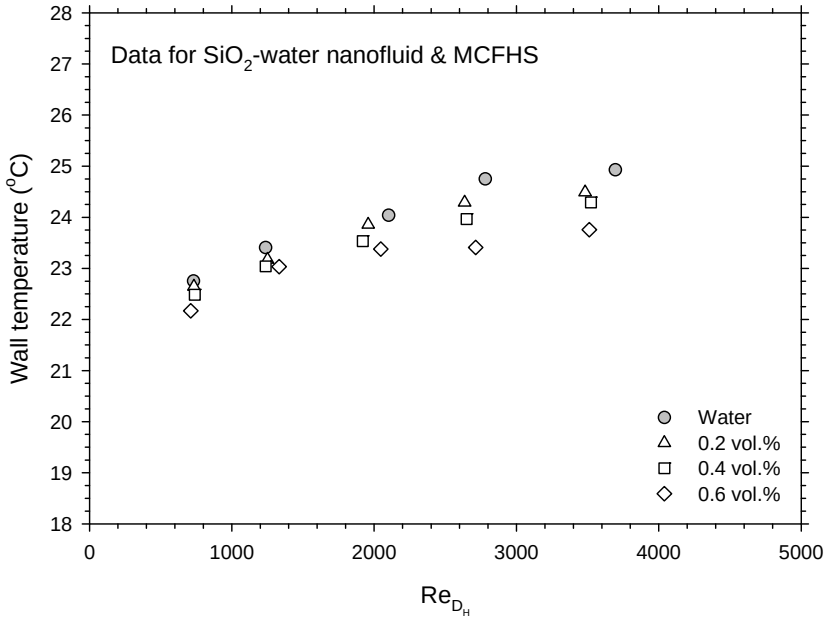

Figure 5.2 Comparison of the wall temperature between the pure water and nanofluids (data for MCFHS)

As shown in Figure 5.2, the wall temperature of test section increases with increasing wall heat flux (see Figure 5.1). From this figure, the important thing is the use of nanofluids lead to decrease in the wall temperature. This is due to the addition of nanoparticles in the base fluid enhances the heat transfer process, which leads to an decrease in the wall temperature. Thus, higher thermal performance of nanofluid-cooled heat sink is obtained to compare with the water-cooled heat sink.

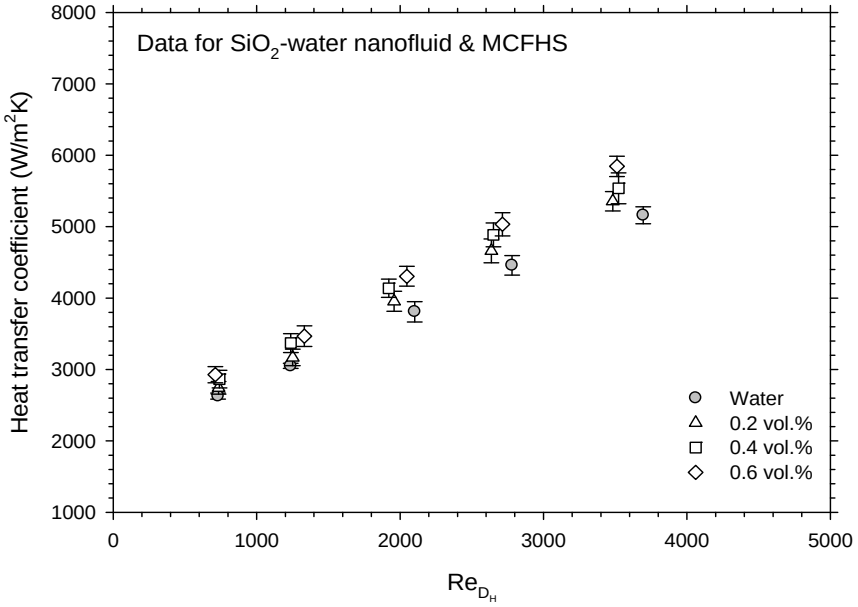

a) Heat transfer coefficient

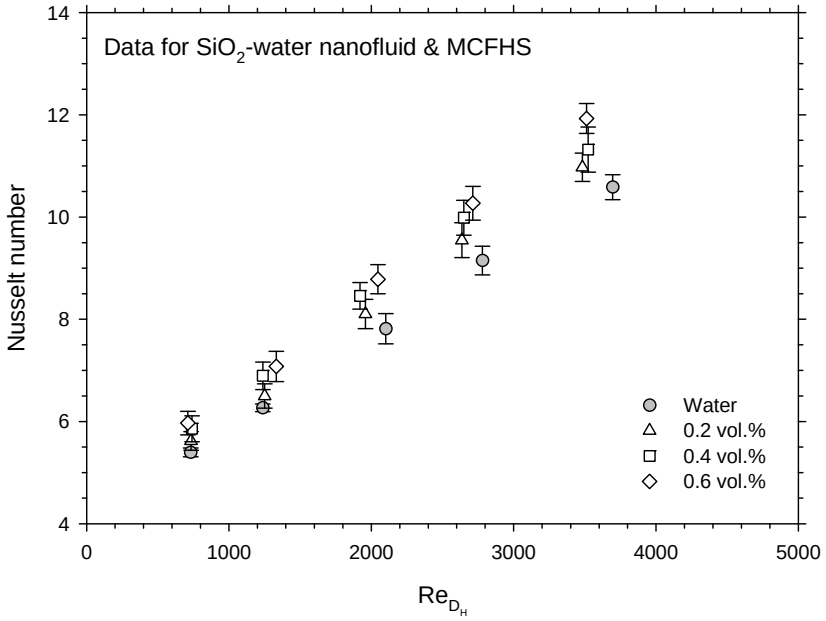

b) Nusselt number

Figure 5.3 Heat transfer coefficient and Nusselt number for water and SiO_2-water nanofluids versus Reynolds number at various volume concentration (data for MCFHS)

As shown in Figure 5.3a-b, the heat transfer coefficient and the Nusselt number of the nanofluids are higher than those of the base liquid, and they increase with increasing the Reynolds number as well as the particle volume concentration. The possible reason for this enhancement may be associated with the following: 1) the nanofluid with suspended nanoparticles increases the thermal conductivity of the mixture and 2) a large energy exchange process resulting from the chaotic movement of nanoparticles.

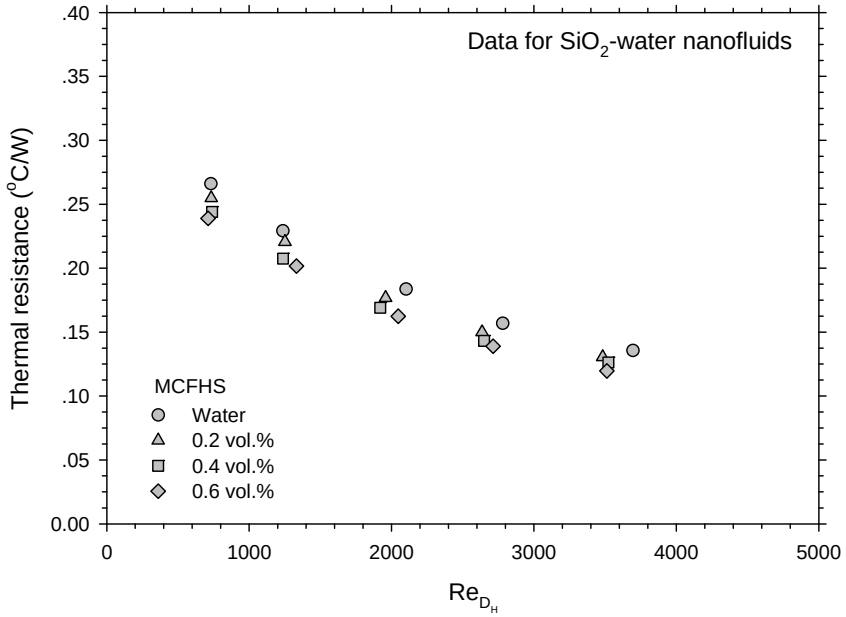

Figure 5.4 Variation of the thermal resistance as a function of Reynolds number and particle concentrations (data for MCFHS)

Figure 5.4 shows the thermal resistance of SiO_2-water nanofluids flowing through a MCHFS as a function of particle volume concentration and Reynolds number. The measured data indicated that nanofluid-cooled heat sink gave lower thermal resistance than that of the water-cooled heat sink and decreased with increasing particle concentrations. This reduction due to the decrease of the bulk thermal resistance as well as the convective thermal resistance.

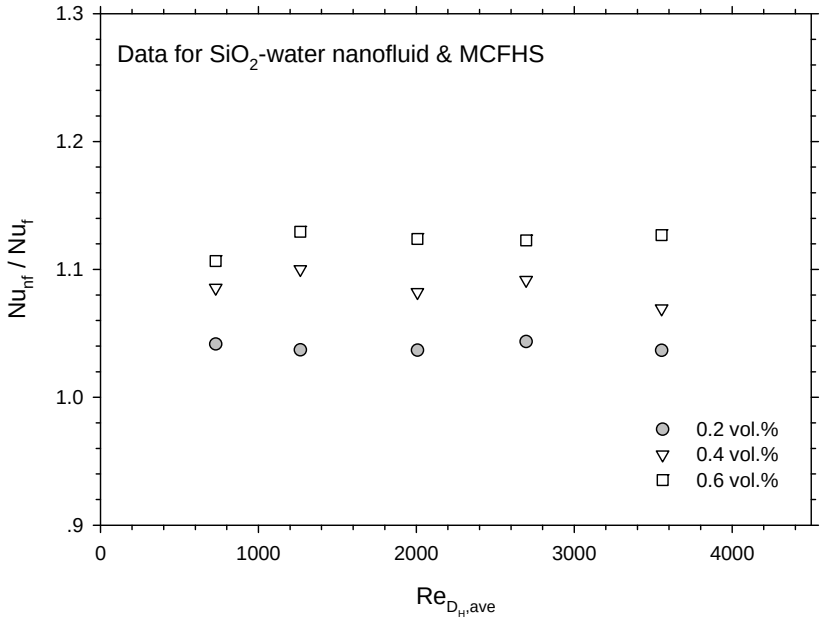

Figure 5.5 Nusselt number ratio as a function of particle concentration for the data of SiO_2-water nanofluids flow in MCFHS

Figure 5.5 shows the Nusslet number ratio as a function of particle volume concentration and Reynolds number. It can be clearly seen that the use of SiO_2 nanoparticles dispersed in base liquid gave greater Nusselt number than the base fluid, about 4 to 13 % for the volume concentration range between 0.2 and 0.6 vol.%.

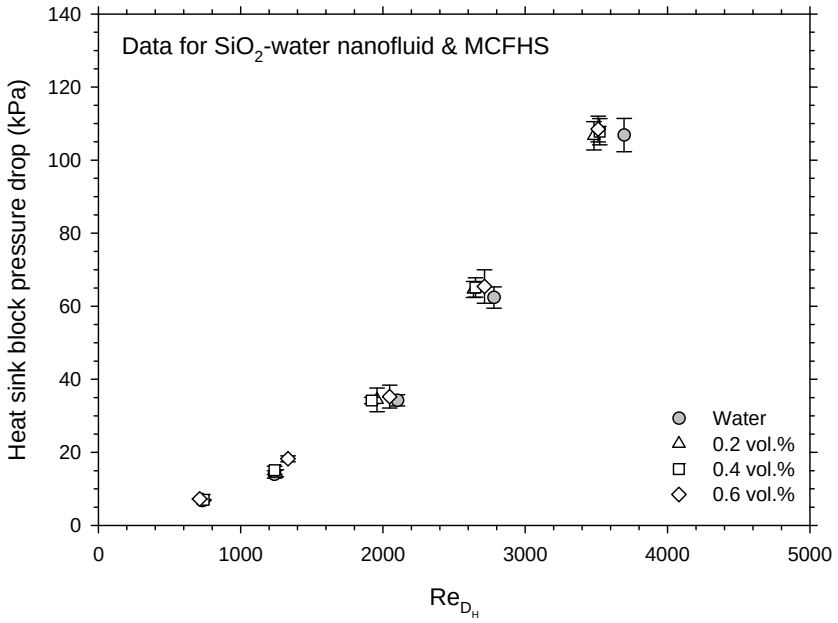

Figure 5.6 Comparison of pressure drop across heat sink block obtained from water and that from the SiO_2-water nanofluids at different volume fraction (data for MCFHS)

As shown in Figure 5.6, the measured data show that the pressure drop of the nanofluids across the MCFHS increase with increasing Reynolds number and that there is a small increase with increasing particle concentrations. This means that using the nanofluids at higher particle volume fraction may create a tiny penalty in pressure drop.

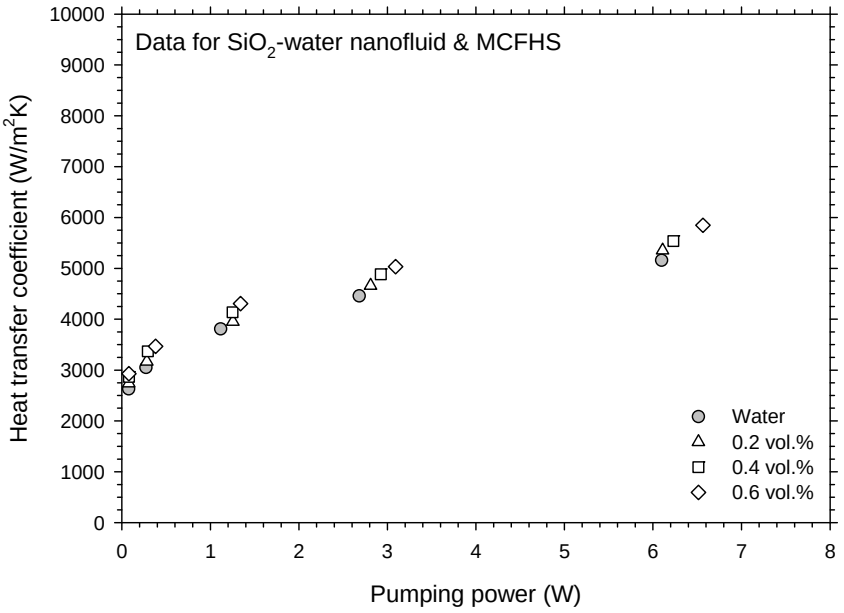

Figure 5.7 Relation between heat transfer coefficient and pumping power as a function of SiO_2 particle concentration (data for MCFHS)

Figure 5.7 also shows the experimental heat transfer coefficients as a function of pumping power and the SiO_2-water nanofluid at different concentrations. The data show that the heat transfer performance of the nanofluids increase with increasing pumping power as well as particle concentrations. Moreover, the results indicate that the thermal performance of nanofluid are higher than those of the water at the given pumping power and increase as particle concentration increase.

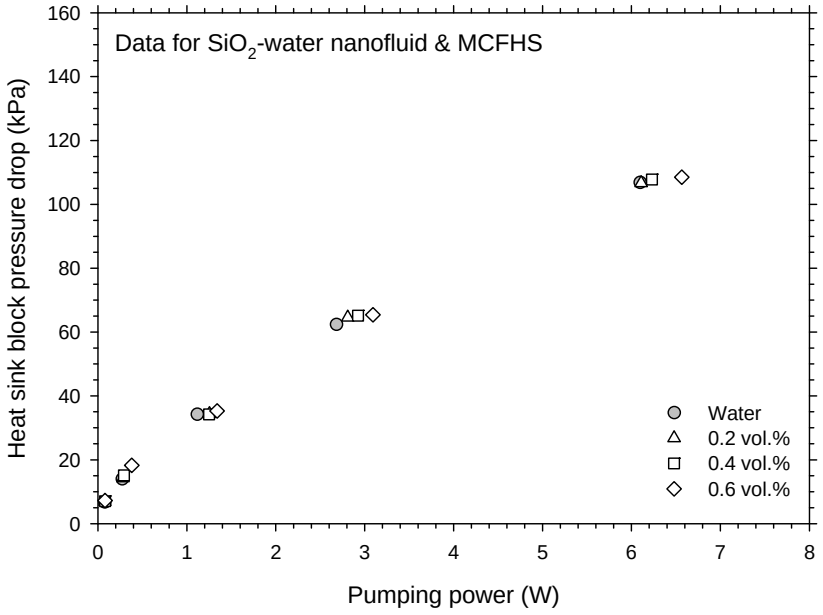

Figure 5.8 Measured pressure drop across MCFHS as a function of pumping power and SiO_2 particle concentration

As shown in Figure 5.8, the pressure drop across MCFHS block increase with increasing pumping and addition of the nanoparticle in the common base liquid create a small increase in the pumping power.

5.1.2 For Miniature Square Fin Heat Sink (MSFHS)

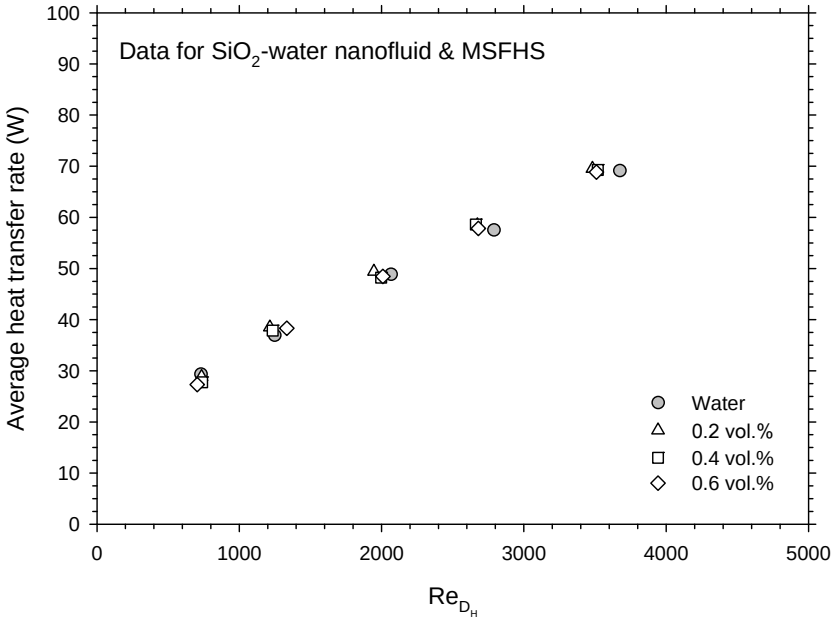

Figure 5.9 Variation of the average heat transfer rate as a function of Reynolds number and particle volume concentration (data for MSFHS)

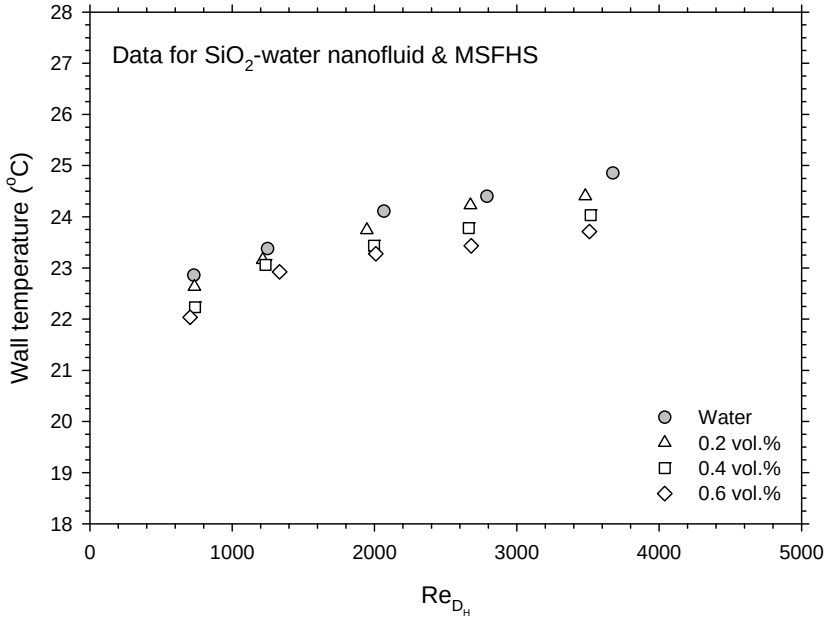

Figure 5.10 Comparison of the wall temperature between the pure water and nanofluids (data for MSFHS)

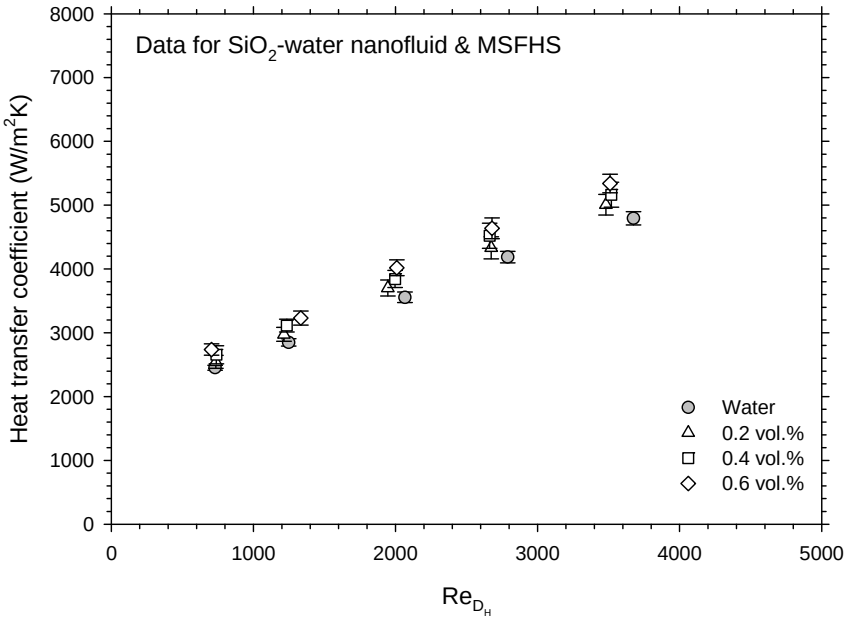

a) Heat transfer coefficient

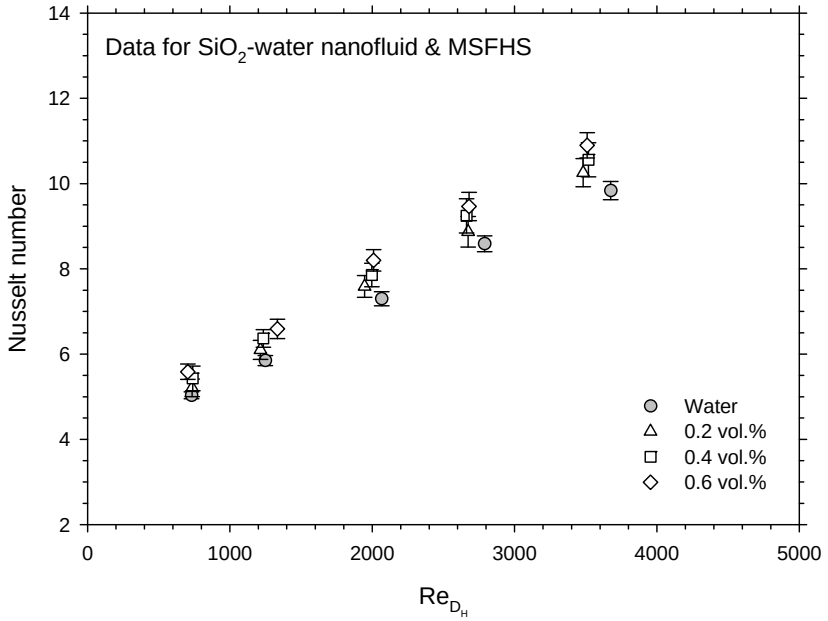

b) Nusselt number

Figure 5.11 Experimental heat transfer coefficient and Nusselt number for water and SiO_2-water nanofluids versus Reynolds number at various volume concentration (data for MSFHS)

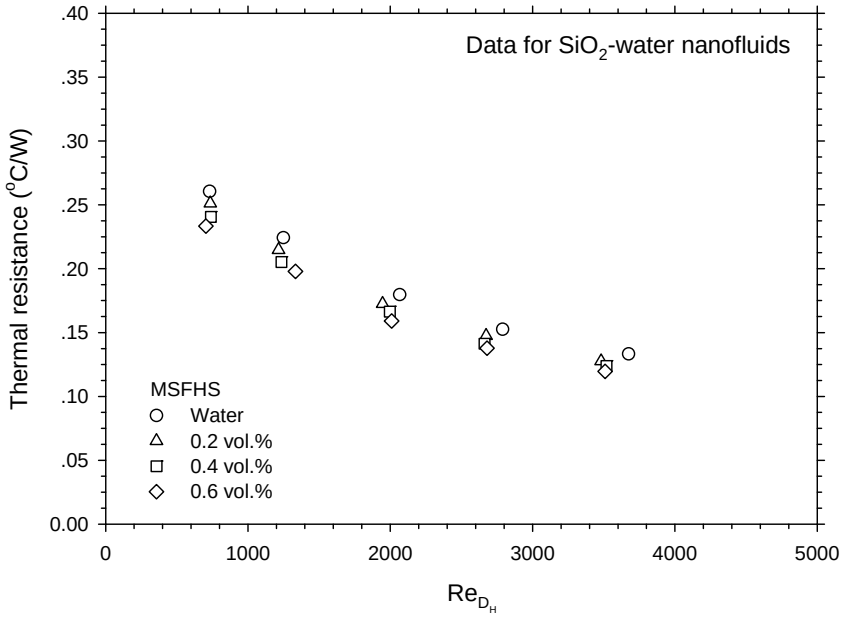

Figure 5.12 Variation of the thermal resistance as a function of Reynolds number and particle concentrations (data for MSFHS)

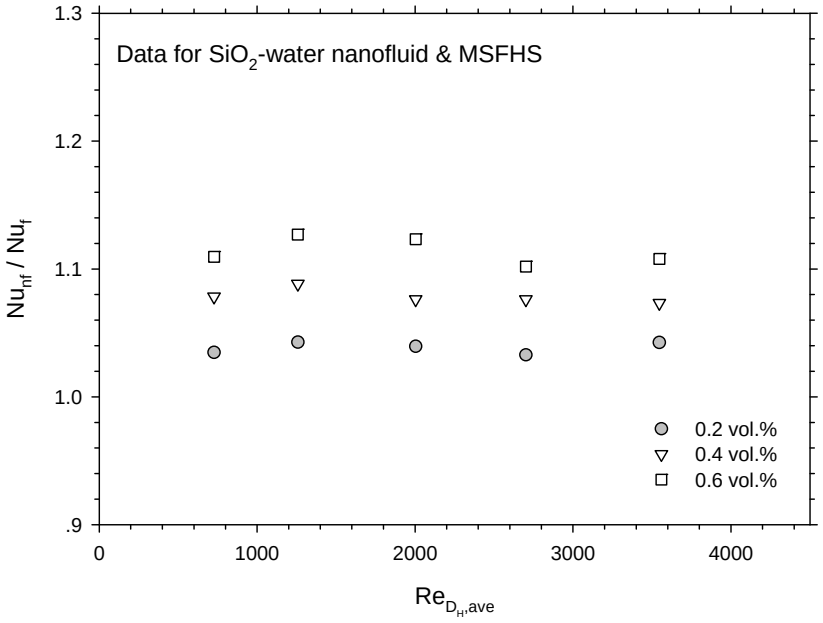

Figure 5.13 Nusselt number ratio as a function of particle concentration for the data of SiO_2-water nanofluids flow in MSFHS

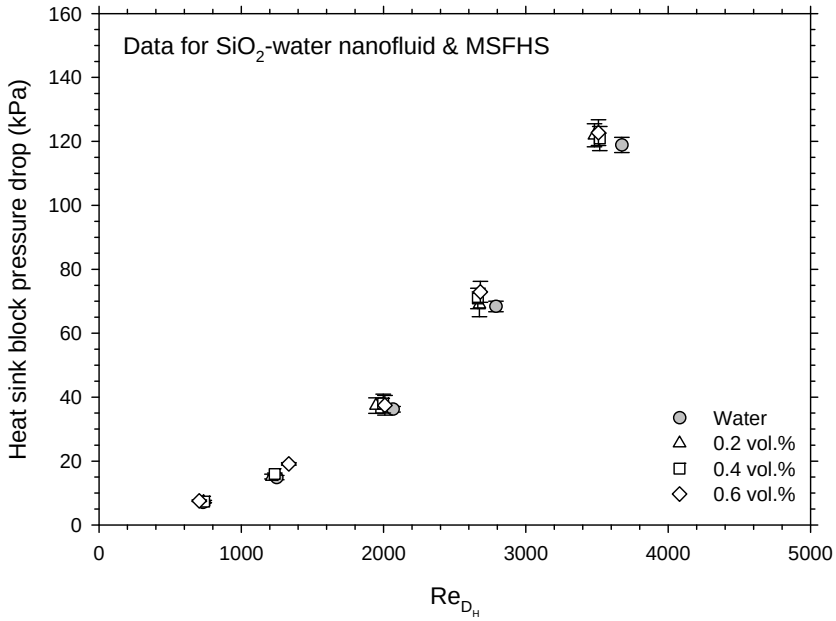

Figure 5.14 Comparison of pressure drop across heat sink block obtained from water and that from the SiO_2-water nanofluids at different volume fraction (data for MSFHS)

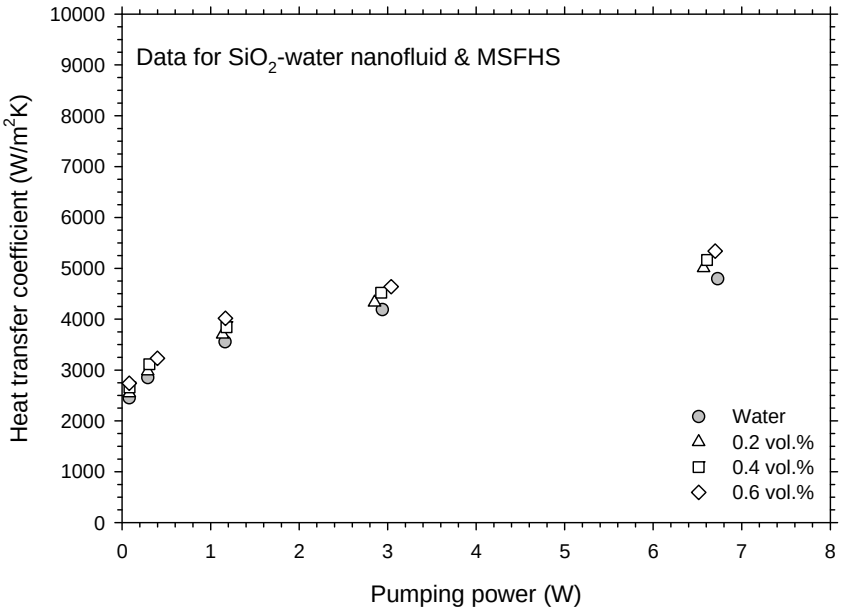

Figure 5.15 Relation between heat transfer coefficient and pumping power as a function of SiO_2 particle concentration (data for MSFHS)

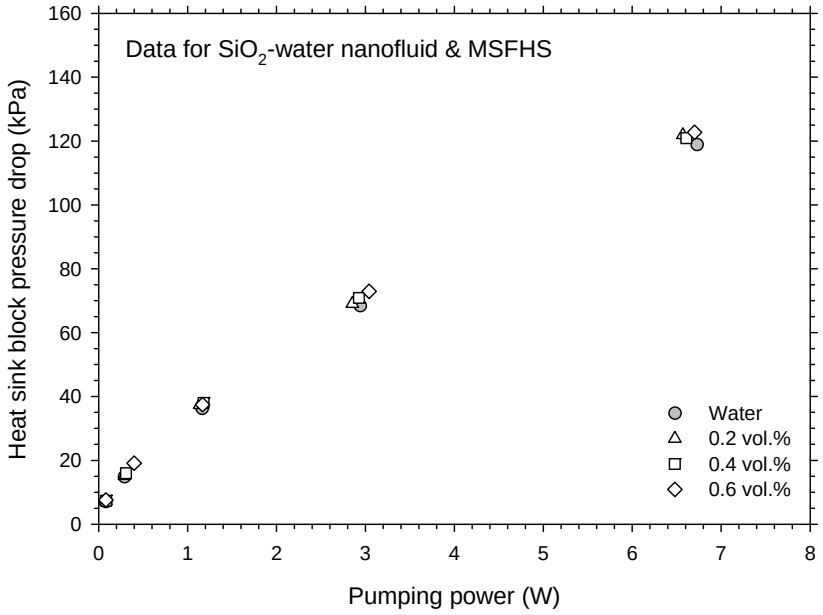

Figure 5.16 Measured pressure drop across MSFHS as a function of pumping power and SiO_2 particle concentration

Similar to the measured data of MCFHS as shown in Figure 5.1 - 5.8, the measured data for SiO_2-water nanofluid flowing through MSFHS are showed in Figures 5.9 – 5-16. Similar trends of the measured data in both heat sinks are observed.

5.2 Data for ZnO-Water Nanofluids

5.2.1 For Miniature Circular Fin Heat Sink (MCFHS)

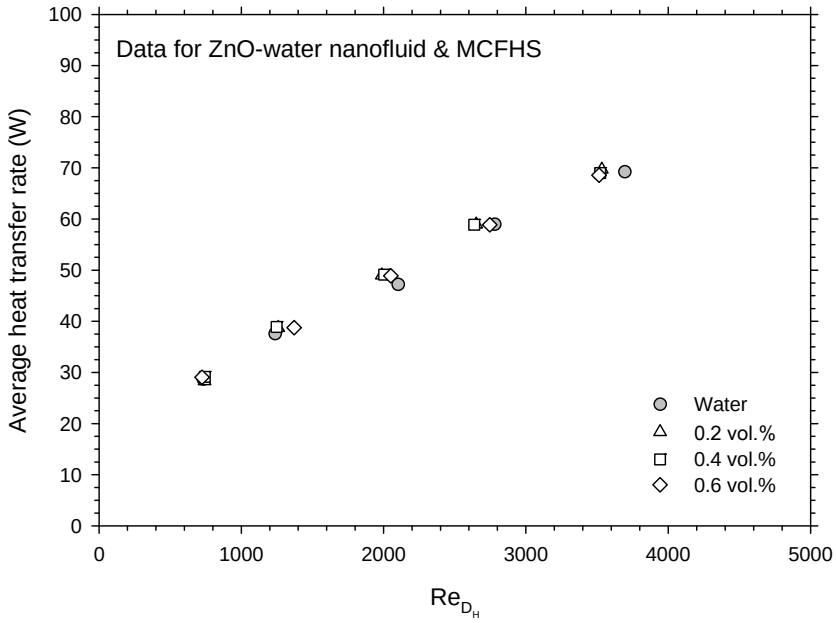

Figure 5.17 Variation of the average heat transfer rate as a function of Reynolds number and particle volume concentration (data for MCFHS)

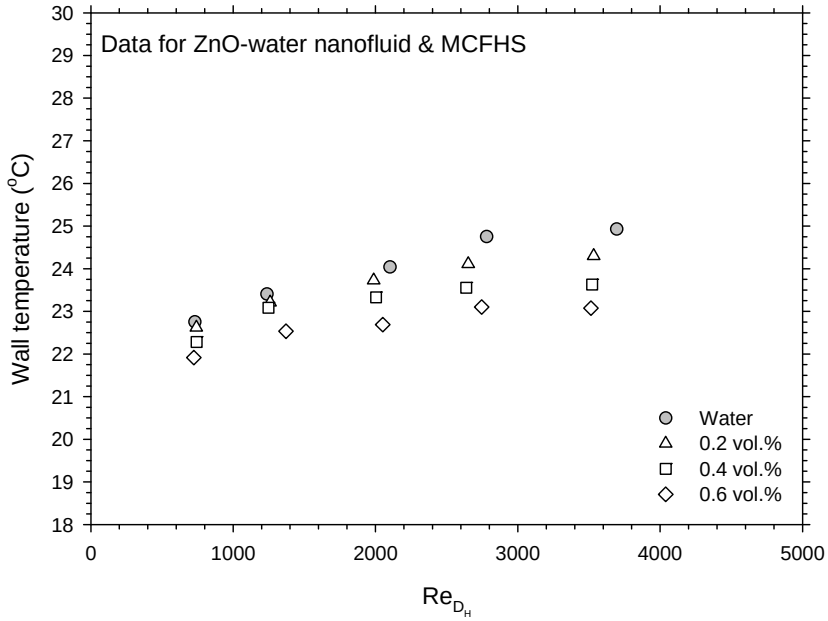

Figure 5.18 Comparison of the wall temperature between the pure water and ZnO-water nanofluids (data for MCFHS)

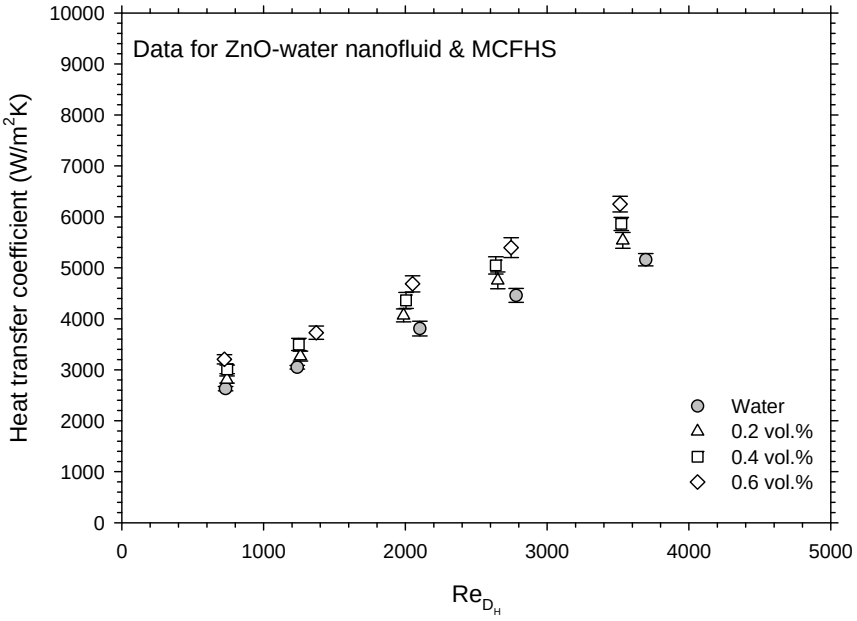

a) Heat transfer coefficient

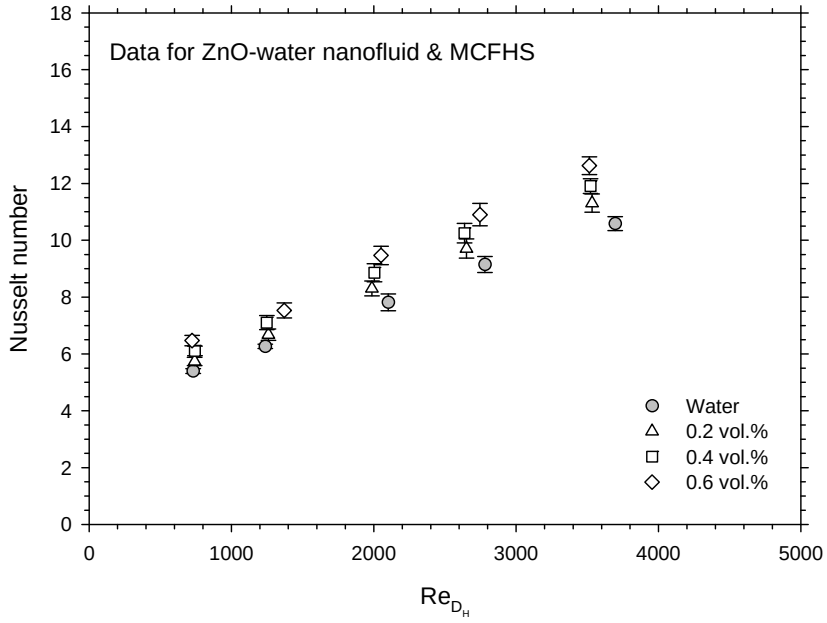

b) Nusselt number

Figure 5.19 Experimental heat transfer coefficient and Nusselt number for water and ZnO-water nanofluids versus Reynolds number at various volume concentration (data for MCFHS)

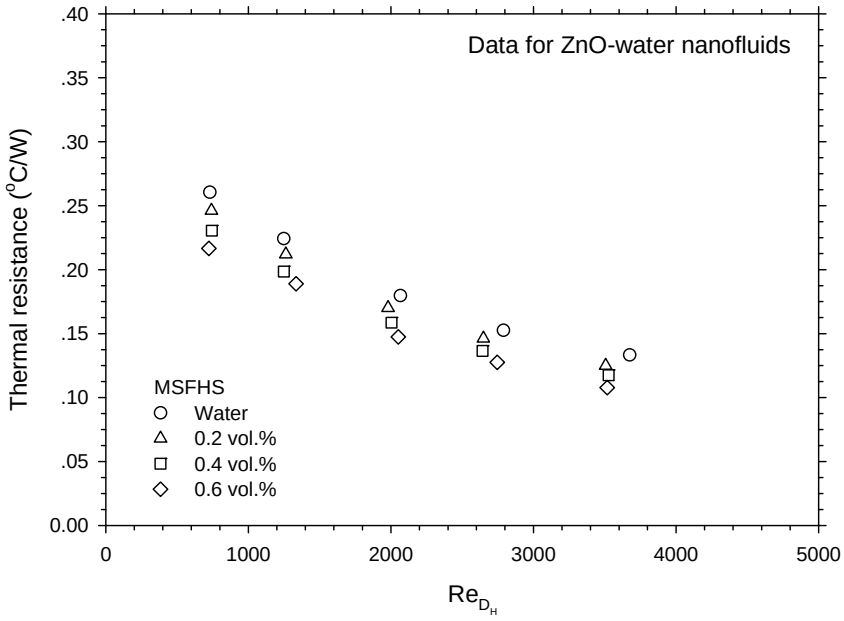

Figure 5.20 Variation of the thermal resistance as a function of Reynolds number and particle concentrations (data for ZnO-water nanofluid and MCFHS)

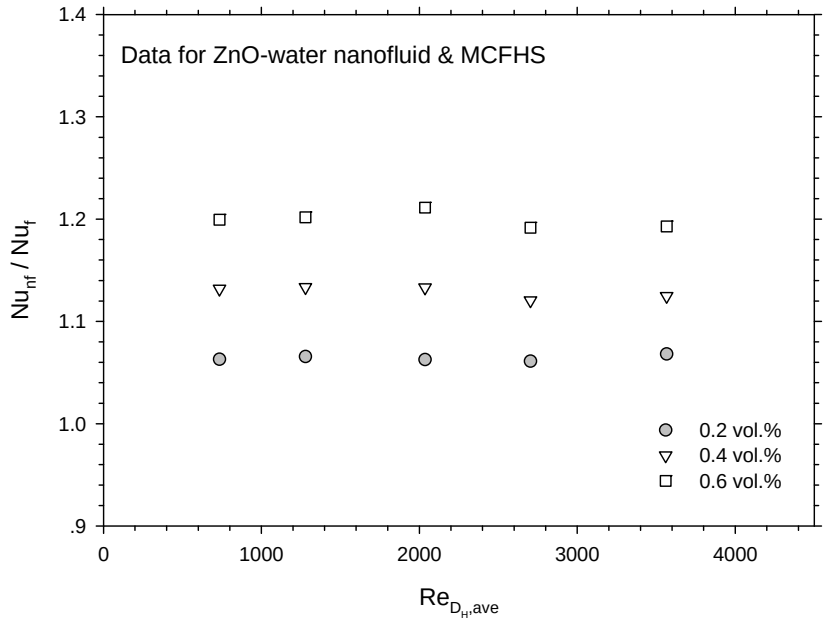

Figure 5.21 Nusselt number ratio as a function of particle concentration for the data of ZnO-water nanofluids flow in MCFHS

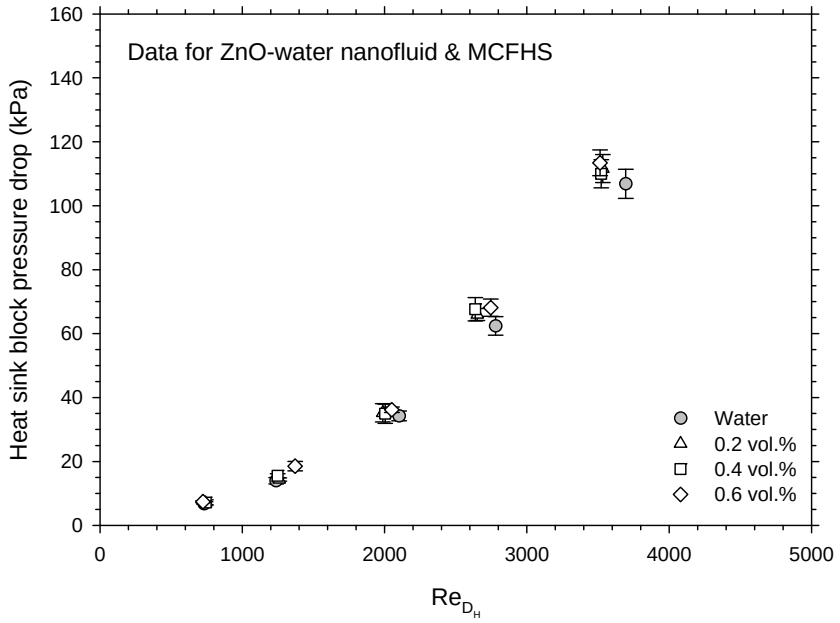

Figure 5.22 Comparison of pressure drop across heat sink block obtained from water and that from the ZnO-water nanofluids at different volume fraction (data for MCFHS)

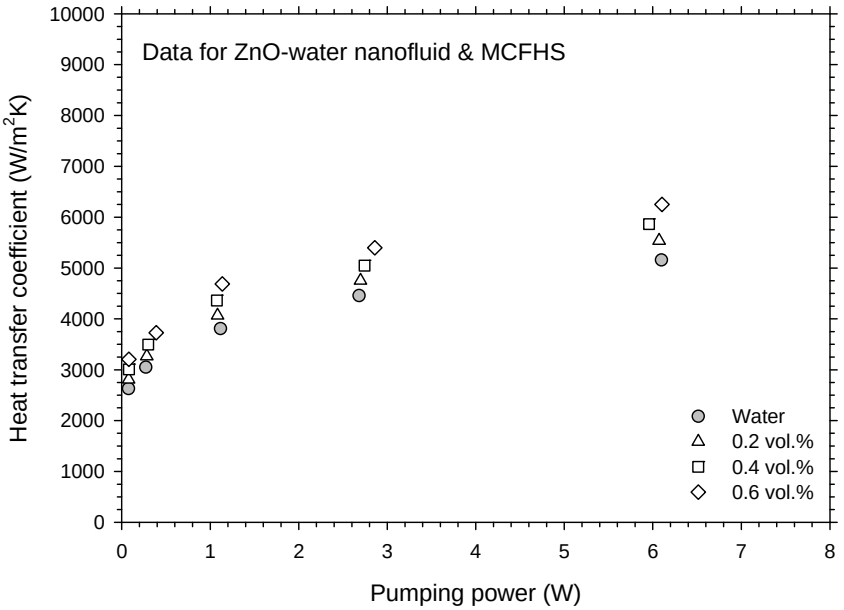

Figure 5.23 Relation between heat transfer coefficient and pumping power as a function of ZnO particle concentration (data for MCFHS)

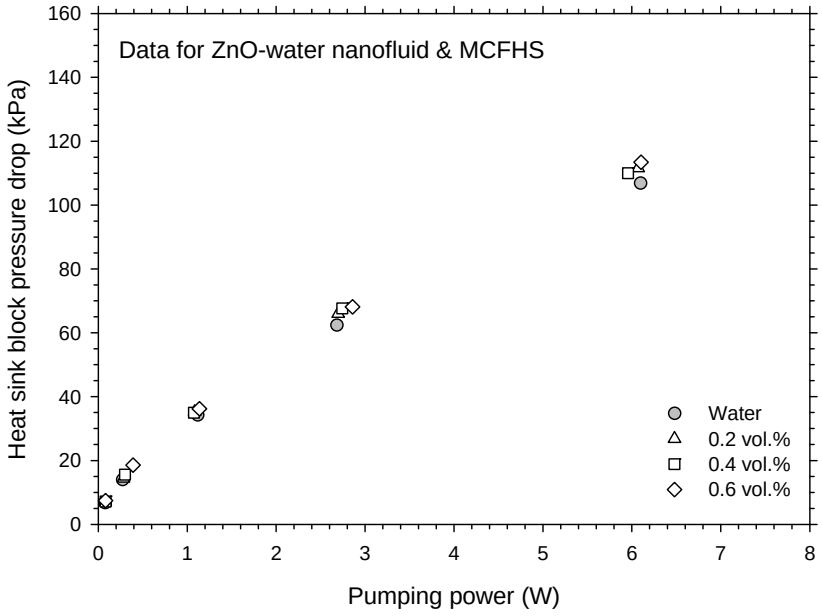

Figure 5.24 Measured pressure drop across MCFHS as a function of pumping power and ZnO particle concentration

Similar to the experimental data for SiO_2-water nanofluids flow in MCFHS (Figure 5.1 - 5.8), the measured data for ZnO-water nanofluid flowing through MCFHS are showed in Figures 5.17 – 5-24. Similar trends of the measured data for both nanoparticles are obtained. However, as shown in Figure 5.21, the heat transfer performances of ZnO-water nanofluids are higher than those of the water between 7 and 20 % which are higher than those of the data for SiO_2-water nanofluids. This may be caused from the fact that the thermal conductivity of ZnO nanoparticle is larger than the SiO_2 nanoparticle which lead to an increase in the heat transfer performance. Furthermore, for pressure drop data, the results indicate that the pressure data for both nanoparticles are quite the same.

5.2.2 For Miniature Square Fin Heat Sink (MSFHS)

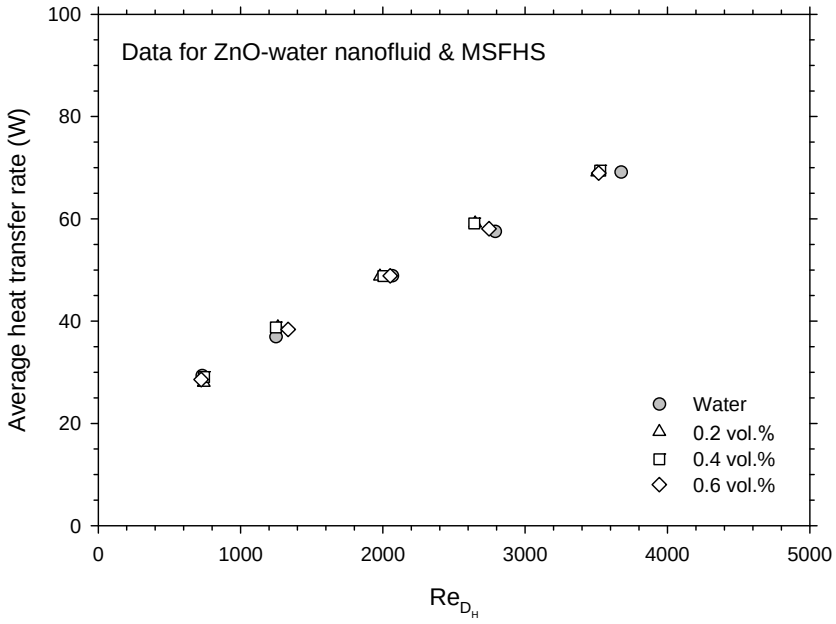

Figure 5.25 Variation of the average heat transfer rate as a function of Reynolds number and ZnO particle concentration (data for MSFHS)

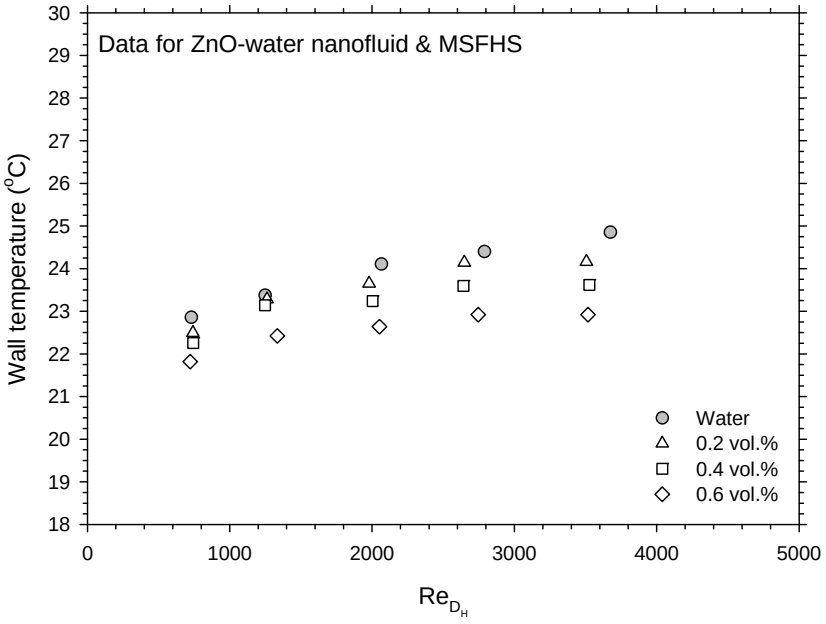

Figure 5.26 Comparison of the wall temperature between the pure water and ZnO-water nanofluids (data for MSFHS)

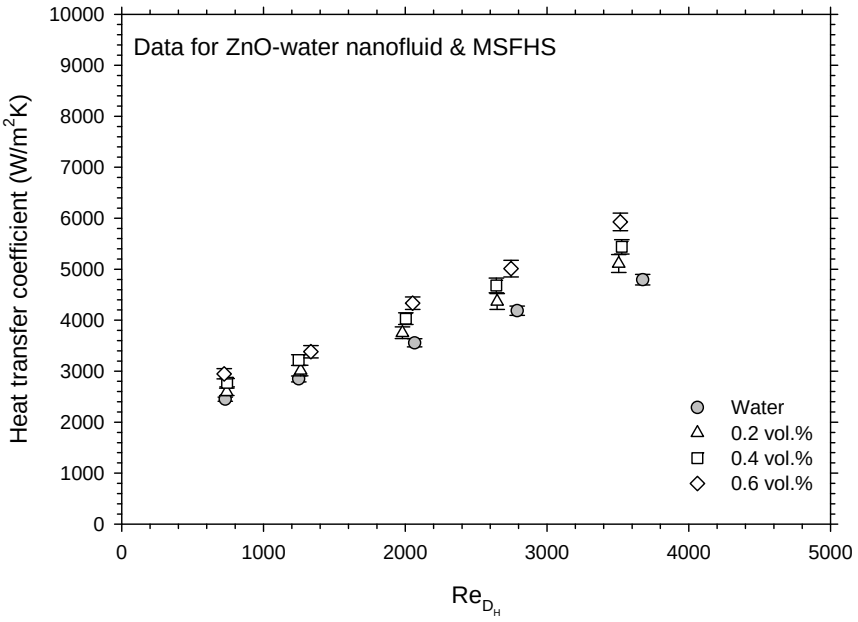

a) Heat transfer coefficient

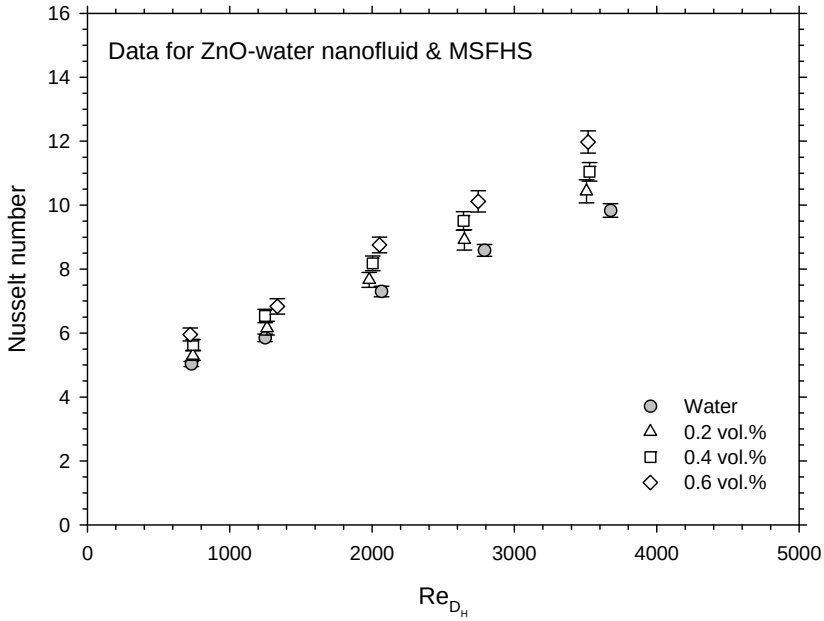

b) Nusselt number

Figure 5.27 Experimental heat transfer coefficient and Nusselt number for water and ZnO-water nanofluids versus Reynolds number at various volume concentration (data for MSFHS)

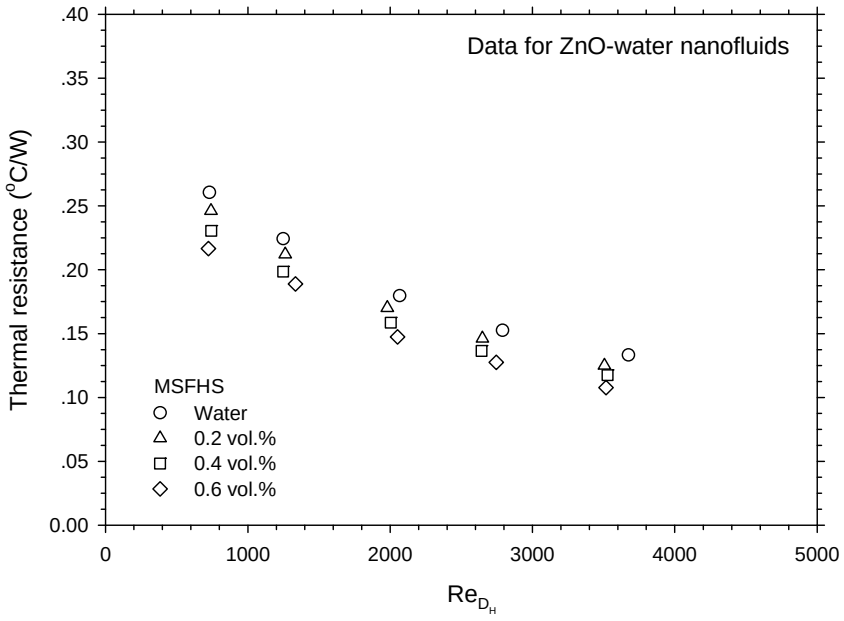

Figure 5.28 Variation of the thermal resistance as a function of Reynolds number and particle concentrations (data for ZnO-water nanofluid and MSFHS)

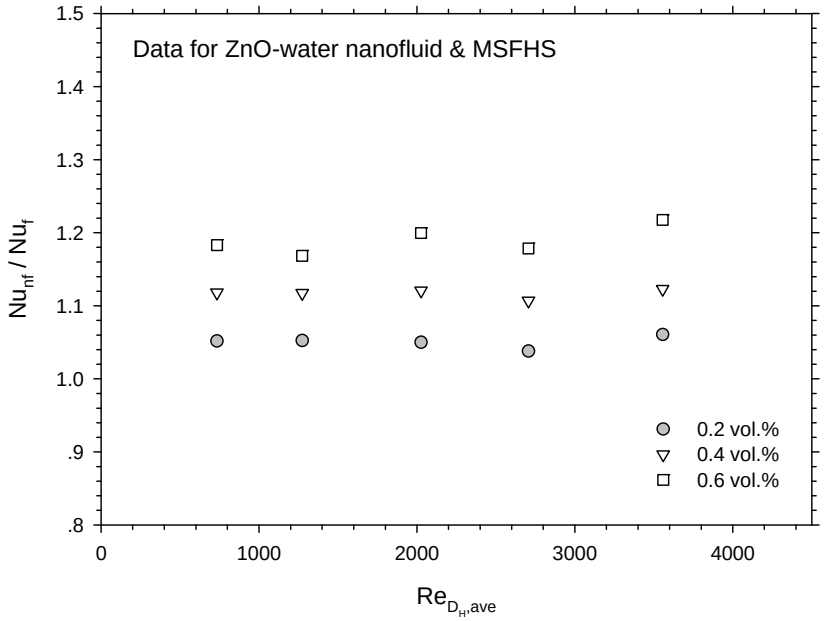

Figure 5.29 Nusselt number ratio as a function of particle concentration for the data of ZnO-water nanofluids flow in MSFHS

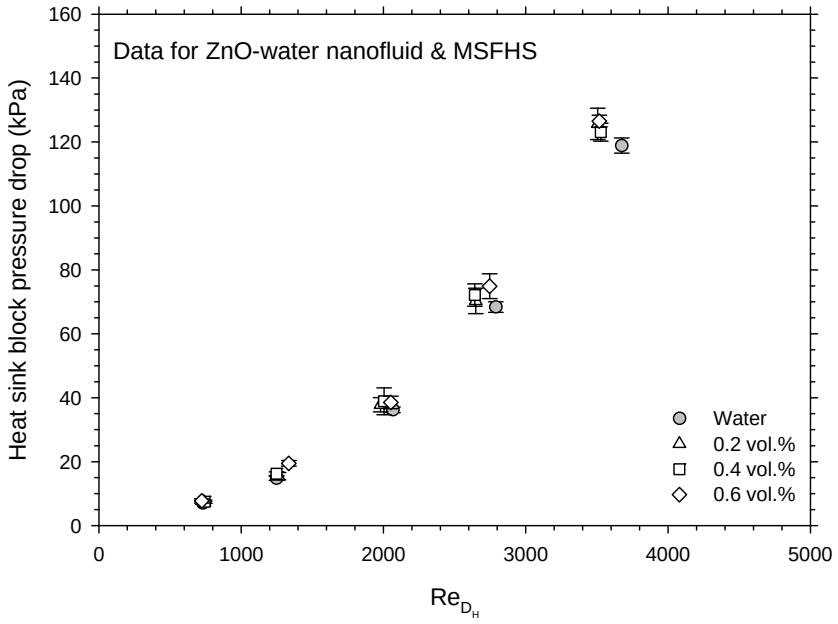

Figure 5.30 Comparison of pressure drop across heat sink block obtained from water and that from the ZnO-water nanofluids at different volume fraction (data for MSFHS)

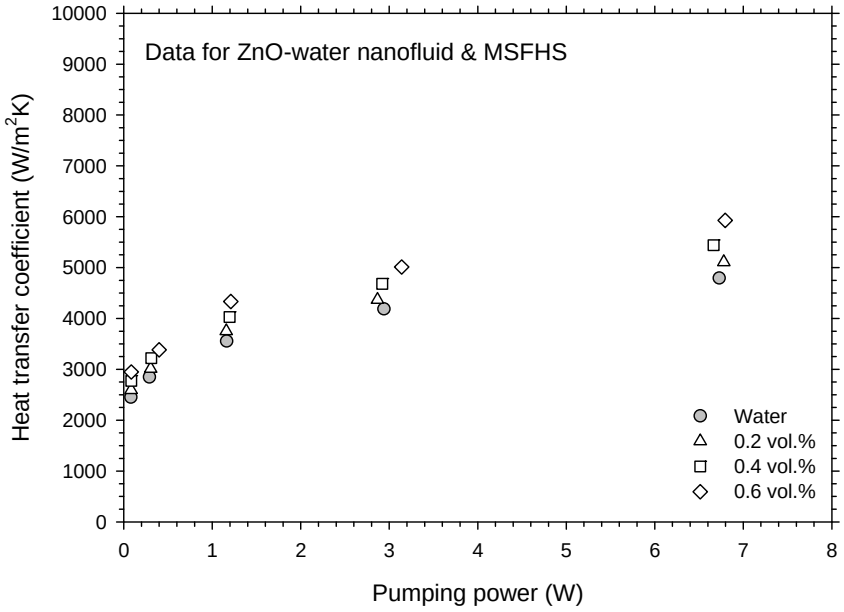

Figure 5.31 Relation between heat transfer coefficient and pumping power as a function of ZnO particle concentration (data for MSFHS)

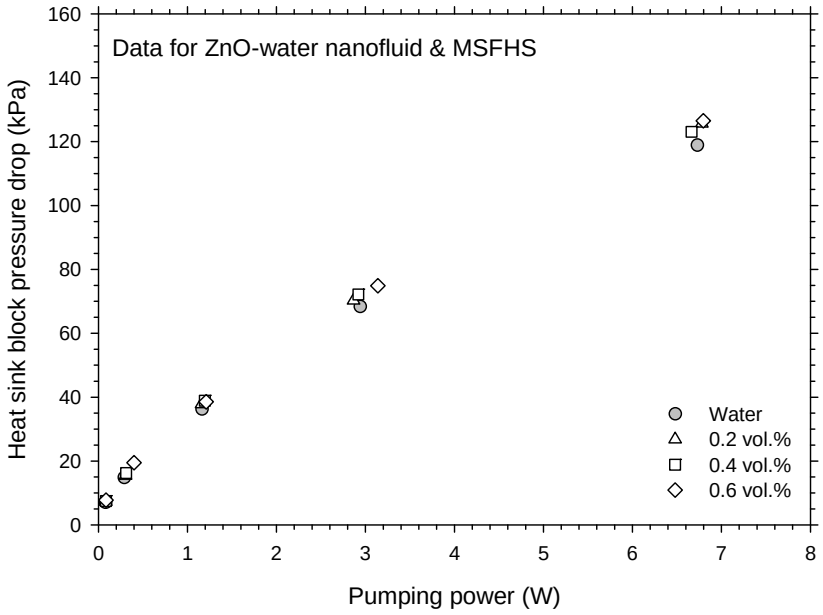

Figure 5.32 Measured pressure drop across MSFHS as a function of pumping power and ZnO particle concentration

Similar to the measured data of ZnO-water nanofluid flowing through MCFHS as shown in Figure 5.17 - 5.24, the measured data for ZnO-water nanofluid flow in MSFHS are showed in Figures 5.25 – 5-32. Similar trends of the measured data are obtained.

5.3 Effect of Pin Fin Configuration on the Heat Transfer Performance and Flow Characteristic

5.3.1 For SiO_2-Water Nanofluid

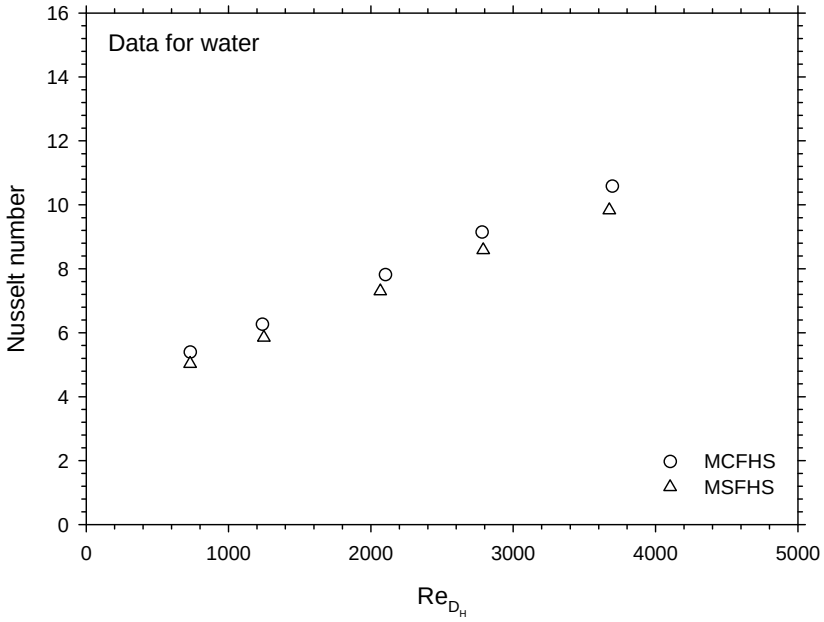

a) Data for water

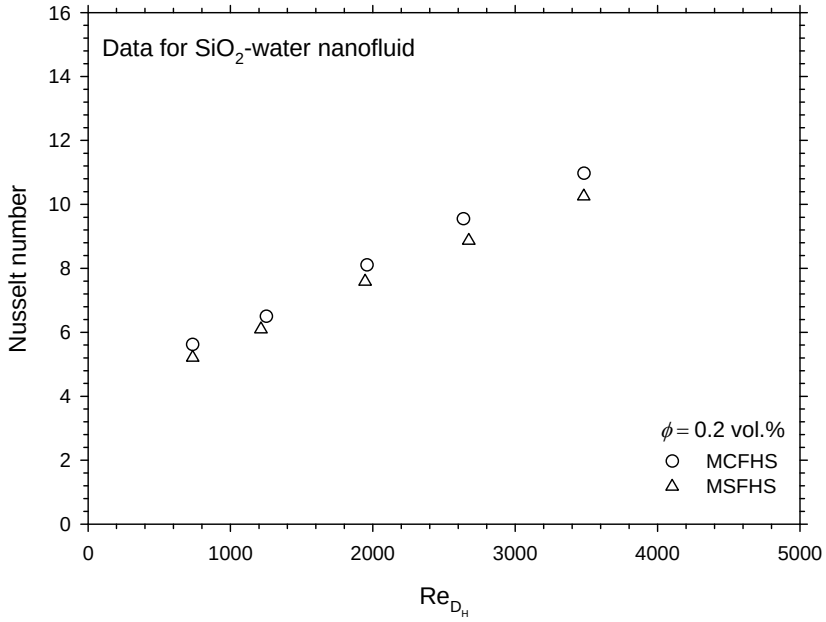

b) Data for SiO_2-water nanofluid at 0.2 vol.%

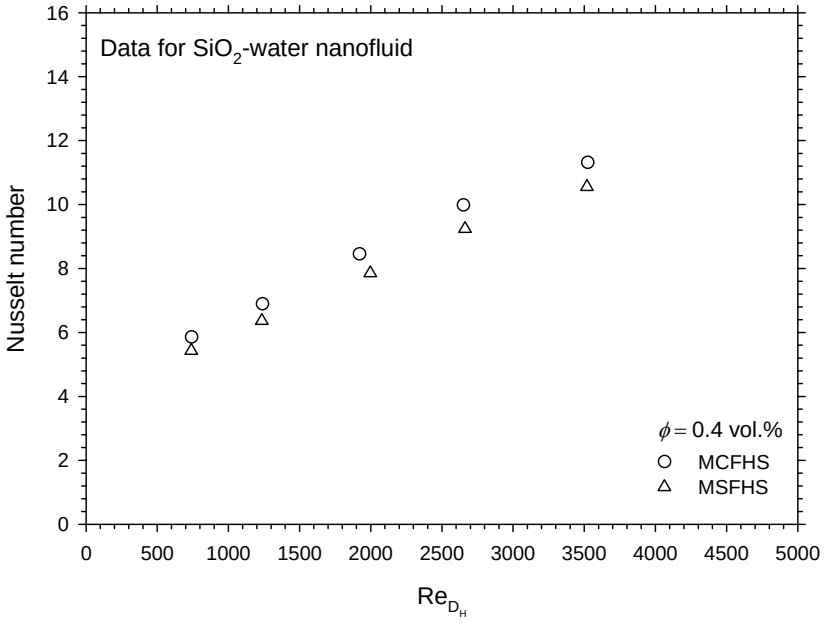

c) Data for SiO_2-water nanofluid at 0.4 vol.%

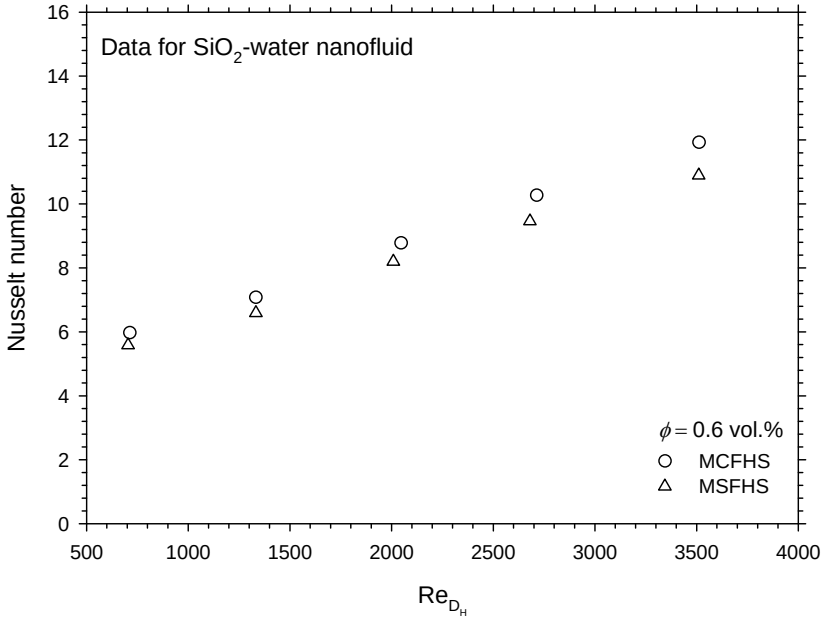

d) Data for SiO_2-water nanofluid at 0.6 vol.%

Figure 5.33 Comparison of Nusselt number between the measured data for MCFHS and MSFHS (data for SiO_2-water nanofluid)

As shown in Figure 5.33 (a) – (d), in spite the heat transfer area of the MSFHS is larger than the MCFHS by about 130 mm^2, the heat transfer performance of the MCFHS are higher than the MSFHS by average about 6 to 9 %. This may due to the fact that the fluid flow passes the circular pin rather ease compared to the square fin configuration which lead to increase in the heat transfer performance. Thus, the author would like to conclude that the effect of fin configuration may overcome the effect of surface area under the same condition.

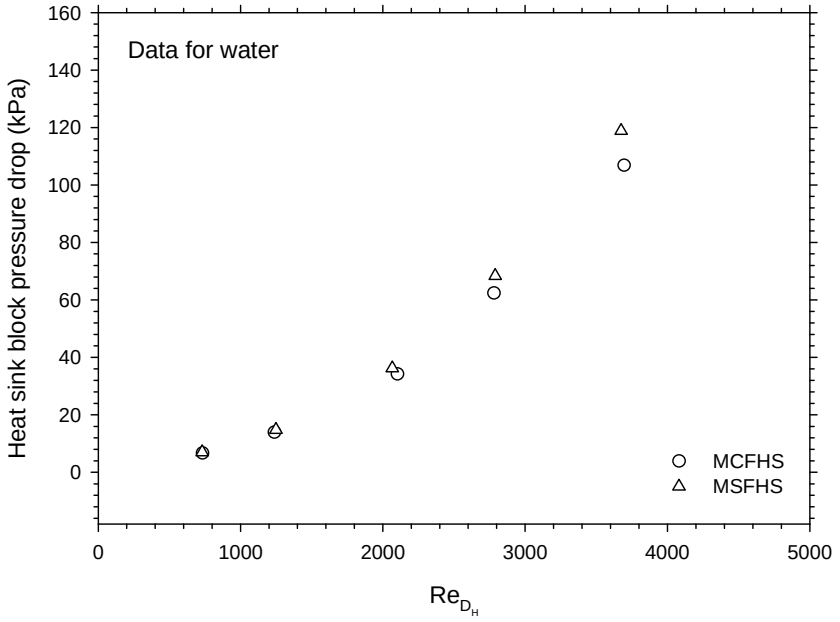

a) Data for water

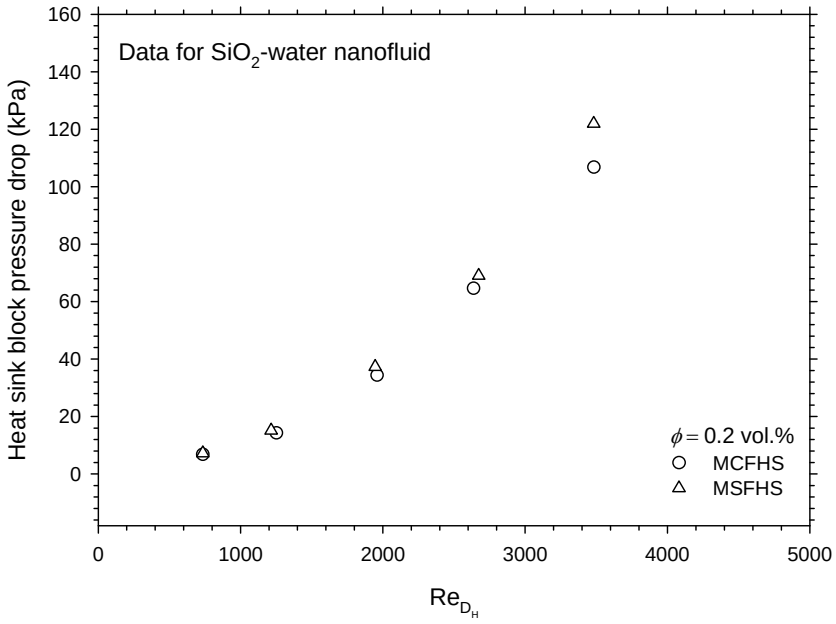

b) Data for SiO_2-water nanofluid at 0.2 vol.%

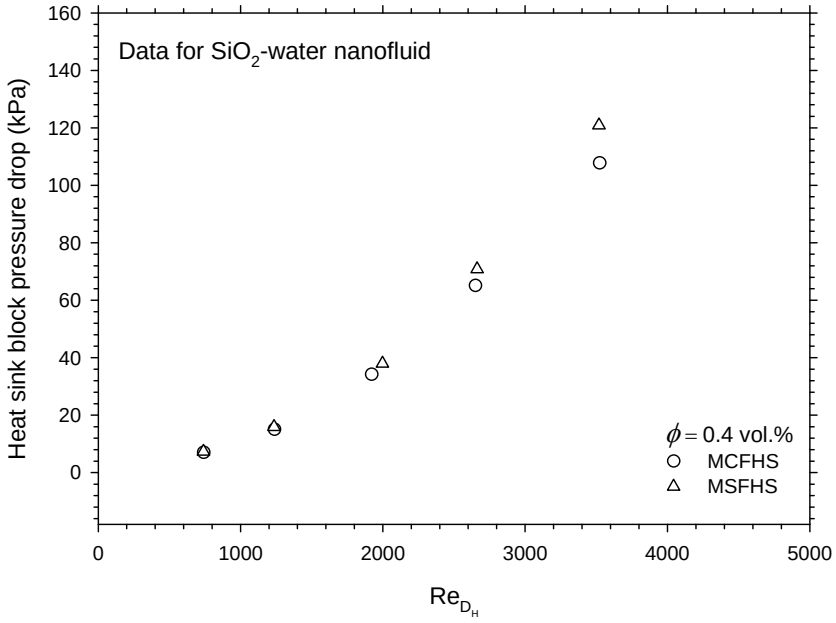

c) Data for SiO_2-water nanofluid at 0.4 vol.%

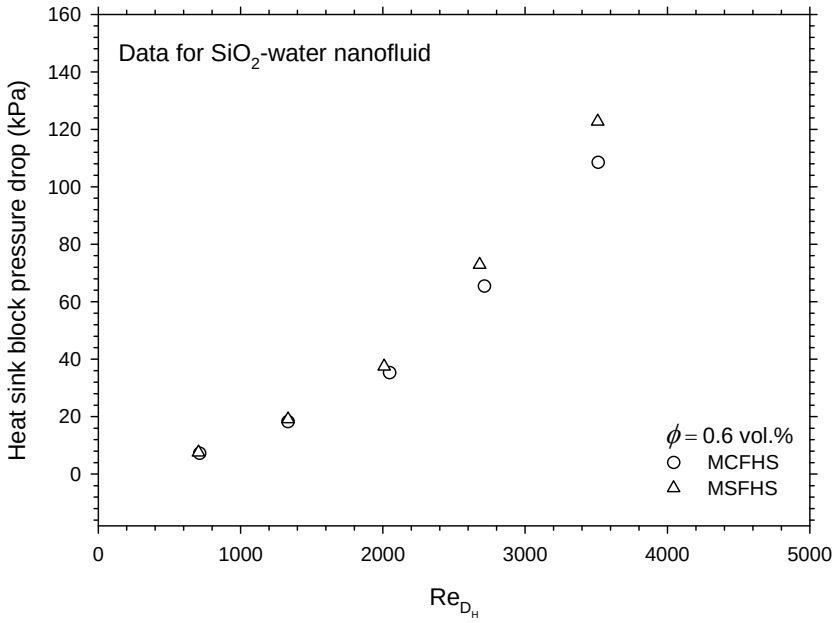

d) Data for SiO_2-water nanofluid at 0.6 vol.%

Figure 5.34 Comparison of pressure drop across MCFHS and MSFHS (data for SiO_2-water nanofluid)

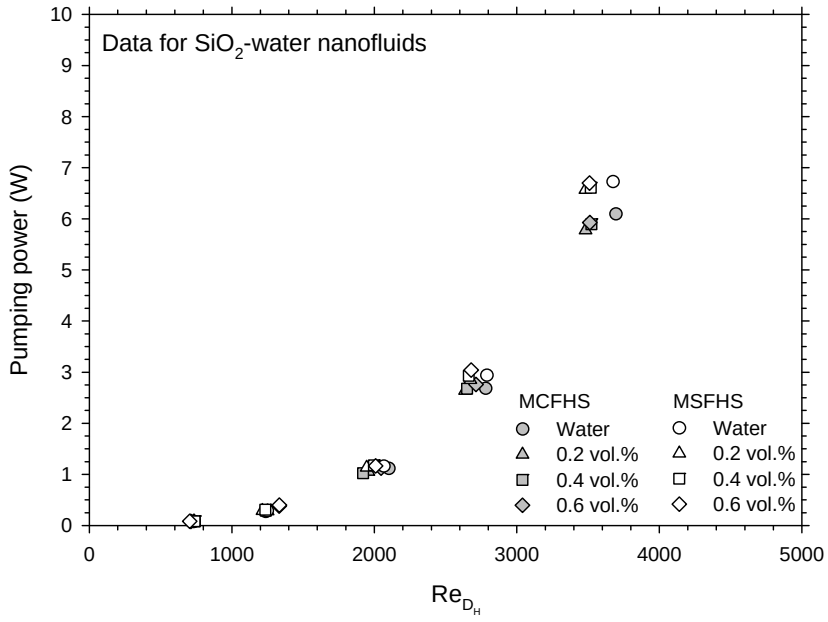

Figure 5.35 Comparison of the pumping power between MCFHS and MSFHS (data for SiO_2-water nanofluid)

Similar to the thermal performance, figures 5.34 and 5.35 show that the pressure drop across the MSFHS are slightly higher than the MCFHS, especially at high flow rate. This behavior may due to the fact that the flow passes the MSFHS rather hard compared to the MCFHS. Thus, higher pressure drop are obtained.

5.3.2 For ZnO-Water Nanofluid

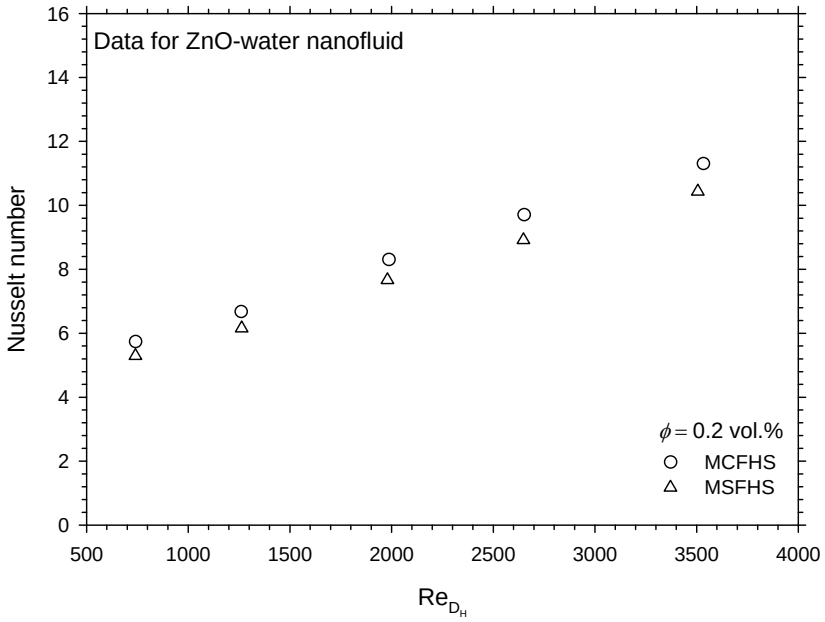

a) Data for ZnO-water nanofluid at 0.2 vol.%

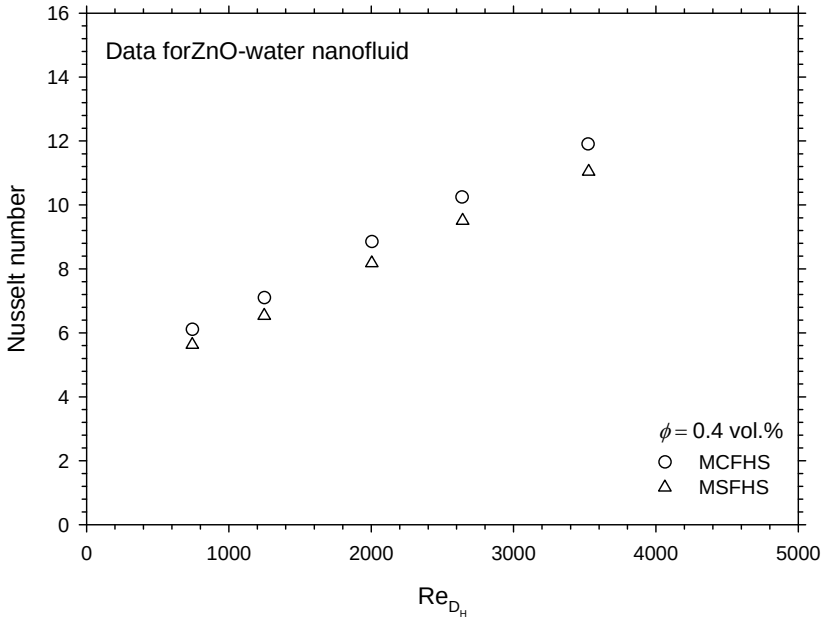

b) Data for ZnO-water nanofluid at 0.4 vol.%

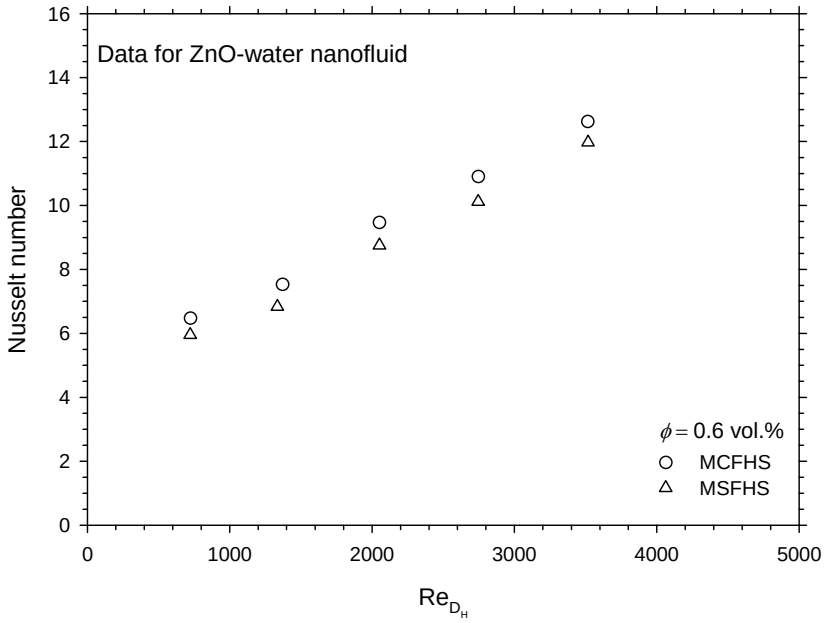

c) Data for ZnO-water nanofluid at 0.6 vol.%

Figure 5.36 Comparison of Nusselt number between the measured data for MCFHS and MSFHS (data for ZnO-water nanofluid)

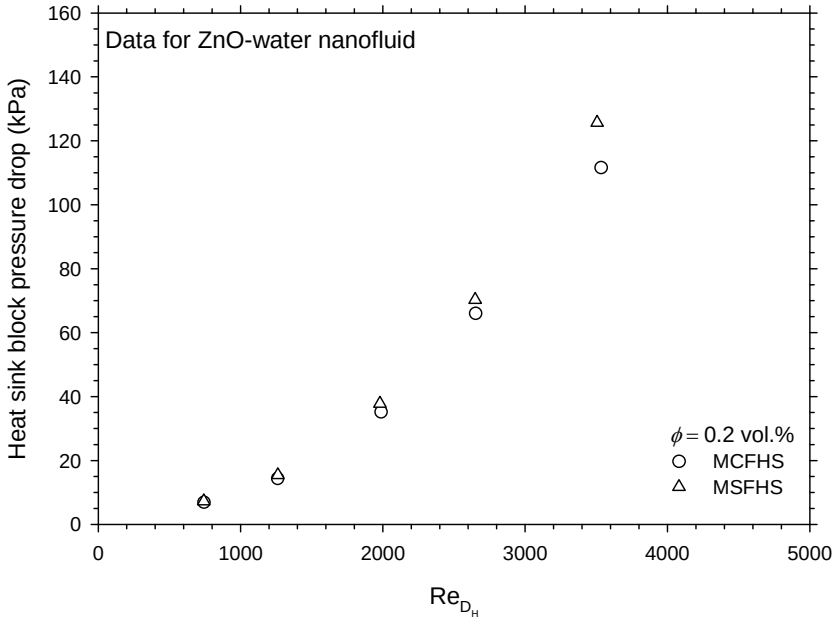

a) Data for ZnO-water nanofluid at 0.2 vol.%

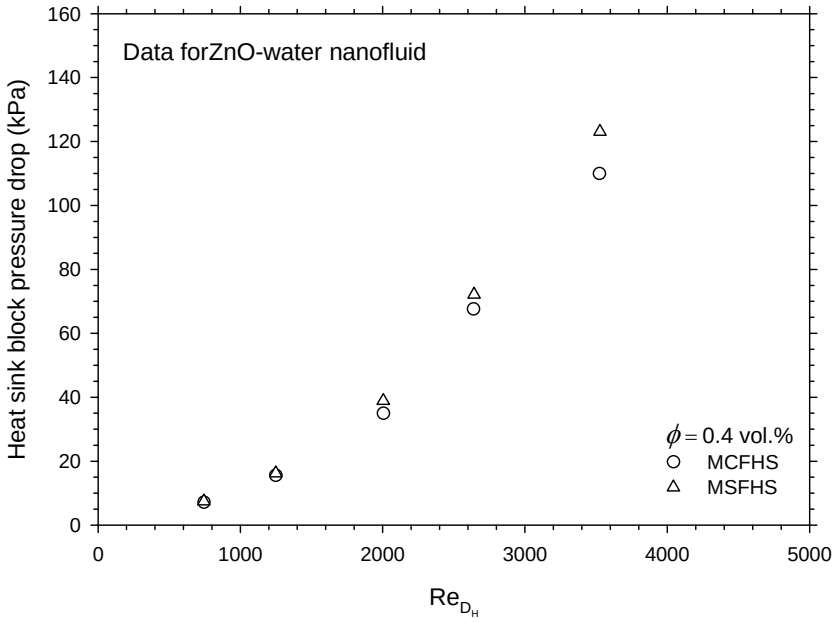

b) Data for ZnO-water nanofluid at 0.4 vol.%

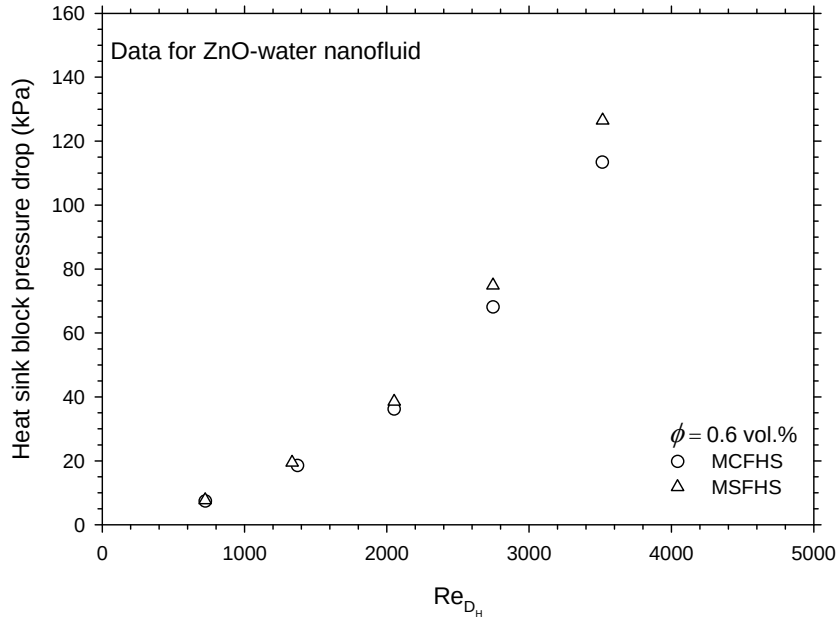

c) Data for ZnO-water nanofluid at 0.6 vol.%

Figure 5.37 Comparison of pressure drop across MCFHS and MSFHS (data for ZnO-water nanofluid)

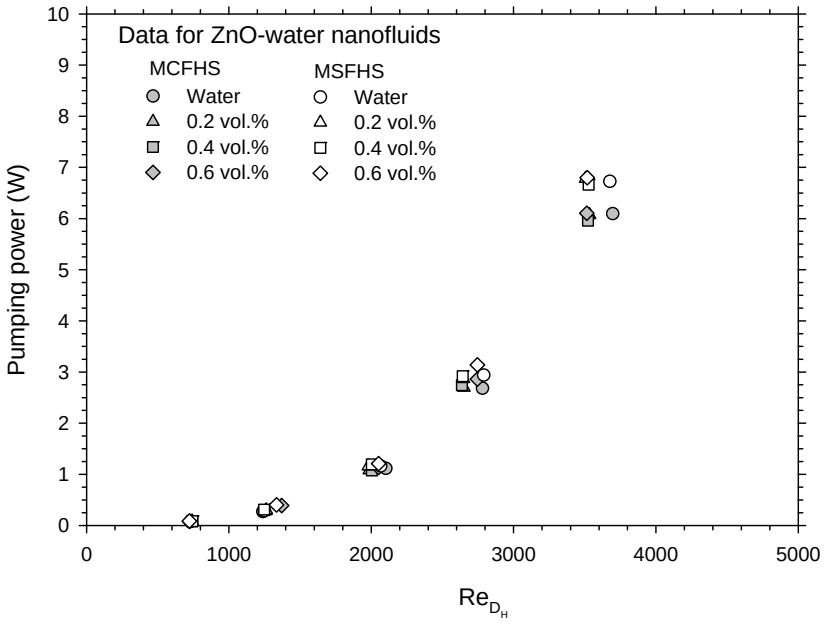

Figure 5.38 Comparison of the pumping power between MCFHS and MSFHS (data for ZnO-water nanofluid)

Similar to the measured data of SiO_2-water nanofluid, the effect of pin fin configurations on the thermal performance and pressure drop characteristic of ZnO-water nanofluid are expressed in Figures 5.36 to 3.38. Similar trends of the measured data are observed.

5.4 Effect of Nanoparticle Type on the Heat Transfer Performance and Flow Characteristic

5.3.1 For MCFHS

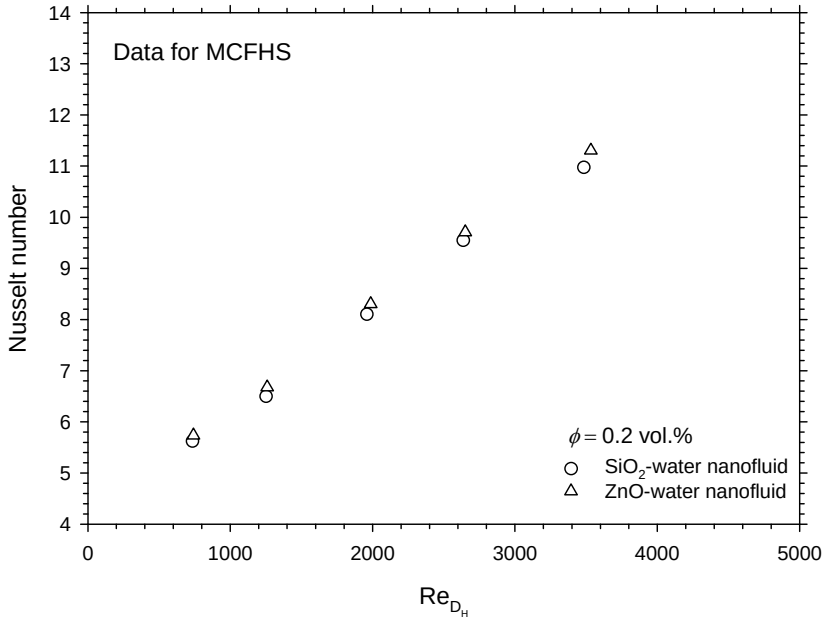

a) at particle fraction of 0.2 vol.%

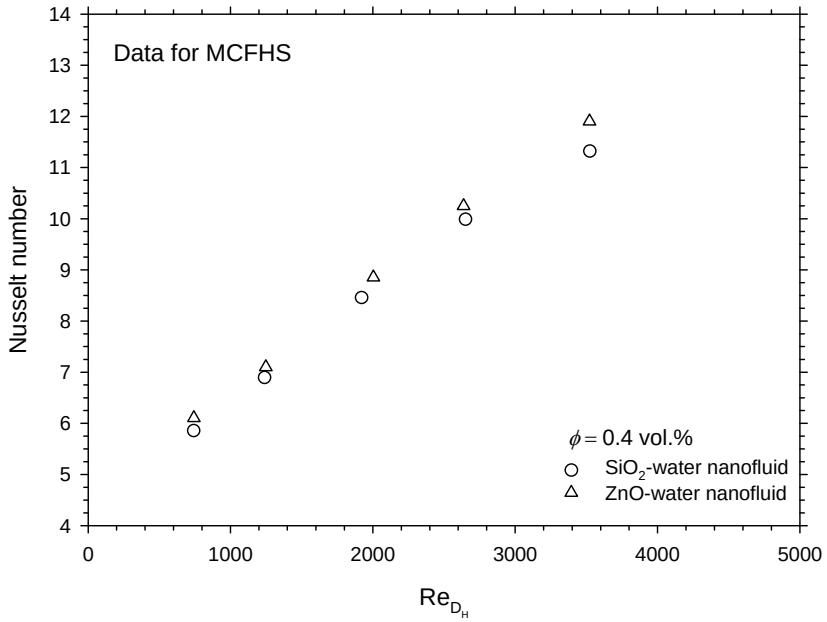

b) at particle fraction of 0.4 vol.%

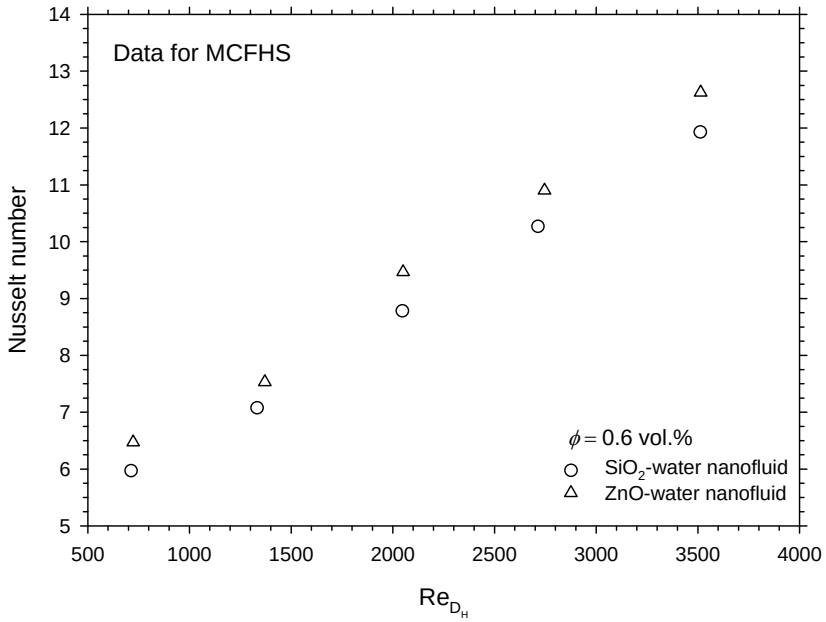

c) at particle fraction of 0.6 vol.%

Figure 5.39 Comparison of the Nusselt number between SiO_2-water and ZnO-water nanofluid at various particle concentration (data for MCFHS)

As shown in Figure 5.39 (a) – (c), the heat transfer performances of ZnO-water nanofluids are higher than those of the SiO_2-water nanofluid by average about 3 to 9. This may be caused from the thermal conductivity of ZnO nanoparticle is larger than the SiO_2 nanoparticle. Thus, higher heat transfer performance are obtained.

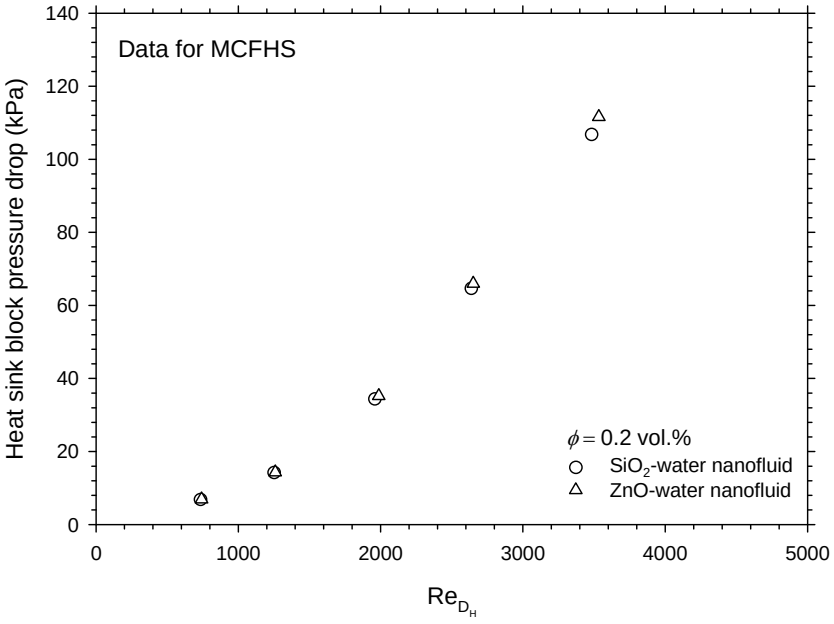

a) at particle fraction of 0.2 vol.%

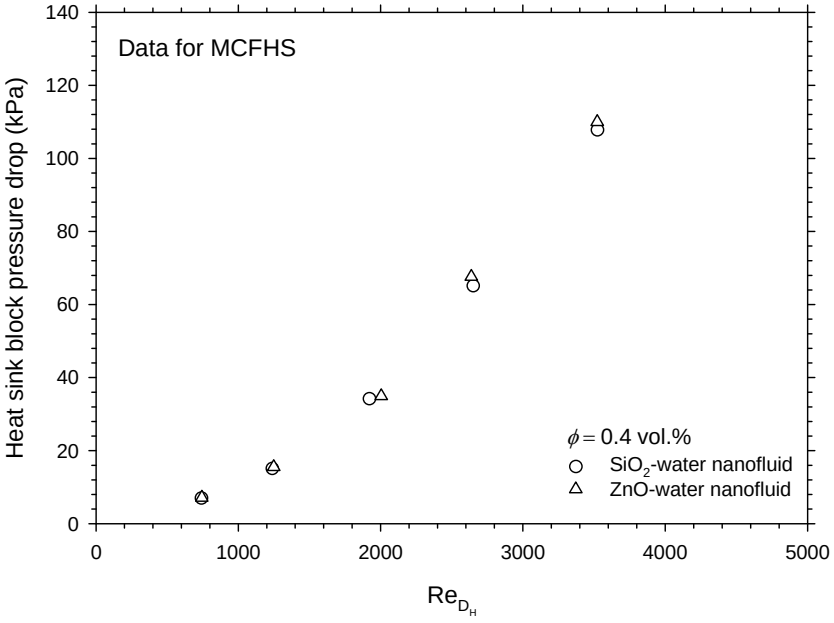

b) at particle fraction of 0.4 vol.%

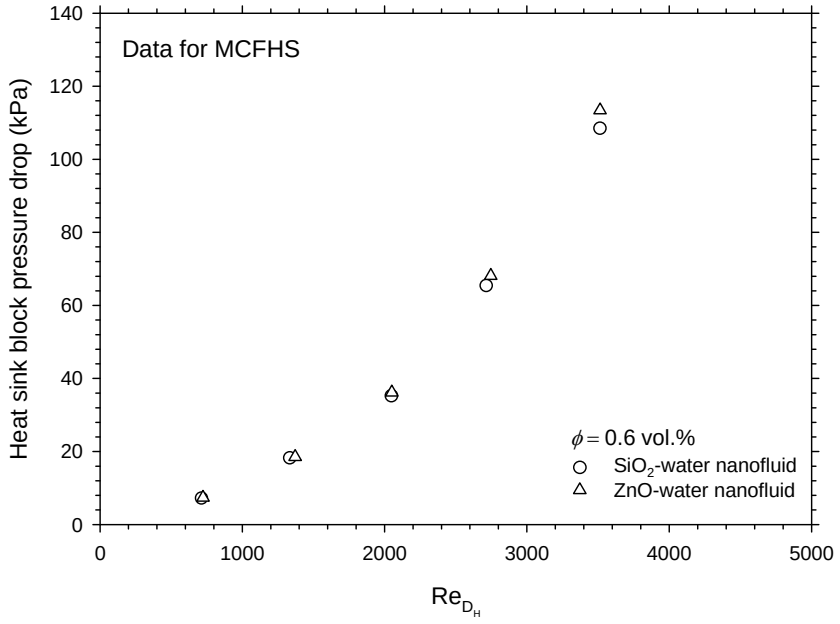

c) at particle fraction of 0.6 vol.%

Figure 5.40 Comparison of the pressure drop heat sink between SiO_2-water and ZnO-water nanofluid at various particle concentration (data for MCFHS)

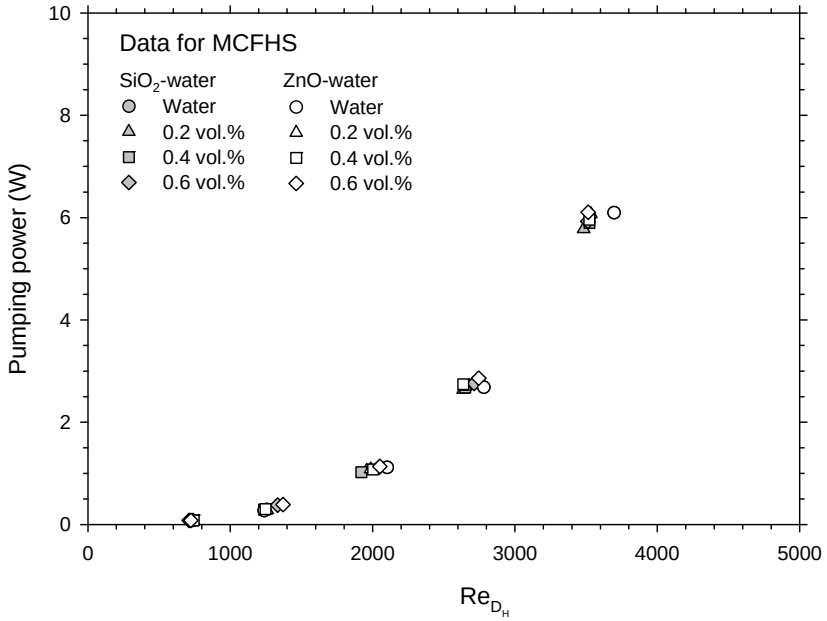

Figure 5.41 Comparison of the pumping power between SiO_2-water and ZnO-water nanofluid at various particle concentration (data for MCFHS)

For pressure data, the results show that the nanoparticle type has no significant effect on the pressure drop across the heat sink. This is due to small amount of particle concentrations are used in the present work.

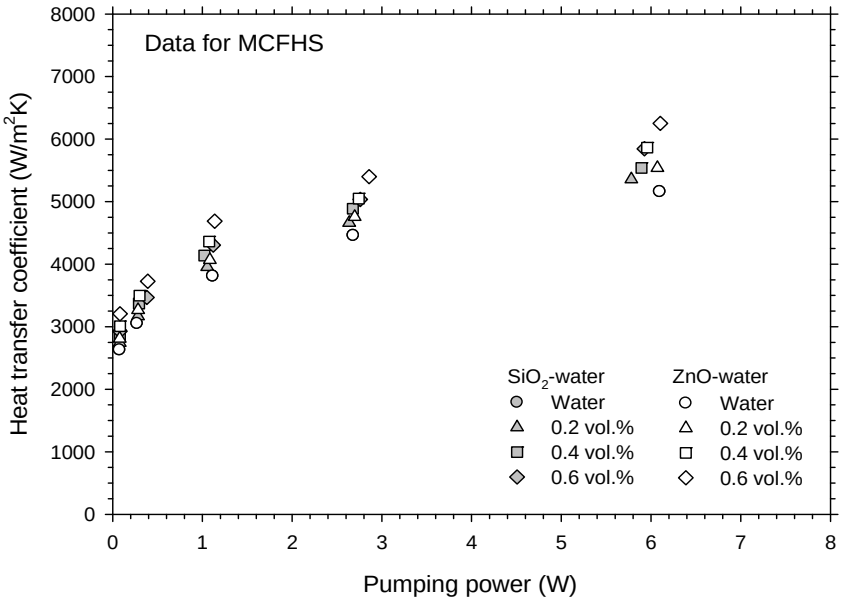

Figure 5.42 Heat transfer coefficient as a function of pumping power and particle type at various concentrations (data for MCFHS)

As shown in Figure 5.42, at a given pumping power, the heat transfer performance of the ZnO-water nanofluids are larger than those of the data for SiO_2-water nanofluids. The reason for this phenomena is explained in the above section.

5.3.2 For MSFHS

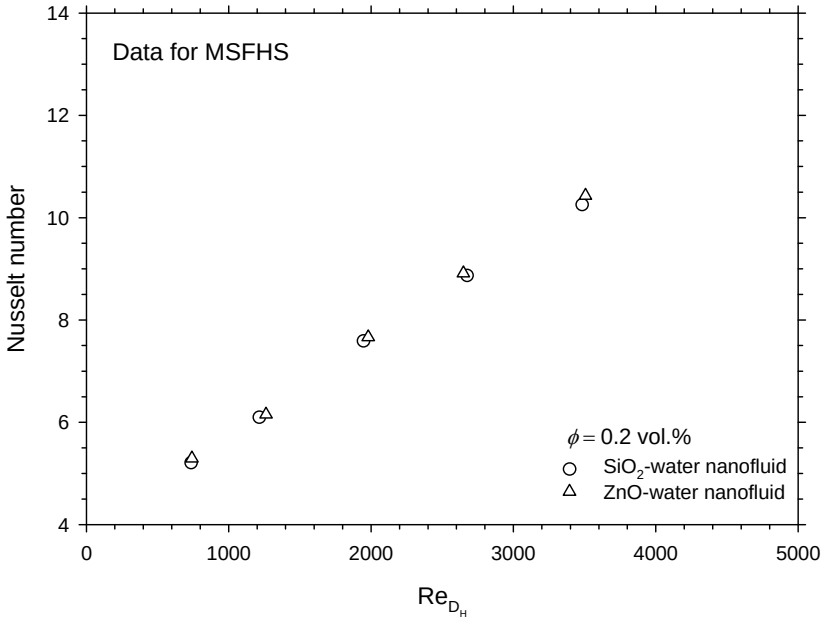

a) at particle fraction of 0.2 vol.%

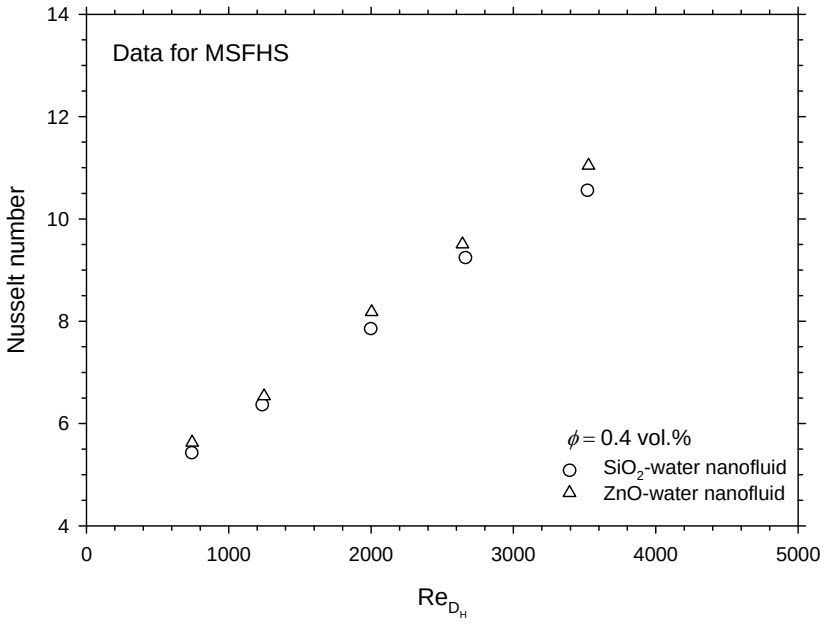

b) at particle fraction of 0.4 vol.%

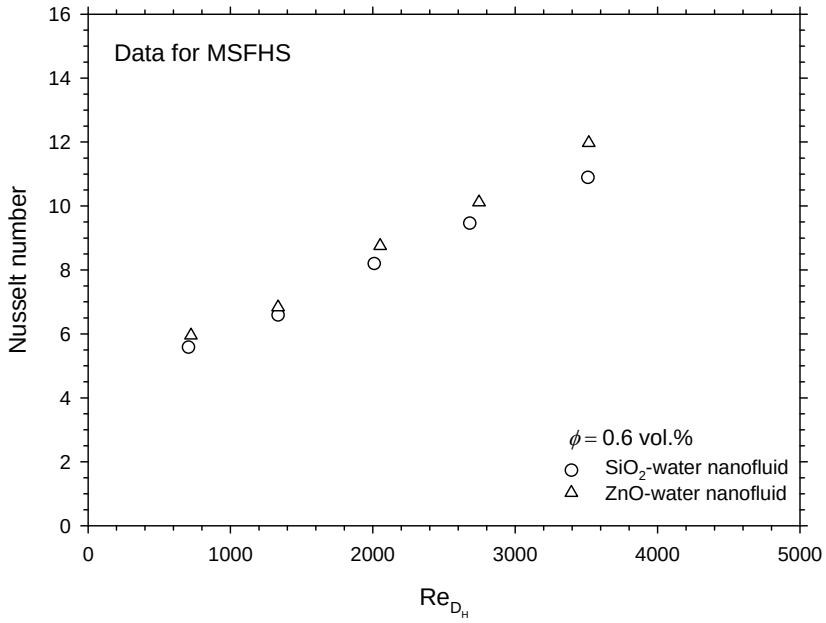

c) at particle fraction of 0.6 vol.%

Figure 5.43 Comparison of the Nusselt number between SiO_2-water and ZnO-water nanofluid at various particle concentration (data for MSFHS)

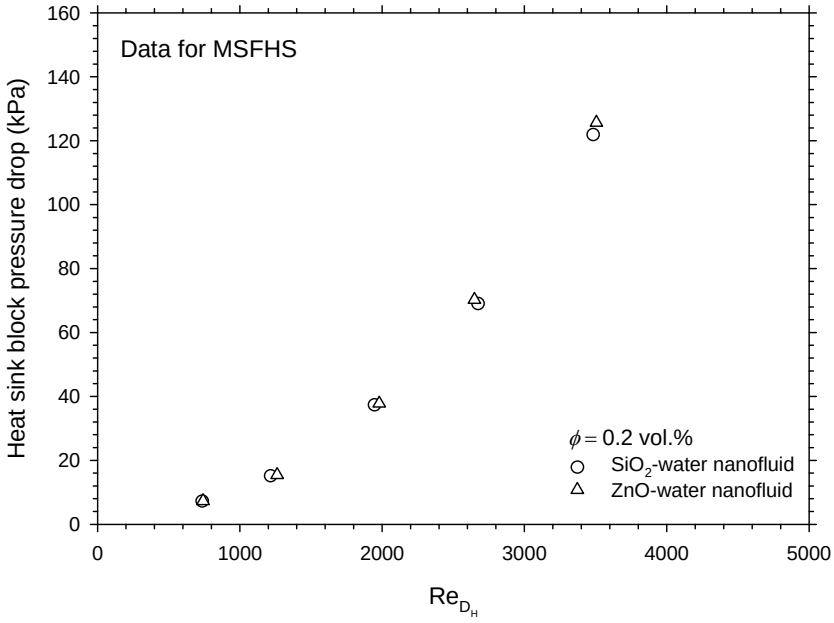

a) at particle fraction of 0.2 vol.%

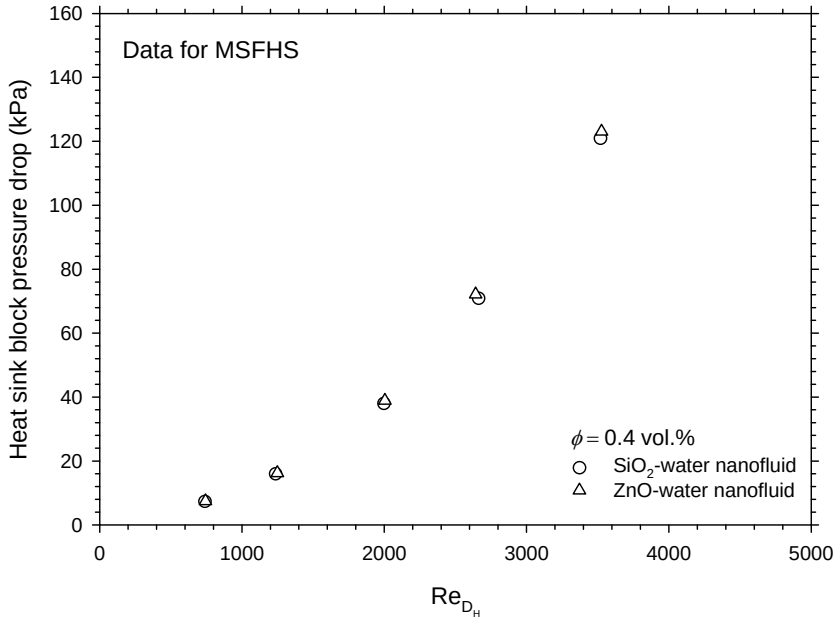

b) at particle fraction of 0.4 vol.%

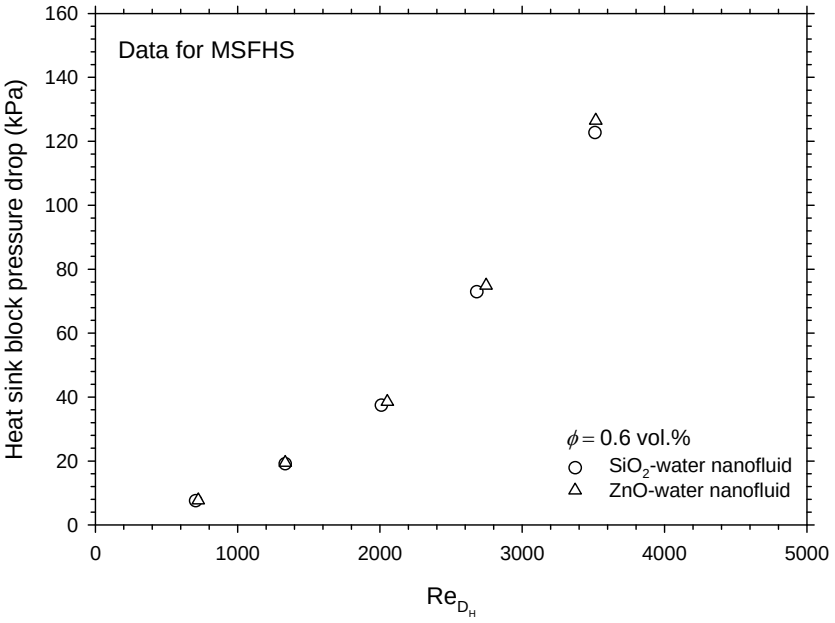

c) at particle fraction of 0.6 vol.%

Figure 5.44 Comparison of the pressure drop heat sink between SiO_2-water and ZnO-water nanofluid at various particle concentration (data for MSFHS)

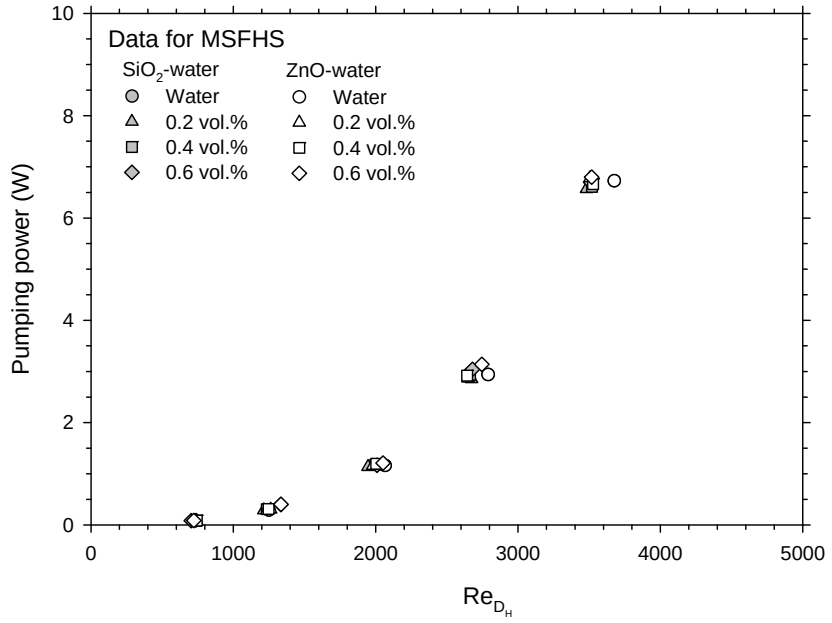

Figure 5.45 Comparison of the pumping power between SiO_2-water and ZnO-water nanofluid at various particle concentration (data for MSFHS)

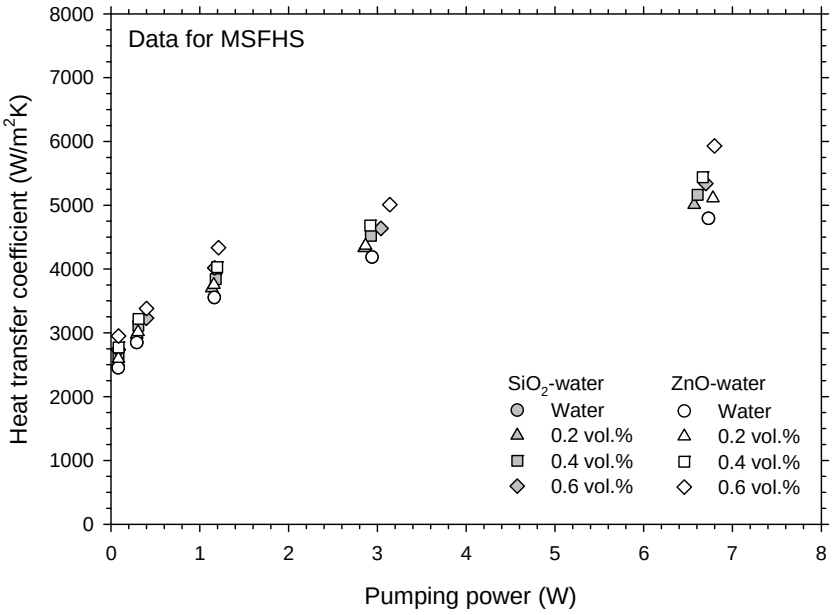

Figure 5.46 Heat transfer coefficient as a function of pumping power and particle type at various concentrations (data for MSFHS)

Similar to the data for MCFHS, same trends of the measured data for MSFHS are observed.

5.5 The Proposed Correlations

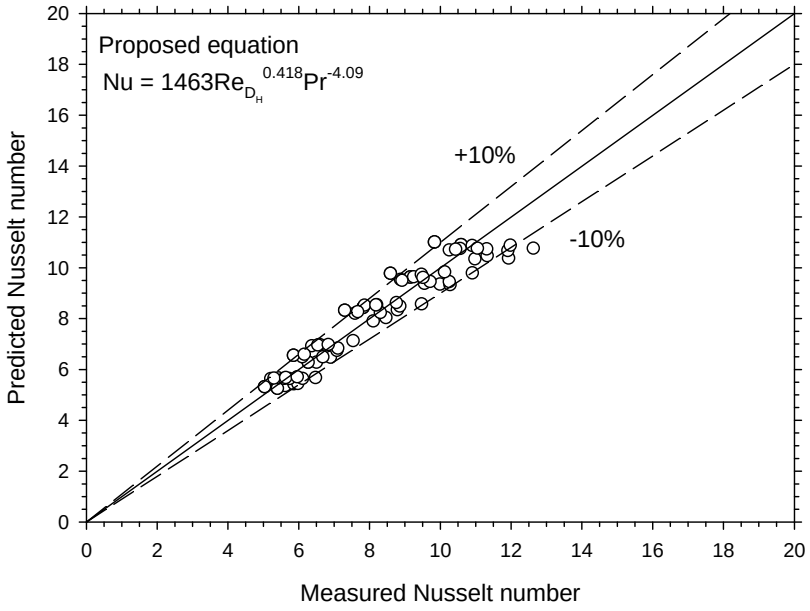

Figure 5.47 Comparison of the Nusselt number of nanofluids flowing through heat sinks between predicted values by presented correlation and measured data

As a results, from the measured data for Nusselt number and pressure drop of two types of nanoparticle and heat sinks are used to establish a new heat transfer and pressure drop correlations for predicting the heat transfer performance of the nanofluids flowing through heat sinks with circular and square pin fin structures. The detail of this concern is expressed as follows:

In general, Nusselt numbers may be related with the parameters as follows:

$$Nu = f\left(\mathrm{Re}_{D_H}, \mathrm{Pr}\right) \tag{5.1}$$

Considering the above mentioned the equation for predicting the heat transfer performance of nanofluid flowing through heat sink with pin fin structure was formed and is proposed in the following form:

$$Nu = 1463\,\mathrm{Re}_{D_H}^{0.418}\,\mathrm{Pr}^{-4.09} \tag{5.2}$$

The above equation is obtained by curve fitting all the experimental data for the SiO_2-water and ZnO-water nanofluids flowing through MCFHS and MSFHS. Comparisons of the experimental Nusselt number with those calculated by the proposed correlation are shown in Figure 5.47. The results show good correspondence between the experimental values and the calculated values by the above equation. It is clearly seen that the majority of the data falls within ± 10% of the proposed equation. The authors would like to introduce that this equation can be used for predicting the heat transfer coefficient of nanofluids flow in heat sink with circular and square pin fin structure and with a volume concentration less than 0.6% and a Reynolds number based on hydraulic diameter range between 700 and 3,800. Moreover, it is very important to note that this equation is only established with respect to the data for SiO_2-water and ZnO-water nanofluids.

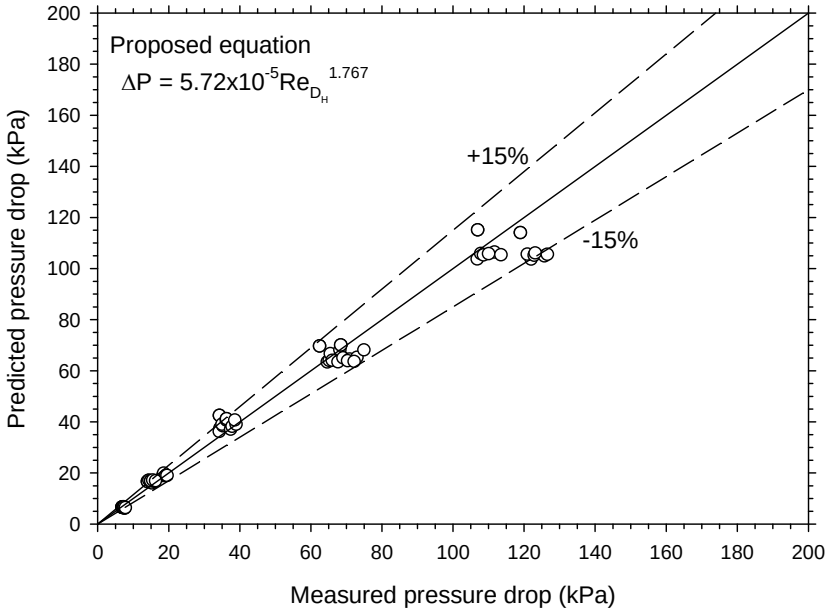

Figure 5.48 Comparison of the pressure drop across heat sinks between predicted values by presented correlation and measured data

Similar to the Nusselt number correlation, a new correlation which is easy to use for calculating the pressure drop of nanofluids across heat sinks with pin fin configuration is proposed in the following form:

$$\Delta P = 5.72x10^{-5}\ \mathrm{Re}_{D_H}^{1.767}\ \text{(kPa)} \qquad (5.3)$$

As shown in Figure 5.48, the results show that the present correlation gave reasonably good agreement with the experimental data. The majority of the data falls within ± 15% of the proposed equation. The limitations of the above equation are the same as that of the Nusselt number equation

CHAPTER 6 CONCLUSION

The objective of this chapter is to present the conclusion of the present work. The important conclusions of this study are expressed as follows:

6.1 Conclusion

The convective heat transfer performance and pressure drop characteristic of a SiO_2–water and ZnO-water nanofluid flowing through heat sinks with circular and square pin fin (MCFHS and MSFHS) structure was experimentally investigated. The following conclusions have been obtained.

- The use of SiO_2–water and ZnO-water nanofluid as coolant gives significantly higher heat transfer coefficients than those of the pure base fluid. For MCFHS, the heat transfer performance are higher than that of water by about 4 - 12% and 7 - 20 %, respectively.
- At the same condition, MCFHS gives roughly 6 – 9% higher thermal performance than that of the MSFHS. Moreover, ZnO-water nanofluid gives 3-9% larger heat transfer performance than that of the SiO_2–water nanofluid.
- The convective heat transfer coefficient increases with an increasing Reynolds number (Re_{DH}) as well as particle concentration.
- The pressure drop of nanofluids increases with increasing Reynolds number and there is a small increase with increasing particle volume concentrations. This implies that the nanofluid incurs small penalty of pumping power and may be suitable for practical application. Moreover, nanoparticle type has no significant effect on the pressure drop data of heat sinks.

- New heat transfer and pressure drop correlations for predicting the Nusselt number and pressure drop of nanofluids flowing through miniature circular and square pin fin structure are proposed in the form of $Nu = 1463\,\mathrm{Re}_{D_H}^{0.418}\,\mathrm{Pr}^{-4.09}$ and $\Delta P = 5.72x10^{-5}\,\mathrm{Re}_{D_H}^{1.767}$, respectively. The majority of the data falls within ± 10% and 15% of the proposed equation, respectively. These equations are valid in the range of Reynolds number based on hydraulic diameter between 700-3,800 and particle volume concentrations in the range of 0 and 0.6 vol.%.

6.2 Recommendations for Future Work

- The test apparatus can be improved to study the heat transfer performance and pressure drop of nanofluids flowing through various heat sink configurations.

REFERENCES

1. Tuckeman, D.B. and Pease, R.F.W., 1981, High performance heat sinking for VLSI, IEEE Electron Device Letters, Vol. 2(5), pp. 126-129.

2. Masuda, H., Ebata, A., Teramae, K. and Hishinuma, N., 1993, "Alteration of Thermal Conductivity and Viscosity of Liquid by Dispersing Ultra-Fine Particles (Dispersion of Al_2O_3, SiO_2 and TiO_2 Ultra-Fine Particles)", Netsu Bussei (Japan), Vol.7, No. 4, pp. 227 - 233.

3. Choi, S.U.S., 1995, "Enhancing Thermal Conductivity of Fluids with Nanoparticle", ASME Fluids Engineering Division, Vol. 231, pp. 99 - 105.

4. Duangthongsuk, W. and Wongwises, S., 2009, "Heat Transfer Enhancement and Pressure Drop Characteristics of TiO_2-Water Nanofluid in a Double-Tube Counter Flow Heat Exchanger" International Journal of Heat and Mass Transfer, Vol. 22, pp. 2059 - 2067.

5. Duangthongsuk, W. and Wongwises, S., 2009, "Measurement of Temperature-Dependent Thermal Conductivity and Viscosity of TiO_2-Water Nanofluids", Experimental Thermal and Fluid Sciences, Vol. 33, pp. 706 - 714.

6. Duangthongsuk, W. and Wongwises, S., 2009, "An Experimental Study on the Heat Transfer Performance and Pressure Drop of TiO_2-Water Nanofluids Flowing under

a Turbulent Flow Regime", International Journal of Heat and Mass Transfer, Vol. 52, pp. 2059 - 2067.

7. Duangthongsuk, W. and Wongwises, S.,"A Dispersion Model for Predicting the Heat Transfer Performance of TiO_2–Water Nanofluids under a Laminar Flow Regime", International Journal of Heat and Mass Transfer, Vol. 55 (2012), pp. 3138-3146.

8. Das, S. K., Choi, S.U.S., Yu, W. and Pradeep, T., 2008, "Nanofluids: Science and Technology", Wiley

9. Duncan, M.A., and Rouvray, D.H., 1989, Microclusters, Scientific American, pp. 110 – 115.

10. Kimoto, K., Kamilaya, Y., Nonoyama, M. and Uyeda, R., 1963, "An Electron Microscope Study on Fine Metal Particles Prepared by Evaporation in Argon Gas at Low Pressure", Japan Journal of Applied Physics, Vol. 2, pp. 702 - 713.

11. Granqvist, C.G., and Buhrman, R.A., 1976, "Ultrafine Metal Particles", Journal of Applied Physics, Vol. 47, No. 5, pp. 2200 – 2219.

12. Suslick, K. S., Fang, M. and Hyeon, T., 1996, "Sonochemical Synthesis of Iron Colloids", Journal of the American Chemical Society, Vol. 118, No. 47, pp. 11960 - 11961.

13. Chopkar, M, Das, P.K. and Manna, I., 2006, “Synthesis and Characterization of Nanofluid for Advanced Heat Transfer Applications”, Scripta Materialia, Vol. 55, pp. 549 – 552.

14. Akoh, H., Tsukasaki, Y., Yatsuya, S. and Tasaki, A., 1978, “Magnetic Properties of Ferro-Magnetic Ultrafine Particles Prepared by a Vacuum Evaporation on Running Oil Substrate”, Journal of Crystal Growth, Vol. 45, pp. 495 - 500.

15. Wagener, M., Murty, B.S. and Gunther, B., 1997, “Preparation of Metal Nanosuspensions by High-Pressure DC-Sputtering on Running Liquids in Nanocrystalline and Nanocomposite Materials II”, Materials Research Society, Pittsburgh, PA, Vol. 457, pp. 149 - 154.

16. Eastman, J.A., Choi, S.U.S., Li, S., Thompson, L.J. and Lee, S., 1997, “Enhanced Thermal Conductivity through the Development of Nanofluids”, Proceeding of the Symposium Nanophase and Nanocomposite Materials II, Materials Research Society, Boston, MA, Vol. 457, pp. 3 - 11.

17. Zhu, H., Lin, Y. and Yin, Y., 2004, “A Novel One-Step Chemical Method for Preparation of Copper Nanofluids”, Journal of Colloid and Interface Science, Vol. 277, pp. 100 - 103.

18. Eastman, J.A., Choi, S.U.S., Li, S., Thompson, L.J. and Lee, S., 2001, “Anomalous Thermal Conductivity Enhancement in Nano-tube Suspensions”, Applied Physics Letters, Vol. 78, pp. 718 - 720.

19. Choi, S.U.S., Zhang, Z.G., Yu, W., Lockwood, F.E. and Grulke, E.A., 2001, "Anomalous Thermal Conductivity Enhancement in Nano-tube Suspensions", Applied Physics Letters, Vol. 79, pp. 2252 - 2254.

20. http://en.wikipedia.org/wiki/Heat_sink

21. Jung, J.Y., Oh, H.S. and Kwak, H.Y., 2009, "Forced Convective Heat Transfer of Nanofluids in Microchannels", International Journal of Heat and Mass Transfer, Vol. 52, pp. 466–472.

22. Ho, C.J., Wei, L.C. and Li, Z.W., 2010, "An Experimental Investigation of Forced Convective Cooling Performance of a Microchannel Heat Sink with Al_2O_3/Water Nanofluid", Applied Thermal Engineering, Vol. 30, pp. 96–103.

23. Roberts, N.A. and Walker, D.G., 2010, "Forced Convective Performance of Nanofluids in Commercial Electronics Cooling Systems", Applied Thermal Engineering, Vol. 30, pp. 2499-2504.

24. Jasperson, B.A., Jeon, Y., Turner, K.T., Pfefferkorn, F.E. and Qu, W., 2010, "Comparison of Micro-Pin-Fin and Microchannel Heat Sinks Considering Thermal-Hydraulic Performance and Manufacturability", IEEE Transactions on Components and Packaging Technologies, Vol. 33, pp. 148 - 160.

25. Escher, W., Brunschwiler, T., Shalkevich, N., Shalkevich, A., Burgi, T., Michel, B., and Poulikakos, D., 2011, “On the Cooling of Electronics with Nanofluids”, Journal of Heat Transfer, Vol.133, pp. 051401-051411.

26. Fazeli, S.A., Hashemi, S.M.H., Zirakzadeh, H., and Ashjaee M., 2012, “Experimental and Numerical Investigation of Heat Transfer in a Miniature Heat Sink Utilizing Silica Nonofluid”, Superlattices and Microstructures, Vol.51, pp. 247-264.

27. Kalteh, M., Abbassi, A., Avval, M.S., Frijns, A., Darhuber, A., and Harting J., 2012, “Experimental and Numerical Investigation of Nanofluid Forced Convection Inside a Wide Microchannel Heat sink”, Applied Thermal Engineering, Vol. 36, pp. 260-268.

28. Selvakumar, P., and Suresh, S., 2012, “Convective Performance of CuO/Water Nanofluid in an Electronic Heat Sink”, Experimental Thermal and Fluid Science, Vol.40, pp.57-63.

29. Nitiapiruk, P., Mahian, O., Dalkilic, A.S., and Wongwises, S., 2013, “Performance Characteristics of a Microchannel Heat Sink Using TiO_2/Water Nanofluid and Different Thermophysical Models”, International Communications in Heat and Mass Transfer, Vol.47, pp.98-104.

30. Deshmukh, P.A., and Warkhedkar, R.M., 2013, “Thermal Performance of Elliptical Pin Fin Heat Sink Under Combined Natural and Forced Convection”, Experimental Thermal and Fluid Science, Vol.50, pp. 61-68.

31. Lee, S., Choi, S.U.S., 1996, “Application of Metallic Nanoparticle of Metallic Nanoparticles Suspensions in Advanced Cooling Systems”, Paper Presented in the International Mechanical Engineering Conference Session on Application of Metallic Materials in Advanced Engineering System, Atlanta, GA, USA

32. Chein, R., Huang, G., 2005, “Analysis of Microchannel Heat Sink Performance using Nanofluids”, Applied Thermal Engineering, Vol. 25, pp. 3104-3114.

33. Koo, J., Kleinstreuer, C., 2005, “Laminar Nanofluid flow in Microheat-Sinks, International Journal of Heat and Mass Transfer”, Vol. 48, pp. 2652–2661.

34. Jang, S.P., Choi, S.U.S., 2006, “Cooling Performance of a Microchannel Heat Sink with Nanofluids”, Applied Thermal Engineering, Vol. 26, pp. 2457-2463.

35. Abbassi, H., Aghanajafi, C., 2006, “Evaluation of Heat Transfer Augmentation in a Nanofluid-Cooled Microchannel Heat Sink”, Journal of Fusion Energy, Vol. 25(3/4), pp. 187-196.

36. Chein, R., Chuang, J., 2007, “Experimental microchannel heat sink performance studies using nanofluids”, International Journal of Thermal Sciences, Vol. 46, pp. 57–66.

37. Tsai, T.S. and Chein, R. (2007). “Performance Analysis of Nanofluid-Cooled Microchannel Heat Sinks”, International Journal of Heat and Fluid Flow, Vol. 28, 2007, pp. 1013–1026.

38. Ghazvini, M. and Shokouhmand, H. (2009). “Investigation of a Nanofluid-Cooled Microchannel Heat Sink Using Fin and Porous Media Approaches”, Energy Conversion and Management, Vol. 50, 2009, pp. 2373–2380.

39. Ebrahimi, S., Sabbaghzadeh, J., Lajevardi, M., Hadi, I., 2010, “Cooling Performance of a Microchannel Heat Sink with Nanofluids Containing Cylindrical Nanoparticles (Carbon Nanotubes)”, Heat Mass Transfer, Vol.46, pp.549–553.

40. Mohammed, H.A., Bhaskaran, G., Shuaib, N.H. and Abu-Mulaweh, H.I., 2011, “Influence of Nanofluids on Parallel Flow Square Microchannel Heat Exchanger Performance”, International Communications in Heat and Mass Transfer, Vol. 38, pp. 1-9.

41. Shokouhmand, H., Ghazvini, M., and Shabanian, J., 2008, “Performance Analysis of Using Nanofluids in Microchannel Heat Sink in Different Flow Regimes and Its Simulation Using Artificial Neural Network”, Proceedings of the World Congress on Engineering, Vol.3, pp. …..

42. Mohammed, H.A., Gunnasegaran, P., and Shuaib, N.H., 2010, “Heat Transfer in Rectangular Microchannels Heat Sink Using Nanofluids”, International Communications in Heat and Mass Transfer, Vol.37, pp. 1496-1503.

43. Ijam, A., Saidur, R., and Ganesan, P., 2012, “Cooling of Minichannel Heat Sink Using Nanofluids”, International Communications in Heat and Mass Transfer, Vol.39, pp. 1188-1194.

44. Ijam, A., and Saidur, R., 2012, “Nanofluid as a Coolant for Electronic Devices (Cooling of Electronic Devices)”, Applied Thermal Engineering, Vol.32, pp.76-82.

45. Hung, T.C., Yan, W.M., Wang, X.D., and Chang, C.Y., 2012, “Heat Transfer Enhancement in Microchannel Heat Sinks Using Nanofluids”, International Journal of Heat and Mass Transfer, Vol.55, pp. 2559-2570.

46. Manay, E., Sahin, B., Yilmaz, M., and Gelis, K., 2012, “Thermal Performance Analysis of Nanofluids in Microchannel Heat Sinks”, World Academy of Science, Engineering and Technology, Vol.6, pp.87-92.

47. Tokit, E.M., Mohammed, H.A., and Yusoff, M.Z., 2012, “Thermal Performance of Optimized Interrupter Microchannel Heat Sink (IMCHS) Using Nanofluids”, International Communications in Heat and Mass Transfer, Vol.39, pp. 1595-1604.

48. Hashemi, S.M.H., Fazile, S.A., Zirakzadeh, H., and Ashjaee, M., 2012, “Study of Heat Transfer Enhancement in a Nanofluid-Cooled Miniature Heat Sink”, International Communications in Heat and Mass Transfer, Vol.39, pp. 877-884.

49. Tabrizi, A.S., and Seyf, H.R., 2012, “Analysis of Entropy Generation and Convective Heat Transfer of Al_2O_3 Nanofluid Flow in a Tangential Micro Heat Sink”, International Journal of Heat and Mass Transfer, Vol.55, pp.4366-4375.

50. Seyf, H.R., and Niiaaein, B., 2012, “Analysis of Brownian Motion and Particle Size Effects on the Thermal Behavior and Cooling Performance of Microchannel Heat Sinks”, International Journal of Thermal Sciences, Vol.58, pp.36-44.

51. Seyf, H.R., and Feizbakhshi M., 2012, “Computation Analysis of Nanofluid Effects on Convective Heat Transfer Enhancement of Micro-Pin Heat Sinks”, International Journal of Thermal Sciences, Vol.58, pp.168-179

52. Shafeie, H., Abouali, O., Jafarpur, K., and Ahmadi, G., 2013, “Numerical Sutdy of Heat Transfer Performance of Single-Phase Heat Sinks With Micro Pin-Fin Structures”, Applied Thermal Engineering, Vol.58, pp. 68-76.

53. John, T.J., Mathew, B., and Hegab, H., 2010, “Parametric Study on the Combined Thermal and Hydraulic Performance of Single Phase Micro Pin-Fin Heat Sinks Part I: Square and Circle Geometries”, International Journal of Thermal Sciences, Vol. 49, pp. 2177-2190.

54. Pak, B. C. and Cho, Y. I., 1998, “Hydrodynamic and Heat Transfer Study of Dispersed Fluids with Submicron Metallic Oxide Particles”, Experimental Heat Transfer, Vol.11, pp.151 - 170.

55. Hamilton, R.L. and Crosser, O.K., 1962, “Thermal Conductivity of Heterogeneous Two-Component Systems”, Industrial & Engineering Chemistry Fundamentals, Vol. 1, No. 3, pp. 187 - 191.

56. Murshed, S.M.S., Leong, K.C. and Yang, C., 2005, “Enhanced Thermal Conductivity of TiO_2-Water Based Nanofluids”, International Journal of Thermal Sciences, Vol.44, pp. 367 - 373.

57. Wasp, F.J., 1977, Solid-Liquid Slurry Pipeline Transportation, Trans. Tech, Berlin

58. Yu, W. and Choi, S.U.S., 2003, "The Role of Interfacial Layers in the Enhanced Thermal Conductivity of Nanofluids: A Renovated Maxwell Model", Journal on Nanoparticle Research, Vol. 5, pp. 167 - 171.

59. Timofeeva, E.V., Gavrilov, A.N., McCloskey, J.M. and Tolmachev, Y.V., 2007, "Thermal Conductivity and Particle Agglomeration in Alumina Nanofluids: Experiment and Theory", Physical Review, Vol. 76, pp. 061203-1 - 061203-16.

60. Batchelor, G.K., 1977, "The Effect of Brownian Motion on the Bulk Stress in a Suspension of Spherical Particles", Journal of Fluid Mechanics, Vol. 83, No. 1, pp. 97 - 117.

61. Drew, D.A. and Passman, S.L., 1999, Theory of Multi Component Fluids, Springer, Berlin

62. Brinkman, H.C., 1952, "The Viscosity of Concentrated Suspensions and Solution", Journal of Chemical Physics, Vol. 20, pp. 571 - 581.

63. Wang, X. Q. and Mujumdar, A. S., 2007, "Heat Transfer Characteristics of Nanofluids: A Review", International Journal of Thermal Sciences, Vol. 46, pp. 1 - 19.

64. Duangthongsuk, W and Wongwises, S., 2009, “Measurement of Temperature-Dependent Thermal Conductivity and Viscosity of TiO_2-Water Nanofluids” Experimental Thermal and Fluid Sciences, Vol. 33, pp. 706 - 714.